

UC Riverside

UC Riverside Electronic Theses and Dissertations

Title

Artificial Cellulosomes and Arsenic Cleanup: From Single Cell Programming to Synthetic Yeast Consortium

Permalink

<https://escholarship.org/uc/item/0fb629h4>

Author

Tsai, Shen-Long

Publication Date

2011

Peer reviewed|Thesis/dissertation

UNIVERSITY OF CALIFORNIA
RIVERSIDE

Artificial Cellulosomes and Arsenic Cleanup:
From Single Cell Programming to Synthetic Yeast Consortium

A Dissertation submitted in partial satisfaction
of the requirements for the degree of

Doctor of Philosophy

in

Chemical and Environmental Engineering

by

Shen-Long Tsai

December 2011

Dissertation Committee:

Dr. Wilfred Chen, Co-Chairperson

Dr. Nosang Myung, Co-Chairperson

Dr. Ashok Mulchandani

Copyright by
Shen-Long Tsai
2011

The Dissertation of Shen-Long Tsai is approved:

Committee Co-Chairperson

Committee Co-Chairperson

University of California, Riverside

ACKNOWLEDGEMENTS

On the last stop of this long and arduous but precious journey, I owe my gratitude to those who ever participated in this journey starting from its inception and assisted me through its completion. Without their help and encouragement, this journey would never have been as memorable.

First of all, I would like to express my sincere gratefulness to my research advisor, Professor Wilfred Chen, who graciously opened the door to the world of science so I may get in. His guidance, understanding, patience and mentorship during my graduate studies at UC Riverside were paramount in providing a well-rounded experience consistent my long-term career goals. He always encouraged me not to be just an experimentalist but also an instructor and an independent scholar. I was so lucky to be one among the graduate students who are given the opportunity to develop their own individuality and self-sufficiency by being allowed to work with such independence. I thank you for everything you've done for me, Dr. Chen.

I would like to thank my dissertation committee members- Professor Ashok Mulchandani and Professor Nosang Myung, and my project collaborator- Professor Nancy Da Silva from UC Irvine. Their insightful comments, constructive criticisms and warm encouragement throughout this work were out of great value. I also wish to thank my undergraduate advisor, Prof. Chi-Wen Lin in Taiwan, for his timely counseling and encouragement whenever I have to make a difficult decision since my undergraduate study. Because of all of these professors, the benefits I have reaped are more than what I deserve.

I would also like to thank all the current and previous members of Prof. Chen, Prof. Mulchandani and Prof. Myung's research group. Special thanks to Miso, Divya, Chong-Hyun, Fang, Lakshmi, Garima G, Qing, Daniel, Charles, Chun-Che, Garima C, Heejae, Bhawna, Ann, Yu-Chen, Seung-Hyun, Shailendra, Payal, Christy, Joun, Zdenek, Jeongseok and Chaokun for their help and encouragement throughout my work, as well as for their contribution of so much needed humor and entertainment in what could have otherwise been a somewhat stressful laboratory environment. I am grateful to have been brought in with such a great group.

I am thankful to the publisher of the journal Applied and Environmental Microbiology for the permission to reprint the articles in Chapter 2 and Chapter 3, and to the publisher of the journal Biotechnology and Bioengineering for the permission to reprint the article in Chapter 5.

For the never ending support and unconditional love of my parents, in laws, siblings and my dearest wife- Yi-Hsun, I feel an immense gratitude which cannot be expressed in words. For them, I believe in more than what I can do. For them, I believe there is always a harbor nearby for an easy and safe refuge. I most want to thank my wife for her love, sacrifice, and kind indulgence. I also credit our children, Charles and William, for inspiring and amazing me every day. Now I am finishing this journey and I would like to dedicate this dissertation to my family.

ABSTRACT OF THE DISSERTATION

Artificial Cellulosomes and Arsenic Cleanup:
From Single Cell Programming to Synthetic Yeast Consortium

by

Shen-Long Tsai

Doctor of Philosophy
Graduate Program in Chemical and Environmental Engineering
University of California, Riverside, December 2011
Dr. Wilfred Chen, Co-Chairperson
Dr. Nosang Myung, Co-Chairperson

As our society marches toward a more technologically-inclined and industrialized future, energy and environmental sustainability are two of the most challenging problems we face today. With the aid of recent advances in recombinant molecular technology, metabolic engineering has been employed on a variety of host organisms to improve biosorption and biocatalytic capabilities. This has shown immense promise and has become an attractive tool for bioremediation and biofuel production. In regards to these challenges, this dissertation focuses on the use of metabolic engineering for biofuel production and arsenic remediation.

The first objective of this dissertation was to create an efficient and inexpensive whole-cell biocatalyst in an effort to produce economically compatible and sustainable biofuels, such as cellulosic ethanol. The approach used was via surface display of versatile cellulolytic enzyme complexes, namely cellulosomes, on the historical ethanol producer *Saccharomyces cerevisiae* for simultaneous and synergistic saccharification and

fermentation of cellulose to ethanol. The feasibility of assembling cellulosome structures on yeast cell surfaces was first demonstrated by incubating the miniscaffoldin displayed yeasts with the *Escherichia coli* cell lysates containing three cellulolytic enzymes that were necessary for hydrolyzing cellulose into glucose. The functionally-assembled minicellulosomes retained the synergism for cellulose hydrolysis, resulting in a higher ethanol production level when compared to that obtained from a free cellulase system.

To create a microorganism suitable for a more cost-effective process, called consolidated bioprocessing (CBP), a synthetic consortium capable of displaying minicellulosomes on the cell surface via intercellular complementation was subsequently created. In this case, the minicellulosomes were assembled *in vivo* on yeast surfaces for direct ethanol production and cell growth from cellulose. To tackle the relatively modest ethanol production of the yeast consortium, a designer cellulosome based on the unique feature of the anchoring -adaptor scaffoldin strategy to amplify the number of enzymatic subunits was created. The increased rate in ethanol production indicated that enzyme proximity was crucial to cellulosomal synergy.

To further extend the metabolic engineering strategy toward environmental sustainability, engineered *S. cerevisiae* strains expressing cysteine desulfhydrase and/or AtPCS were created for enhanced accumulation of arsenic as an efficient biosorbent for environment cleanup.

TABLE OF CONTENTS

CHAPTER 1	1
METABOLIC ENGINEERING OF BAKER’S YEAST	2
ENGINEERING CELLULOLYTIC CAPABILYIES IN BAKER’S YEAST	5
ARSENIC METABOLISM IN YEAST	12
SCOPE OF THIS DISSERTATION.....	18
REFERENCES	20
CHAPTER 2	35
ABSTRACT.....	36
INTRODUCTION	37
MATERIALS AND METHODS.....	40
RESULTS	45
DISCUSSION	51
REFERENCES	53
CHAPTER 3	67
ABSTRACT.....	68
INTRODUCTION	69
MATERIALS AND METHODS.....	72
RESULTS	78
DISCUSSION	83
REFERENCES	86
CHAPTER 4	100

ABSTRACT.....	101
INTRODUCTION	102
MATERIALS AND METHODS.....	106
RESULTS AND DISCUSSION	112
REFERENCES	121
CHAPTER 5.....	134
ABSTRACT.....	135
INTRODUCTION	136
MATERIALS AND METHODS.....	139
RESULTS AND DISCUSSION	142
REFERENCES	145
CHAPTER 6.....	154

LIST OF TABLES

Table 2.1. Scaffoldins and dockerin-tagged cellulases used in this study	58
Table 2.2. Amount of reducing sugars released from Avicel after 24 h of incubation at 30°C either by cells displaying cellulosomes or by the same amount of free enzymes.	59
Table 3.1. Primers used in this study	90
Table 3.2. Strains and plasmids used in this study.....	91
Table 3.3. Consortia generated in this study	92
Table 5.1. Cell densities (O.D.) of the yeast strain BY4742 with or without cysteine desulfhydrase expression after 15 h cultivation at various cysteine concentrations. Data shown below were the average from three independent experiments.	149

LIST OF FIGURES

Figure 1.1. Potential strategies for genetically engineering yeasts	32
Figure 1.2. Native cellulolytic systems in (A) aerobic microorganisms and (B) anaerobic microorganisms.....	33
Figure 1.3. Arsenic metabolism in yeasts.	34
Figure 2.1. Functional assembly of minicellulosomes on the yeast cell surface	60
Figure 2.2. Phase-contrast and immunofluorescence micrographs of yeast cells displaying minicellulosomes	62
Figure 2.3. Fluorescence intensity of cells either displaying scaffoldin Scaf-ctf or with different combinations of dockerin-tagged cellulases (At [A], Ec [E], and Gf [G]) docked on the displayed Scaf-ctf.	63
Figure 2.4. Whole-cell hydrolysis of CMC by different cellulase pairs (CelE-Dc [Ec], CelA-Dt [At], or CelG-Df [Gf]) docked on the displayed Scaf-ctf protein ..	64
Figure 2.5. Production of glucose (A) and reducing sugars (B) from the hydrolysis of PASC by free enzymes and by surface-displayed cellulosomes.....	65
Figure 2.6. Time profiles of ethanol production (A) and cellulose hydrolysis (B) from PASC by control strain EBY100 plus free enzymes and yeast cells displaying functional cellulosomes.	66
Figure 3.1. Surface assembly of a functional mini-cellulosome through intracellular complementation using a synthetic yeast consortium.....	93
Figure 3.2. Secretion of dockerin-tagged enzymes.....	94
Figure 3.3. Cellulose hydrolysis and ethanol production by different synthetic consortia (See Table 3.3). established using a strain.....	96
Figure 3.4. Constitutive surface display of scaffoldin Scaf-ctf using the Ag α 1 anchor and the constitutive PGK promoter	97
Figure 3.5. (A) Cell growth and (B) ethanol production and (C) PASC hydrolysis by the different yeast consortia, i.e., consortium C1 without secreting	

enzymes (●), consortium C8 only secreting enzymes (■) and consortium C1 forming cellulosome structure (▲)..	99
Figure 4.1. A schematic diagram of the complex cellulosome assembled on the yeast surface	125
Figure 4.2. Phase-contrast micrographs and immunofluorescence micrographs of the yeast displaying the anchoring scaffoldin pCohAcBc and the control yeast.....	126
Figure 4.3. Expression and Avicel purification of adaptor scaffoldins analyzed by (A) 10% SDS-PAGE gel and (B) western-blot analysis with goat IgG-alkaline phosphatase conjugate.	127
Figure 4.4. Fluorescent intensity of the anchoring scaffoldin displayed yeast after incubated with one and two adaptor scaffoldins..	128
Figure 4.5. Fluorescent intensity of the anchoring scaffoldin displayed yeast after incubated with adaptor scaffoldins and (A) endoglucanase CelGt, (B) β -glucosidase BglAf or (C) both enzymes.	130
Figure 4.6. Illustration of the different cellulosome systems used in this research.	131
Figure 4.7. Production of glucose (A) and reducing sugars (B) from the hydrolysis of PASC by the yeasts displaying different cellulosomes.....	132
Figure 4.8. Time profiles of ethanol production (A) and cellulose hydrolysis (B) from PASC by the yeasts displaying different cellulosomes.....	133
Figure 5.1. Plasmid maps of the construct (A) pYES3-atPCS::FLAG and (B) p181CysDes.	150
Figure 5.2. (A) Sulfide production and (B) intracellular As(III) accumulation from the engineered <i>S. cerevisiae</i> strain BY4742 expressing cysteine desulfhydrase at various cysteine concentrations.....	151
Figure 5.3. PC production and intracellular As(III) accumulation from the engineered <i>S. cerevisiae</i> strain BY4742 expressing AtPCS.....	152
Figure 5.4. Intracellular As(III) accumulation from engineered <i>S. cerevisiae</i> strains expressing either cysteine desulfhydrase, AtPCS, or both enzymes.....	153

CHAPTER 1

Background

METABOLIC ENGINEERING OF BAKER'S YEAST

Baker's yeast *Saccharomyces cerevisiae* expression platform

Since 1990, the concept of metabolic engineering has been developed and applied to the production of metabolites (Bailey, 1991). With the unexpectedly fast progress in recombinant DNA technology, metabolic engineering has allowed the production of peptides, proteins and biomolecules from naturally non-producing microorganisms (Porro et al., 2005). Combined with extensive works on genomic data, central metabolic processes, and cellular enzymes, metabolic engineering has become one of the most important technologies developed in this era.

Many microorganisms, including archaea, prokaryotes and eukaryotes, have been employed as hosts for the production of recombinant proteins and molecules (Keasling, 2010). Several criteria, such as efficient mass production, safety, and available genetic tools, should be taken into consideration while choosing a host cell for metabolic engineering applications. In this aspect, yeasts offer considerable benefits over other host systems. Among more than 800 yeast species described, the baker's yeast *Saccharomyces cerevisiae* is the one with the longest use in industry (Graf et al., 2009).

The completion of the *S. cerevisiae*'s genome project was accomplished in 1996, making it the first eukaryote whose genome has been completely documented (Goffeau et al. 1996). Because of the well-established knowledge on its physiology, genetics, and biochemistry, *S. cerevisiae* is an ideal model eukaryote for fundamental research and heterologous gene expression (Gellissen and Hollenberg 1997). Moreover, *S. cerevisiae* is recognized by the US Food and Drug Administration (USFDA) as a safe organism

because of the absence of endotoxins as well as oncogenic or viral DNA. Unlike bacteria, which lack the capability for post-translational modifications such as glycosylation, *S. cerevisiae* either possesses many of these characteristics or can be engineered to produce a wider range of functionally active proteins.

Strategies for heterologous protein production in yeast

A wide range of vectors has been developed for molecular cloning in *S. cerevisiae*. Together with the well-characterized genetics, chemistry, and physiology, the most appealing aspect of *S. cerevisiae* for metabolic engineering is perhaps the ease of genetic manipulation. Past efforts in genetic engineering has made it easy to delete, insert, replace, over-express or down-regulate any gene of interest (Siewers 2010).

There are many different ways that heterologous proteins can be expressed in *S. cerevisiae* (Figure 1.1). Depending on the applications, they can be deposited intracellularly, displayed on the cell surfaces, or targeted to the secretory apparatus. Cytoplasmic expression often leads to relatively higher expression levels as the potential limitations of the secretory pathways are not involved (Boer et al., 2007). However, in many cases, disulfide bond formation is required for correct protein folding and processing, which pose a sever limitation for cytoplasmic expression. Alternatively, heterologous proteins can be secreted into the culture supernatant by adding a secretion signal sequence. The most popular secretion signal sequence is the α -mating factor (MF α 1). However, compared to intracellular expression, the level of secreted proteins is often impaired.

Yeast surface-display of heterologous proteins is of particular interesting as it provides several advantages over other strategies. As the active enzymes are displayed on the surface of the yeast, reactions can occur at the surface. Therefore, this method is quite useful when dealing with a substrate that cannot enter the cell or is highly toxic to the cell (Kuroda and Ueda, 2011). While many cell surface proteins have been identified in *S. cerevisiae*, glucanase extractable proteins that have glycosylphosphatidylinositol (GPI) anchors are the major group used for heterologous-protein display (Fleet and Manners 1977). Among these GPI anchor proteins, mating-type sexual agglutinins (Aga1 and Aga1), which mediate the direct cell-cell adhesion during mating, are two of most commonly used fusion partners for surface display (Lipke and Kurjan, 1992). Proteins ranging from 0.93 to 136 KDa have been successfully displayed on the yeast surface, and in many cases up to 10^4 - 10^5 molecules can be displayed per cell (Shibasaki et la., 2001; Nakamura et al., 2002).

With these versatile tool sets for the genetic manipulations, *S. cerevisiae* has been engineered to solve a wide range of current issues in environment and energy such as bioremediation, biosensors, and biofuel production.

ENGINEERING CELLULOLYTIC CAPABILITIES IN BAKER'S YEAST

Cellulosic ethanol and the evolution of its production process

Biomass is one of the most abundant renewable-feedstock for sustainable production of biofuels. Among different forms of biomass, lignocellulose is particularly well-suited for energy applications because of its large-scale availability, low cost and environmental benign production (Lynd, 1999). This natural and abundant polymer is found as agricultural waste (wheat straw, corn stalks, and soybean residues), industrial waste (Pulp and paper industry), forestry residues, and municipal solid waste. In addition, many energy production and utilization cycles based on cellulosic materials have near-zero greenhouse gas emissions on a life cycle basis (Lynd, 2005).

Extensive researches have been performed in the area of reactor design, pretreatment protocols, and separation technologies in an effort to make the bioconversion processes more economically competitive with petroleum fuel technologies. Ethanol is particularly attractive since it is a good transportation fuel and in some respects superior to gasoline (Lynd et al., 1991). (1) Neat (unblended) ethanol burns more cleanly and efficiently due to its high octane rating. (2) Ethanol by fermentation offers a more favorable trade balance and enhanced energy security. (3) Ethanol also reduces smog formation due to its low volatility and low photochemical reactivity. (4) Ethanol is considerably less toxic to human than is gasoline.

However, the main technological obstacle to more widespread usages of this resource is the lack of low-cost technologies to overcome the recalcitrant nature of the cellulosic structure, especially the hydrolysis step on highly ordered cellulose (Lynd et al.,

2002). As plants have evolved mechanisms over millennia to protect the structure forms of polysaccharides from which cell wall has been compromised, only a small fraction of microorganisms possess the ability to degrade cellulose efficiently. A great deal of effort has gone into the development of methods for the conversion of cellulose to glucose. Several events have to happen for cellulose to be amenable to ethanol fermentation: (1) production of cellulases, (2) hydrolysis of the cellulose present in pretreated biomass, (3) fermentation of hexose sugars (van Zyl et al., 2007). Further, it has been reported that a substantially cost reduction can be obtained when two or more steps are combined. Although the cost of ethanol production can become more competitive by combining the hydrolysis and fermentation steps in simultaneous saccharification and cofermentation (SSCF), it has been shown that the overall cost can be even further reduced by four-fold using a one-step consolidated bioprocessing (CBP), where cellulase production, cellulose hydrolysis and sugar fermentation can be carried out in a single reactor (Lynd., 2005).

While CBP is a promising approach to reduce the cost of biofuel production, microorganisms that are suitable for CBP do not exist in nature. Numerous attempts have been made to create recombinant organisms for CBP. These recombinant microorganisms can be roughly divided into three groups: (1) recombinant solventgenic microorganisms that possess superior saccharolytic capabilities, but into which solvent-production capabilities were engineered, (2) recombinant cellulolytic microorganisms that naturally give high product yields, but into which saccharolytic systems were engineered, and (3) recombinant microorganisms that do not possess saccharolytic and solventgenic abilities, but into which solvent production and saccharolytic capabilities were engineered.

1.3.2. Natural cellulolytic systems

Cellulose is a linear condensation polymer consisting of D-anhrolocopyranose jointed together by β -1,4-glycosidic bonds with a degree of polymerization (DP) from 100 to 20,000 (Zhang and Lynd 2004). By hydrogen bonds and van der Waal's forces, adjacent cellulose forms a parallel alignment and a crystalline structure with great tensile strength and low accessibility (Zhang et al., 2006).

Cellulolytic bacteria and fungi employ a diversity of contrasting but complementary mechanisms for the hydrolysis of cellulose and related complex plant cell-wall polysaccharides. Since these microbes have been selected by nature, they have evolved different strategies to survive and thrive in their environments either independently or by collaborating with other bacteria and fungi.

Although it is widely recognized that the mechanism for enzymatic cellulose hydrolysis involves the synergistic action of three distinct classes of enzymes: (1) endoglucanases which act randomly on the accessible β -1,4-glycosidic bonds of the cellulose substrate and release the smaller-size oligosaccharides, (2) exoglucanases which liberate cellobiose in a processive manner from the end of cellulose or the end of the released oligosaccharides, and (3) β -glucosidases which release glucose from cellobiose for cell growth and to eliminate the inhibition of the other two enzymes from cellobiose (Lynd et al., 2002). These three reactions occur simultaneously, but the classification of the three enzymes is not strictly rigid since some enzymes may spill over from one category to another.

While microbial-based cellulose hydrolysis naturally occurs in both aerobic and anaerobic biotopes, nature has developed two different strategies to degrade this recalcitrant polymer (Figure 1.2). In the aerobic biotope, aerobic microorganisms secrete copious amounts of free cellulases to breakdown cellulose (Wilson, 2004; Bayer et al., 2000). For example, fungi of the genus *Trichoderma* express free, non-complexed cellulolytic enzymes and are known to produce high titers of extracellular enzymes reaching up to 100 g/L (Cherry and Fidantsef, 2003). In contrast, anaerobic organisms, due to energetic constraints, can only produce a limited amount of enzymes. Therefore, in response, they have developed an elaborately structured enzyme complex, called cellulosome, to maximize catalytic efficiency (Bayer et al, 2004; Doi and Kosugi, 2004; Demain et al., 2005). This self-assembled system brings multiple enzymes in close proximity to the substrate, and provides a structure that ensures a high local concentration and the correct ratio and orders of the enzymes, thereby maximizing synergy. Consequently, it has a much higher catalytic efficiency than soluble enzymes present in a non-organized fashion.

Cellulosome and artificial cellulosomes

Cellulosome is a cell-bound multienzyme complex responsible for the synergistic deconstruction of both cellulose and hemicellulose, two of the most abundant carbon-rich polymers in the world. The main feature of this nanomachine is a structural scaffoldin consisting of at least one cellulose-binding domain (CBD) and repeating cohesin domains, which are docked individually with a different cellulases tagged with a corresponding

dockerin domain. This highly ordered structure allows the assembly of multiple enzymes in close proximity, mediated by the high-affinity protein-protein interaction ($>10^{-9}$ M) between the dockerin and cohesin modules, resulting in a high level of enzyme-substrate-microbe synergy.

Because of the modular nature of the cellulosomal subunits, artificial “designer” cellulosomes have been created (Fierobe et al., 2001 and 2005). A trifunctional chimeric scaffoldin containing the cohesin domains from three different species was constructed and was shown to bind specifically to the corresponding dockerin-borne cellulolytic enzymes (Fierobe et al., 2005). Not surprisingly, several cellulosome-like nanostructures have been explored (Cho et al., 2007; Cha et al., 2007; Heyman et al., 2007; Mingardon et al., 2007). Two of the most popular are based on rosettazyme-derived and stable protein-derived nanoscaffolds (Mitsuzawa et al., 2009; Morais et al., 2010). Rosettasomes from the hyperthermo-acidophilic archaeon *Sulfolobus shibatae* are thermostable, group II chaperonins, which in the presence of ATP/Mg²⁺ assembled into 18-subunit, double-ring structures. Another protein scaffold SP1, first isolated from aspen (*Populus tremula*) trees, is a ring-shaped, highly stable homododecamer protein with a diameter of 11 nm and an internal cavity of 3 nm, which can be potentially utilized to self-assemble different modules and enzymes in a specific and oriented manner. In both cases, they fused a cohesin module to a circular permutant of the self-assembled protein complex subunit, resulting in nanoscaffolds displaying functional cohesin domains. Again, binding of dockerin-tagged cellulases onto these cohesin-containing

nanoscaffoldins increased cellulose-degrading activity compared to their activity in solution.

Engineering cellulolytic systems in baker's yeast

One of the most attractive strategies to create an efficient CBP microorganism for cellulosic ethanol production is by expressing multiple components of a cellulolytic system from either fungi or bacteria in *S. cerevisiae*, which has a highly efficient ethanol production system and a naturally high ethanol tolerance. Expression and secretion of cellulases in *S. cerevisiae* have been attempted for more than two decades and well documented (van Zyl et al., 2007).

Due to a similar glycosylation mechanism and the cellulolytic nature, *Trichoderma reesei* is one of the most common sources for heterologous cellulases in *S. cerevisiae*. However, cellulases from mesophilic and thermophilic bacteria have also been used. Den Haan and colleagues described the successful secretion of four individual cellobiohydrolases (CBHs) in *S. cerevisiae* originating from *T. reesei* (*cbh1* and *cbh2*), *Aspergillus niger* (*cbhB*) and *Phanerochaete chrysosporium* (*cbh1-4*), and the direct ethanol production from several model cellulose substrates (Den Haan et al., 2007a). The same group later demonstrated that co-secretion of an endoglucanase from *T. reesei* (*EG1*) and a β -glucosidase from *Saccharomycopsis fibuligera* (*BGL1*) allowed 1.0 g/L of ethanol to be produced from 10 g/L of phosphoric acid swollen cellulose (PASC) (Den Haan et al., 2007b). Jeon and colleagues described the production of ethanol from an engineered *S. cerevisiae* strain expressing the *Clostridium thermocellum* endoglucanase

(*EgE*) and the *S. fibuligera* β -glucosidase (*BGLI*) using β -glucan as the substrate (Jeon et al., 2009b).

Apart from secreting cellulases from yeast, several attempts have also been made to create biocatalysts by displaying cellulases on the yeast surface. Muri and colleagues constructed yeast with the ability to hydrolyze cellulosic biomass for ethanol production by co-displaying a carboxymethylcellulase (CMCase) and a β -glucosidase (*BGLI*) from *Aspergillus aculeatus* (Muri et al., 1998). In another report, direct ethanol production from PASC was achieved when the endoglucanase (*EGII*) and exoglucanase (*CBHII*) from *T. reesei* and a β -glucosidase (*BGLI*) from *A. acculeatus* were co-displayed on the yeast cell surface (Fujita et al., 2004). Interestingly, a higher level of ethanol production was reported by the same group using this three-enzyme system from a surface-display strain than a secretion strain (Yanase et al., 2010).

With the substantial improvement in cellulose hydrolysis over free enzymes by the designer cellulosomes, it is of great interest to exam whether a similar strategy could be exploited to improve whole-cell hydrolysis of cellulose and ethanol production. In this dissertation, progress in the quest of extending the cellulolytic capability of yeast via cell surface-display of different cellulosomes was described in CHAPTER 2 to CHAPTER 4.

ARSENIC METABOLISM IN YEAST

Introduction of arsenic

Arsenic (As) is a natural and ubiquitous element that presents in many environmental compartments and is released through various natural processes or by anthropogenic inputs. It is recognized as carcinogenic (Rosen, 1971) and chronic exposure to arsenic results in a wide range of adverse health effects (Chen et al., 2005; Tapio and Grosche, 2006). Depending on the physical–chemical conditions of the environment, some arsenic compounds can be easily solubilized in water (Oremland et al., 2005) and taken up by microorganisms, resulting in high levels of bioavailability (Bryan et al., 2009).

Arsenic occurs in several oxidation states including arsenate As(V), arsenite As(III), elemental As(0) and arsenide As(–III). In natural waters, arsenic is mostly found in its inorganic forms as trivalent arsenite [As(III)] or pentavalent arsenate [As(V)] (Cullen and Reimer, 1989). Among them, As(III) is generally considered to be more mobile and more toxic than As(V) (Liu et al., 2001). Owing to its extreme toxicity, arsenic is ranked number one on the Environmental Protection Agency's (EPA) priority list of drinking water contaminants and effective from 2006 the maximum contaminant level for arsenic in drinking water was reduced by the US Environmental Protection Agency from 50 ppb to 10 ppb.

Several treatment technologies have been applied in laboratory-scale and/or field-scale testing for the removal of arsenic from waters, such as coagulation, filtration, ion exchange, adsorption, and reverse osmosis (Kartinen and Martin, 1995; Zouboulis and

Katsoyiannis, 2002; DeMarco et al., 2003). However, these technologies are either too expensive or ineffective for low arsenic concentration treatment. To comply with the current regulatory limit of 10 ppb would require extensive technological developments that are highly selective and economically competitive.

In nature, microbes respond to arsenic in a variety of different ways (Figure 1.3). Depending on the species of different microorganisms, the responses could be chelation, compartmentalization, exclusion, and immobilization (Toppi and Gabbriellini, 1999). Understanding the molecular and genetic level of arsenic metabolism will be, therefore, an important knowledge base for developing efficient and selective arsenic bioremediation approaches, which has so far been considered as a cost-effective and environmental friendly way for heavy-metal removal.

Arsenic uptake and metabolism by baker's yeast

Arsenic uptake by *S. cerevisiae* occurs through three different transport systems. The pentavalent arsenate, because of the similarity to phosphate (Nidhubhghaill and Sadler, 1991), is taken up through a phosphate transporter, Pho87p (Persson et al., 1999). In addition, two transporter systems for the trivalent arsenite have been identified. Similar to bacterial systems, arsenite is taken up by an aquaglyceroporin Fps1p, a glycerol transporter (Wysocki et al., 1997; Wysocki et al., 2001). In 2004, Liu *et al.* found that a class of hexose permeases (Hxt1p to Hxt1 plus Gal2p) of *S. cerevisiae* adventitiously catalyzed the uptake of arsenite (Liu et al., 2004). Arsenite uptake was reduced by 80% in

the presence of glucose even when FPS1 was deleted, confirming that the hexose transporters are mainly responsible for arsenite uptake.

Once arsenic enters the cells, a series of detoxification steps are used to reduce the acute cytotoxic effects. The most comprehensive mechanism of arsenic tolerance in yeast is provided by three contiguous gene clusters: ARR1, ARR2, and ARR3. ARR1 encodes a transcription factor that regulates the transcription of arsenate reductase Arr2p and the arsenite extrusion transporter Arr3p (Ghosh et al., 1999). After arsenate is transported inside the yeast cells, arsenate is reduced to arsenite by an arsenate reductase Arr2p (Mukhopadhyay et al., 200). The disruption of ARR2 in *S. cerevisiae* eliminated arsenate resistance (Mukhopadhyay and Rosen, 1998). To date Arr2p is still the sole arsenate reductase in eukaryote and no ARR2 gene has yet been found with the fission yeast *S. pombe* or other fungi.

Intracellular sequestration of arsenic

Questions have been raised as to why cells were designed to reduce arsenate to the more reactive arsenite, which is at least 100 times more toxic (Knowles and Benson, 1983). The answer is that by taking advantage of the chemical reactivity, arsenite can bind to many intracellular chelating proteins or peptides containing thiol ligands, such as GSH, PCs, and MTs to form inactive complexes (Cobbett and Goldsbrough, 2002; Singhal et al., 1987; Ngu et al., 2008). GSH is a major reservoir of nonprotein thiols (Noctor, 2006), and the availability of GSH is important in arsenate reduction as well as in arsenite transport into the vacuoles (Wysocki et al., 2003). Guo *et al.* showed that

overexpression of the *S. cerevisiae* GSH1 gene encoding a γ -glutamylcysteine synthetase (γ -ECS), the first enzyme in the GSH biosynthesis pathway (Foyer and Noctor, 2005), elevated the tolerance and accumulation of arsenic in *Arabidopsis thaliana* (Guo et al., 2008). MTs belong to a family of cysteine-rich proteins with the unique ability to form stable metal-thiolate clusters with their two metal-binding, cysteine-rich domains (Morris et al., 1999), and are the major metal-binding ligands in animals. Although As-binding MTs have been described in the alga *Fucus vesiculosus* (Merrifield et al., 2004), none have been isolated in bacteria. On the other hand, PCs are small enzymatically synthesized cysteine-rich peptides widely found in plants and yeasts, and have been shown to bind arsenite efficiently (Maitani et al., 1996; Schmoger et al., 2000; Wunschmann et al., 2007). Overexpression of a tobacco PC synthase in yeast *S. cerevisiae* resulted in increased tolerance for Cd and As (Kim et al., 2005) without any enhancement in accumulation. However, our lab reported enhanced accumulation of arsenite by engineered *S. cerevisiae* expressing the *Arabidopsis thaliana* PC synthase (Singh et al., 2008).

For some yeasts such as *Candida glabrata*, extracellular sulfate is metabolized to sulfide (Thomas and SurdinKerjan, 1997), which acts as an electron donor for arsenate reduction (Rochette et al., 2000). In some eukaryotes, incorporation of sulfide to form a more stable, high-molecular-weight PC–metal–sulfide complex in the vacuole has been demonstrated (Kneer and Zenk, 1997; Mendoza-Cozatl and Moreno-Sanchez, 2005; Mendoza-Cozatl et al., 2006). In addition, the formation of metal sulfide particles in

Schizosaccharomyces pombe and *C. glabrata* is also part of their intracellular detoxification (Dameron and Winge, 1990; Krumov et al., 2007).

Arsenic resistant via intracellular and extracellular transport

S. cerevisiae has two different mechanisms to reduce arsenite cytotoxicity. One is through the arsenite extrusion pump Arr3p, which transports the As(III)–GSH complexes out of the membrane. A second mechanism of arsenic resistance is via the transport of GSH-conjugated arsenite into the vacuole (Ghosh et al., 1999). The Ycf1p protein associated with the vacuolar membrane is a member of the ABC transporter superfamily that is responsible for the ATP-dependent transport of a wide range of GSH-conjugated substrates (such as As(GS)₃) into the vacuole. Further genetic analyses support the notion that these two pathways function in a synergistic fashion as the hypersensitivity of yeast cells to arsenic is additive in a mutant lacking both genes. While *S. cerevisiae* transports the GSH–As complex into the vacuole, *S. pombe* transports high-molecular PC–Cd–S complexes into the vacuole via the Hmt1 transporter (Ortiz et al., 1995).

Ways to create arsenic biosorbents

The use of engineered microbes as selective biosorbents is an attractive green technology for the low-cost and efficient removal of arsenic. Although efforts have been reported in engineering microbes for the removal of cadmium or mercury by expressing metal-binding peptides such as human MTs or synthetic peptides (Bae et al., 2000), the relatively low affinity of these peptides for arsenic make them ineffective for arsenic

remediation. Development of an arsenic accumulating microbe should comprise the ability to firstly, modify the naturally existing defense mechanisms and secondly, develop novel or hybrid pathways into one easily manipulated microorganism. In CHAPTER 5, the possibility of creating engineered microbes as efficient biosorbents for arsenic removal was investigated, in which baker's yeast *S. cerevisiae* was metabolically programmed for arsenic clean-up by coexpressing AtPCS and cysteine desulphydrase.

SCOPE OF THIS DISSERTATION

Energy and environmental sustainability are two of the most challenging problems for the next several decades. As our society marches toward a more technologically inclined and industrialized future, the need for clean water supply and renewable energy has never been more pertinent. In this dissertation, metabolic engineering has been applied to create several yeast strains with new functionalities suitable for arsenic remediation and biofuel production.

While it is well recognized that fuels made from cellulosic biomass would be one of the most sustainable way to address the issue of gasoline crisis, the first objective of this dissertation was to create an efficient and inexpensive whole-cell biocatalyst in an effort to produce economically compatible biofuels. The approach used was via surface display of versatile cellulosomes on the historical ethanol producer *S. cerevisiae* for simultaneous and synergistic saccharification and fermentation of cellulose to ethanol.

In CHAPTER 2, I investigate the possibility of functionally assembling a mini-cellulosme on the yeast surface by incubating the scaffoldin displayed yeast with the *E. coli* cell lysates containing the endoglucanase from *C.thermocellum* (CelA), the exoglucanase from *C. cellulolyticum* (CelE), and the β -glucosidase from *C. thermocellum* (BglA). The capability and the synergic effect of the engineered yeast strain to directly convert PASC to ethanol were described.

In CHAPTER 3, I subsequently created a synthetic consortium capable of displaying mini-cellulosmes on the cell surface for the direct ethanol production from PASC via intercellular complementation. The ability of the created consortium to

hydrolyze PASC and use the released sugar for cell growth and ethanol production was investigated.

In CHAPTER 4, a more complex cellulosome structure bearing a higher enzyme loading was designed and successfully assembled on the yeast surface to further improve the cellulolytic capability of the engineered yeast strain toward cellulosic ethanol production. In this part of study, the benefit of having all enzymes in the same cellulosome structure over that in heterogeneous cellulosome structure was also discussed.

To further extend the metabolic engineering strategy toward environmental sustainability, another objective of this dissertation was to create an efficient biosorbent for arsenic cleanup. In CHAPTER 5, the baker's yeast was genetically engineered to express both the PC synthase (AtPCS) and cysteine desulfhydrase. The enhanced capability of the engineered yeast coexpressing both enzymes versus that of the yeast expressing only one enzyme was compared.

REFERENCES

1. **Bae, W., W. Chen, A. Mulchandani, and R. K. Mehra.** 2000. Enhanced bioaccumulation of heavy metals by bacterial cells displaying synthetic phytochelatins. *Biotechnol Bioeng* **70**:518–524.
2. **Bailey, J. E.** 1991. Toward a science of metabolic engineering. *Science* **252**:1668-1675.
3. **Bayer, E. A., J. P. Belaich, Y. Shoham, and R. Lamed.** 2004. THE CELLULOSOMES: Multienzyme Machines for degradation of Plant Cell Wall Polysaccharides. *Ann Rev Microbiol* **58**:521-554.
4. **Bayer, E. A., R. Lamed, and M. E. Himmel.** 2007. The potential of cellulases and cellulosomes for cellulosic waste management. *Curr Opin Biotechnol* **18**:237-245.
5. **Bayer, E. A., Y. Shoham, and R. Lamed.** 2000. Cellulose-decomposing prokaryotes and their enzyme systems. In *The Prokaryotes: An Evolving Electronic Resource for the Microbiological Community*, 3rd edition. Springer-Verlag, New York.
6. **Boer, V. M., S. L. Tai, Z. Vuralhan, Y. Arifin, M. C. Walsh, M. D. Piper, J. H. de Winde, J. T. Pronk, and J. M. Daran.** 2007. Transcriptional responses of *Saccharomyces cerevisiae* to preferred and nonpreferred nitrogen sources in glucose-limited chemostat cultures. *FEMS Yeast Res* **7**:604-20.
7. **Bryan, C. G., M. Marchal, F. Battaglia-Brunet, V. Kugler, C. Lemaitre-Guillier, D. Lievremont, P. N. Bertin, and F. Arsene-Pløetze.** 2009. Carbon and arsenic

- metabolism in *Thiomonas* strains: differences revealed diverse adaptation processes. BMC Microbiol **9**:127S.
8. **Cha, J., S. Matsuoka, H. Chan, H. Yukawa, M. Inui, and R. H. Doi.** 2007. Effect of multiple copies of cohesins on cellulase and hemicellulase activities of *Clostridium cellulovorans* mini-cellulosomes. J Microbiol Biotechnol **17**:1782-1788.
 9. **Chen, Y., P. Factor-Litvak, F. Parvez, J. Graziano, G. Howe, and H. Ahsan.** 2005. Association between lower-dose arsenic exposure from drinking water and high blood pressure in Bangladesh. Am J Epidemiol **161**:S30–S130.
 10. **Cherry, J. R., and A. L. Fidantsef.** 2003. Directed evolution of industrial enzymes: an update. Curr Opin Biotechnol **14**:438-443.
 11. **Cho, H. Y., H. Yukawa, M. Inui, R. H. Doi, and S. L. Wong.** 2004. Production of minicellulosomes from *Clostridium cellulovorans* in *Bacillus subtilis* WB800. Appl Environ Microbiol **70**:5704-5707.
 12. **Cobbett, C., and P. Goldsbrough.** 2002. Phytochelatins and metallothioneins: roles in heavy metal detoxification and homeostasis. Annu Rev Plant Biol **53**:159–182.
 13. **Cullen, W. R., and K. J. Reimer.** 1989. Arsenic speciation in the environment. Chem Rev **89**:713–764.
 14. **Dameron, C .T., and D. R. Winge.** 1990. Peptide-mediated formation of quantum semiconductors. Trends Biotechnol **8**:3–6.
 15. **Demain, A. L., M. Newcomb, and J. H. D. Wu.** 2005. Cellulase, Clostridia, and ethanol. Microbiol Mol Biol Rev **69**: 124-154.

16. **DeMarco, M. J., A. K. SenGupta, and J. E. Greenleaf.** 2003. Arsenic removal using a polymeric/inorganic hybrid sorbent. *Water Res* **37**:164–176.
17. **Den Haan, R., J. E. McBride, D. C. La Grange, L. R. Lynd, and W. H. Van Zyl.** 2007. Functional expression of cellobiohydrolases in *Saccharomyces cerevisiae* towards one-step conversion of cellulose to ethanol. *Enzyme Microb Technol* **40**:1291-1299.
18. **Den Haan, R., S. H. Rose, L. R. Lynd, W. H. van Zyl.** 2007. Hydrolysis and fermentation of amorphous cellulose by recombinant *Saccharomyces cerevisiae*. *Metab Eng* **9**:87-94.
19. **Di, L. S. Toppi, and R. Gabrielli.** 1999. Response to cadmium in higher plants. *Environ Exp Bot* **41**:105–130.
20. **Doi, R. H., and A. Kosugi.** 2004. Cellulosomes: plant-cell-wall-degrading enzyme complexes. *Nat Rev Microbiol* **2**:541-551.
21. **Fierobe, H. P., A. Mechaly, C. Tardif, A. Belaich, R. Lamed, Y. Shoham, J. P. Belaich, and E. A. Bayer.** 2001. Design and production of active cellulosome chimeras - Selective incorporation of dockerin-containing enzymes into defined functional complexes. *J Biol Chem* **276**:21257-21261.
22. **Fierobe, H. P., F. Mingardon, A. Mechaly, A. Belaich, M. T. Rincon, S. Pages, R. Lamed, C. Tardif, J. P. Belaich, and E. A. Bayer.** 2005. Action of designer cellulosomes on homogeneous versus complex substrates - Controlled incorporation of three distinct enzymes into a defined trifunctional scaffoldin. *J Biol Chem* **280**:16325-16334.

23. **Fleet, G. H., and D. J. Manners.** 1977. The enzymatic degradation of an alkali-soluble glucan from cell walls of *Saccharomyces cerevisiae*. *J Gen Microbiol* **98**: 315-327.
24. **Foyer, C. H., and G. Noctor.** 2005. Oxidant and antioxidant signalling in plants: a re-evaluation of the concept of oxidative stress in a physiological context. *Plant Cell Environ* **28**:1056–1071.
25. **Fujita, Y., I. Junji, M. Ueda, H. Fukuda, and A. Kondo.** 2004. Synergistic saccharification, and direct fermentation to ethanol, of amorphous cellulose by use of an engineered yeast strain codisplaying three types of cellulolytic enzyme. *Appl Environ Microbiol* **70**: 1207-1212.
26. **Gellissen, G., and C. P. Hollenberg.** 1997. Application of yeasts in gene expression studies: a comparison of *Saccharomyces cerevisiae*, *Hansenula polymorpha* and *Kluyveromyces lactis*—a review. *Gene* **190**:87–97
27. **Ghosh, A. S., A. K. Kar, and M. Kundu.** Impaired imipenem uptake associated with alterations in outer membrane proteins and lipopolysaccharides in imipenem-resistant *Shigella dysenteriae*. *J Antimicrob Chemother* **43**:195–201.
28. **Ghosh, M., J. Shen, and B. P. Rosen.** 1999. Pathways of As(III) detoxification in *Saccharomyces cerevisiae*. *Proc Natl Acad Sci USA* **96**:5001–5006.
29. **Goffeau, A., B. G. Barrell, H. Bussey, R. W. Davis, B. Dujon, H. Feldmann, F. Galibert, J. D. Hoheisel, C. Jacq, M. Johnston, E. J. Louis, H. W. Mewes, Y. Murakami, P. Philippsen, H. Tettelin, and S. G. Oliver.** 1996. Life with 6000 genes. *Science* **274**:546, 563–567.

30. **Graf, A., M. Dragosits, B. Gasser, and D. Mattanovich.** 2009. Yeast systems biotechnology for the production of heterologous proteins. *FEMS yeast Res* **9**:335-348.
31. **Guo, J. B., X. J. Dai, W. Z. Xu, and M. Ma.** 2008. Overexpressing GSH1 and AsPCS1 simultaneously increases the tolerance and accumulation of cadmium and arsenic in *Arabidopsis thaliana*. *Chemosphere* **72**:1020–1026.
32. **Heyman, A., Y. Barak, J. Caspi, D. B. Wilson, A. Altman, E. A. Bayer, and O. Shoseyov.** 2007. Multiple display of catalytic modules on a protein scaffold: nano-fabrication of enzyme particles. *J Biotechnol* **131**:433-439.
33. **Himmel, M. E., S.Y. Ding, D. K. Johnson, W. S. Adney, M. R. Nimlos, J. W. Brady, and T. D. Foust.** 2007. Biomass recalcitrance: engineering plants and enzymes for biofuels production. *Science* **315**:804-807.
34. **Jeon, E., J. E. Hyeon, D. J. Suh, Y. W. Suh, S. W. Kim, K. H. Song, and S. O. Han.** 2009. Production of cellulosic ethanol in *Saccharomyces cerevisiae* heterologous expressing *Clostridium thermocellum* endoglucanase and *Saccharomycopsis fibuligera* betaglucosidase genes. *Mol Cell* **28**:369-373.
35. **Kartinen, E. O., and C. J. Martin.** 1995. An overview of arsenic removal processes. *Desalination* **130**:79–88.
36. **Keasling J. D.** 2010. Manufacturing molecules through metabolic engineering. *Science* **330**:1355-1358.
37. **Kim, Y. J., K. S. Chang, M. R. Lee, J. H. Kim, C. E. Lee, Y. J. Jeon, J. S. Choi, H. S. Shin, and S. B. Hwang.** 2005. Expression of tobacco cDNA encoding

- phytochelatin synthase promotes tolerance to and accumulation of Cd and As in *Saccharomyces cerevisiae*. *J Plant Biol* **48**:440–447.
38. **Kneer, R., and M. H. Zenk.** 1997. The formation of Cd–phytochelatin complexes in plant cell cultures. *Phytochemistry* **44**:69–74.
 39. **Knowles, F. C., and A. A. Benson.** 1983. The biochemistry of arsenic. *Trends Biochem Sci* **8**:178–180.
 40. **Krumov, N., S. Oder, I. Perner-Nochta, A. Angelov, and C. Posten.** 2007. Accumulation of CdS nanoparticles by yeasts in a fed-batch bioprocess. *J Biotechnol* **132**:481–486.
 41. **Kuroda, K., and M. Ueda.** 2011. Cell surface engineering of yeast for applications in white biotechnology. *Biotechnol Lett* **33**:1-9.
 42. **Lipke, P. N., and J. Kaujan.** 1992. Sexual agglutination in budding yeasts: structure, function, and regulation of adhesion glycoproteins. *Microbiol Rev* **56**:180-194
 43. **Liu, S. X., M. Athar, I. Lippai, C. Waldren, and T. K. Hei.** 2001. Induction of oxyradicals by arsenic: implication for mechanism of genotoxicity. *Proc Natl Acad Sci USA* **98**:1643–1648.
 44. **Liu, Z. J., E. Boles, and B. P. Rosen.** 2004. Arsenic trioxide uptake by hexose permeases in *Saccharomyces cerevisiae*. *J Biol Chem* **279**:17312–17318.
 45. **Lynd, L. R., C. E. Wyman, and T. U. Gerngross.** 1999. Biocommodity engineering. *Biotechnol Prog* **15**:777-793.

46. **Lynd, L. R., J. H. Cushman, R. J. Nichols, and C. E. Wyman.** 1991. Fuel ethanol from cellulosic biomass. *Science* **251**: 1318-1323.
47. **Lynd, L. R., P. J. Weimer, W. H. van Zyl, and I. S. Pretorius.** 2002. Microbial cellulose utilization: fundamentals and biotechnology. *Microbiol Mol Biol Rev* **66**:506-577.
48. **Lynd, L. R., W. H. van Zyl, J. E. McBride, and M. Laser.** 2005. Consolidated bioprocessing of cellulosic biomass: an update. *Curr Opin Biotechnol* **16**:577-583.
49. **Maitani, T., H. Kubota, K. Sato, and T. Yamada.** 1996. The composition of metals bound to class III metallothionein (phytochelatin and its desglycyl peptide) induced by various metals in root cultures of *Rubia tinctorum*. *Plant Physiol* **110**:1145–1150.
50. **Mendoza-Cozatl, D. G., and R. Moreno-Sanchez.** 2005. Cd²⁺ transport and storage in the chloroplast of *Euglena gracilis*. *Biochim Biophys Acta Bioenerget* **1706**:88–97.
51. **Mendoza-Cozatl, D. G., J. S. Rodriguez-Zavala, S. Rodriguez-Enriquez, G. Mendoza-Hernandez, R. Briones-Gallardo, and R. Moreno-Sanchez.** 2006. Phytochelatin–cadmium–sulfide high-molecular-mass complexes of *Euglena gracilis*. *FEBS J* **273**:5703–5713.
52. **Merrifield, M. E., T. Ngu, and M. J. Stillman.** 2004. Arsenic binding to *Fucus vesiculosus* metallothionein. *Biochem Biophys Res Commun* **324**:127–132.

53. **Mingardon, F. A. Chanal, C. Tardif, E. A. Bayer, and H. P. Fierobe.** 2007. Exploration of new geometries in cellulosome-like chimeras. *Appl Environ Microbiol* **73**:7138-49.
54. **Mingardon, F., A. Chanal, A. M. Lopez-Contreras, C. Dray, E. A. Bayer, and H. P. Fierobe.** 2007. Incorporation of fungal cellulases in bacterial minicellulosomes yields viable, synergistically acting cellulolytic complexes. *Appl Environ Microbiol* **73**:3822-3832.
55. **Mitsuzawa, S., H. Kagawa, Y. Li, S.L. Chan, C. D. Paavola, and J. D. Trent.** 2009. The rosettazyme: a synthetic cellulosome. *J Biotechnol* **143**:139-44.
56. **Morais, S., A. Heyman, Y. Barak, J. Caspi, D. B. Wilson, R. Lamed, O. Shoseyov, and E. A. Bayer.** 2010. Enhanced cellulose degradation by nano-complexed enzymes: Synergism between a scaffold-linked exoglucanase and a free endoglucanase. *J Biotechnol* **147**:205-11.
57. **Morris, C. A., B. Nicolaus, V. Sampson, J. L. Harwood, and P. Kille.** 1999. Identification and characterization of a recombinant metallothionein protein from a marine alga, *Fucus vesiculosus*. *Biochem J* **338**:553–560.
58. **Mukhopadhyay, R., and B. P. Rosen.** 1998. *Saccharomyces cerevisiae* ACR2 gene encodes an arsenate reductase. *FEMS Microbiol Let* **168**:127–136.
59. **Mukhopadhyay, R., J. Shi, and B. P. Rosen.** 2000. Purification and characterization of Acr2p, the *Saccharomyces cerevisiae* arsenate reductase. *J Biol Chem* **275**:21149–21157.

60. **Murai, T., M. Ueda, T. Kawaguchi, M. Arai, and A. Tanaka.** 1998. Assimilation of cellooligosaccharides by a cell surface-engineered yeast expression β -glucosidase and carboxymethylcellulase from *Aspergillus aculeatus*. *Appl Environ Microbiol* **64**:4857-4861.
61. **Nakamura, Y., S. Shibasaki, M. Ueda, A. Tanaka, H. Fukuda, and A. Kondo.** 2001. Development of novel whole-cell immunoadsorbents by yeast surface display of the IgG-binding domain. *Appl Microbiol Biotechnol* **57**:500-505.
62. **Ngu, T. T., A. Easton, and M. J. Stillman.** 2008. Kinetic analysis of arsenic-metalation of human metallothionein: significance of the two-domain structure. *J Am Chem Soc* **130** :17016–17028.
63. **Nidhubhghail, O. M., and P. J. Sadler.** 1991. The structure and reactivity of arsenic compounds — biological-activity and drug design. *Struct Bond* **78**:129–190.
64. **Noctor, G.** 2006. Metabolic signalling in defence and stress: the central roles of soluble redox couples. *Plant Cell Environ* **29**:409–425.
65. **Oremland, R. S., T. R. Kulp, J. S. Blum, S. E. Hoefft, S. Baesman, L. G. Miller, and J. F. Stolz.** 2005. A microbial arsenic cycle in a salt-saturated, extreme environment. *Science* **308**:1305–1308.
66. **Ortiz, D. F., T. Ruscitti, K. F. McCue, and D. W. Ow.** 1995. Transport of metal-binding peptide by HMT1, a fission yeast ABC-type vacuolar membrane-protein. *J Biol Chem* **270**:4721–4728.

67. **Persson, B. L., J. Petersson, U. Fristedt, R. Weinander, A. Berhe, and J. Pattison.** 1999. Phosphate permeases of *Saccharomyces cerevisiae*: structure, function and regulation. *Biochim Biophys Acta Rev Biomembr* **1422**:255–272.
68. **Porro, D., M. Sauer, P Branduardi, and D Mattanovich.** 2005. Recombinant protein production in yeasts. *Mol Biotechnol* **31**:245-259.
69. **Rochette, E. A., B. C. Bostick, G. C. Li, and S. Fendorf.** 2000. Kinetics of arsenate reduction by dissolved sulfide. *Environ Sci Technol* **34**:4714–4720.
70. **Rosen, P.** 1971. Theoretical significance of arsenic as a carcinogen. *J Theor Biol* **32**: 425-426.
71. **Schmoger, M. E. V., M. Oven, and E. Grill.** 2000. Detoxification of arsenic by phytochelatins in plants. *Plant Physiol* **122**:793–801.
72. **Shibasaki, S., M. Ueda, T. Izuka, M. Hirayama, Y. Ikeda, M. Kamasawa, M. Osumi, and A. Tanaka.** Quantitative evaluation of the enhanced green fluorescent protein displayed on the cell surface of *Saccharomyces cerevisiae* by the fluorometric and confocal laser scanning microscopic analyses. *Appl Microbiol Biotechnol* **55**:471-475.
73. **Siewers, V., R. San-Bento, and J. Nielsen.** 2010. Implementation of communication-mediating domains for non-ribosomal peptide production in *Saccharomyces cerevisiae*. *Biotechnol Bioeng* **106**:841-844.
74. **Singh, S., W. Lee, and N. A. DaSilva.** 2008. A. Mulchandani and W. Chen, Enhanced arsenic accumulation by engineered yeast cells expressing *Arabidopsis thaliana* phytochelatin synthase. *Biotechnol Bioeng* **99**:333–340.

75. **Singhal, R. K., M. E. Anderson, and A. Meister.** 1987. Glutathione, a 1st line of defense against cadmium toxicity. *FEBS J* **1**:220–223.
76. **Tapio, S., and B. Grosche.** 2006. Arsenic in the aetiology of cancer. *Mutat Res Rev Mutat Res* **612**:215–246.
77. **Thomas, D., and Y. SurdinKerjan.** 1997. Metabolism of sulfur amino acids in *Saccharomyces cerevisiae*. *Microbiol Mol Biol Rev* **61**:503–512.
78. **Van Zyl H. W., L. R. Lynd, R. D. Haan, J. E. McBride.** 2007. Cosolidated bioprocessing for bioethanol production using *Saccharomyces cerevisiae*. *Adv Biochem Eng Biotechnol* **108**: 205-235.
79. **Wilson, D. B.** 2004. Studies of *Thermobifida fusca* plant cell wall degradation enzymes. *Chem Rec* **4**:72-82.
80. **Wunschmann, J., A. Beck, L. Meyer, T. Letzel, E. Grill, and K. J. Lenzian.** 2007. Phytochelatins are synthesized by two vacuolar serine carboxypeptidases in *Saccharomyces cerevisiae*. *FEBS Lett* **581**:1681–1687.
81. **Wysocki, R., C. C. Chery, D. Wawrzycka, M. Van Hulle, R. Cornelis, J. M. Thevelein, and M. J. Tamas.** 2001. The glycerol channel Fps1p mediates the uptake of arsenite and antimonite in *Saccharomyces cerevisiae*. *Mol Microbiol* **40**:1391–1401.
82. **Wysocki, R., P. Bobrowicz, and S. Ulaszewski.** 1997. The *Saccharomyces cerevisiae* ACR3 gene encodes a putative membrane protein involved in arsenite transport. *J Biol Chem* **272**:30061–30066.

83. **Wysocki, R., S. Clemens, D. Augustyniak, P. Golik, E. Maciaszczyk, M. J. Tamás, and D. Dziadkowiec.** 2003. Metalloid tolerance based on phytochelatins is not functionally equivalent to the arsenite transporter Acr3p. *Biochem Biophys Res Commun* **304**:293–300.
84. **Yanase, S, R. Yamada, S. Kaneko, H. Noda, T. Hasunuma, T. Tanaka, C. Ogino, H. Fukuda, A. Kond.** 2010. Ethanol production from cellulosic materials using cellulase-expressing yeast. *Biotechnol J* **5**:449-455.
85. **Zhang, Y. H. P., and L. R. Lynd.** 2004. Toward an aggregated understanding of enzymatic hydrolysis of cellulose: noncomplexed cellulose systems. *Biotechnol Bioeng* **88**:797-824.
86. **Zhang, Y. H. P., M. Himmel, J. R. Mielenz.** 2006. Outlook for cellulase improvement: Screening and selection strategies. *Biotechnol Adv* **24**:452–481.
87. **Zouboulis, A. I., and I. A. Katsoyiannis.** 2002. Arsenic removal using iron oxide loaded alginate beads. *Ind Eng Chem Res* **41**:6149–6155.

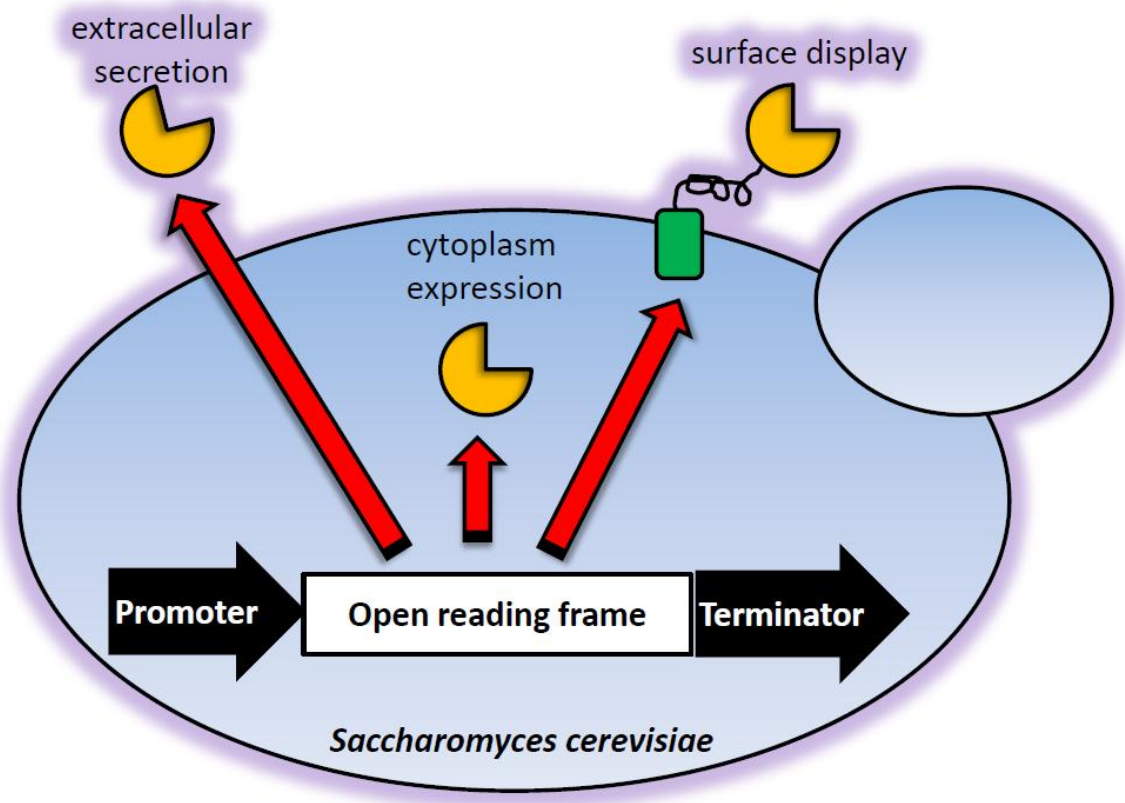


Figure 1.1. Potential strategies for genetically engineering yeasts

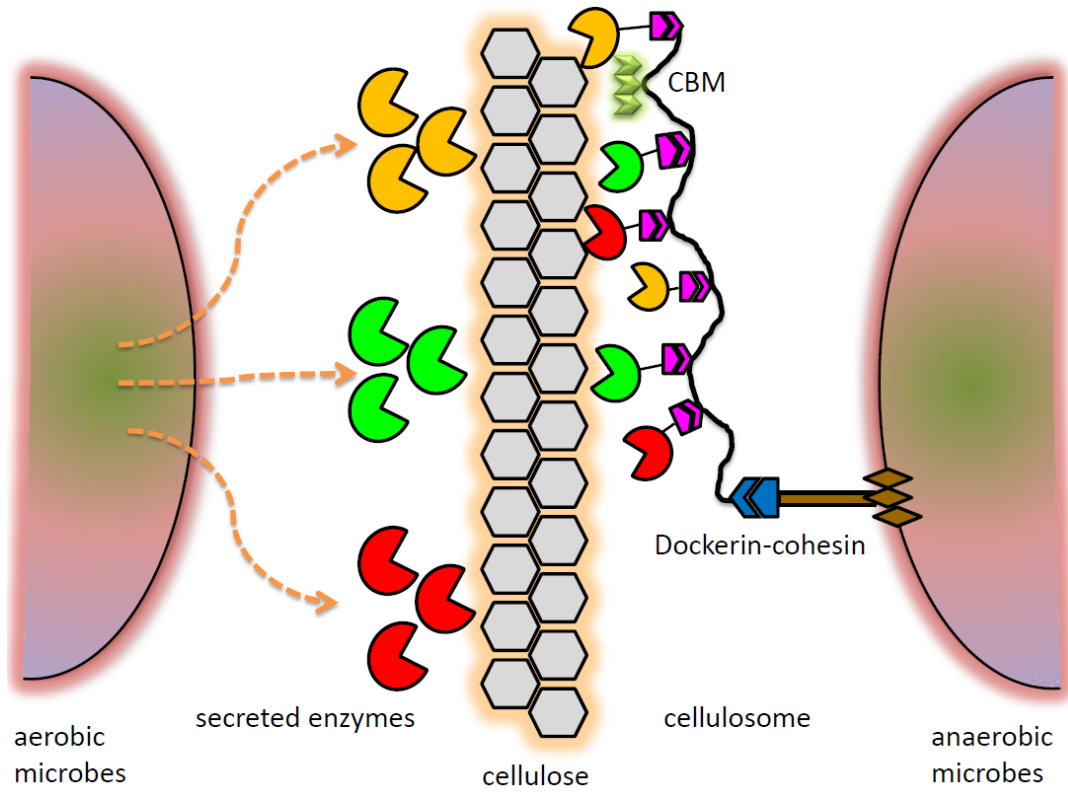


Figure 1.2. Native cellulolytic systems in (A) aerobic microorganisms and (B) anaerobic microorganisms.

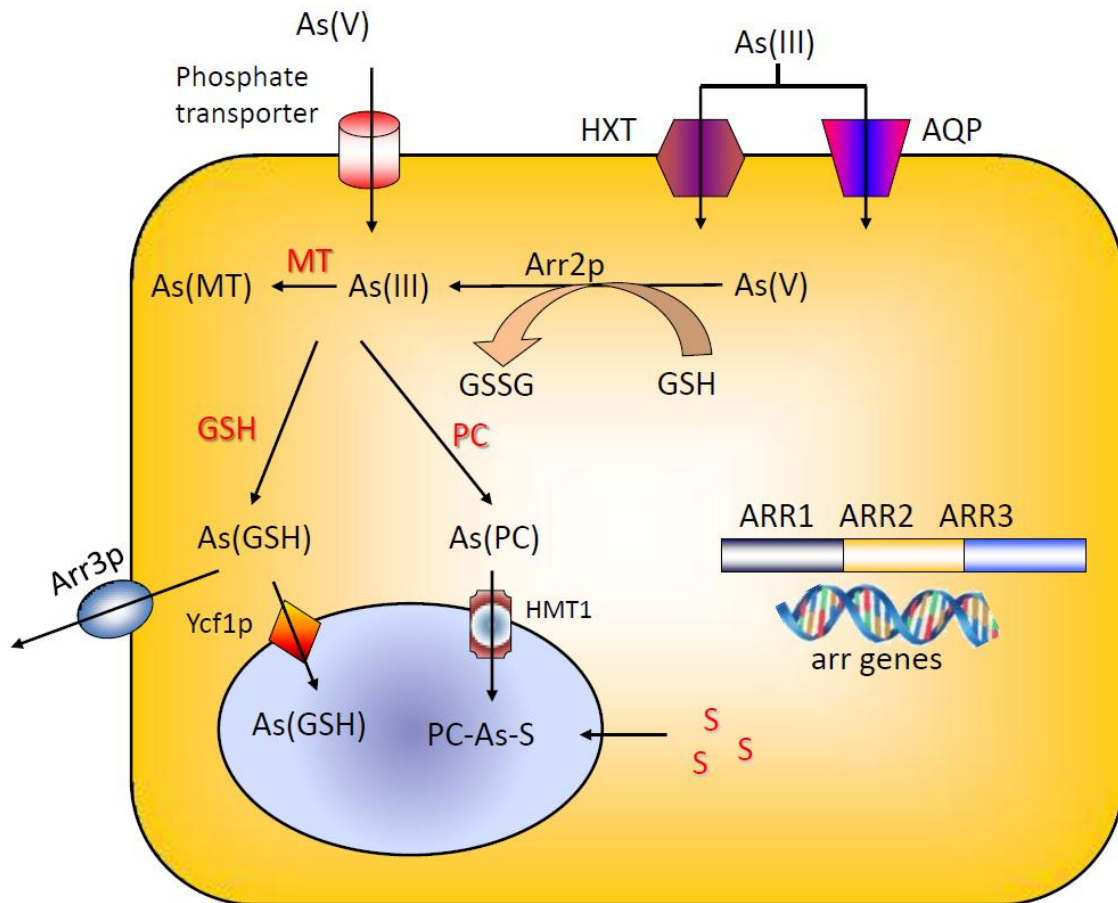


Figure 1.3. Arsenic metabolism in yeasts.

CHAPTER 2

Functional assembly of minicellulosomes on the *Saccharomyces cerevisiae* cell surface for cellulose hydrolysis and ethanol production

ABSTRACT

We demonstrated the functional display of a mini-scaffoldin on the yeast cell surface, consisting of three divergent cohesin domains from *Clostridium thermocellum* (t), *Clostridium cellulolyticum* (c) and *Ruminococcus flavefaciens* (f). Incubation with *E. coli* lysates containing an endoglucanase (CelA) fused with a dockerin domain from *C. thermocellum* (At), an exoglucanase (CelE) from *C. cellulolyticum* fused with a dockerin domain from the same species (Ec), and an endoglucanase (CelG) from *C. cellulolyticum* fused with a dockerin domain from *R. flavefaciens* (Gf) resulted in the assembly of a functional minicellulosome on the yeast surface. The displayed minicellulosome retained the synergistic effect for cellulose hydrolysis. When a β -glucosidase (BglA) from *C. thermocellum* tagged with the dockerin from *R. flavefaciens* was used in place of Gf, cells displaying the new mini-cellulosome exhibited significantly enhanced glucose liberation and produced ethanol directly from phosphoric acid swollen cellulose (PASC). The final ethanol concentration of 3.5 g/L was 2.6-fold higher than that using the same amounts of added purified cellulases. The overall yield was 0.49 g of ethanol produced per g of carbohydrate consumed, which corresponds to 95% of the theoretical value. This result confirms that simultaneous and synergistic saccharification and fermentation of cellulose to ethanol can be efficiently accomplished using a yeast strain displaying a functional minicellulosome containing all three required cellulolytic enzymes.

INTRODUCTION

Production of bioethanol from biomass has recently attracted attention due to the mandate for a billion gallons of renewable fuel by the new Energy Policy Act (Lynd et al., 2005). Current production processes using sugar cane and cornstarch are well established (Lynd et al., 1999; Lee et al., 2008). However, utilization of a cheaper substrate would render bioethanol more competitive with fossil fuel (Zaldivar et al., 2001). Cellulosic biomass found in many low value agricultural or wood pulping wastes is particularly well-suited because of its large-scale availability, low cost and environmentally benign production (Lynd et al., 1999). The primary obstacle impeding the more widespread production of ethanol from cellulose is the absence of a low-cost technology for overcoming its recalcitrant nature (Lynd et al., 2008).

Recently, a new method known as consolidated bioprocessing (CBP) has been proposed that combines enzyme production, cellulose saccharification and fermentation into a single process to dramatically reduce the cost for ethanol production (Lynd et al., 2005). An ideal microorganism for CBP should possess the capability for simultaneous cellulose saccharification and ethanol fermentation. One attractive candidate is *Saccharomyces cerevisiae*, which is widely used for industrial ethanol production due to its high ethanol productivity and high inherent ethanol tolerance (Nevoigt, 2008). Attempts have been made to engineer *S. cerevisiae* to hydrolyze cellulose (Cho et al., 1999; Curry et al., 1988; Haan et al., 2007). However, due to energetic limitations under anaerobic conditions, only a small amount of cellulases can often be secreted. An alternative is to display the cellulolytic enzymes on the yeast surface (Fujita et al., 2004;

2002). Up to three different cellulases have been displayed, permitting the hydrolysis of cellulose with concomitant ethanol production. While these results point to a potential strategy of combining the ethanol-producing capability with cellulose hydrolysis, the efficiency of hydrolysis must be significantly improved before it can be employed for practical applications.

Many anaerobic bacteria have developed an elaborately structured enzyme complex on the cell surface, called the cellulosome, to maximize the catalytic efficiency of cellulose hydrolysis using only a limited amount of enzymes (Bayer et al., 2004; Doi and Kosugi, 2004; Demain et al., 2005). The major component of these cellulosome complexes is a structural scaffoldin consisting of at least one cellulose binding domain (CBD) and repeating cohesin domains, which are docked individually with a different cellulase tagged with the corresponding dockerin domain (Shoham et al., 1999). Since the interaction between dockerin and cohesin is species specific (Pages et al., 1997; Haimovitz et al., 2008), designer mini-cellulosomes composed of three different dockerin/cohesion pairs have been generated with up to 6-fold higher efficiency in cellulose hydrolysis over similar free enzymes (Fierobe et al., 2005). Recently, it has been shown that the specific cellulose hydrolysis rates are more than 4-fold higher using metabolically active cultures of *C. thermocellum* displaying cellulosomes as compared to purified cellulosomes (Lu et al., 2006). This significant improvement appears to be a surface phenomenon involving adhesion onto the cellulose for enhanced substrate capture.

In the present study, we demonstrate the functional assembly of mini-cellulosomes onto the surface of *S. cerevisiae* and the subsequent feasibility for cellulosic

ethanol production using the engineered yeast strains. The success of displaying a functional cellulosome onto the surface of an organism that already produces high titers of ethanol could lay a foundation towards the goal of an industrially relevant CBP-enabling microorganism.

MATERIALS AND METHODS

Strains, plasmids, and media

Escherichia coli strain JM109 [endA1, recA1, gyrA96, thi, hsdR17 (rk⁻, mk⁺), relA1, supE44, Δ(lac-proAB)] was used as the host for genetic manipulations. *E. coli* BL21 (DE3) [F- ompT gal hsdSB (rB⁻ mB⁻) dcm lon λDE3] was used as production host for cellulase expressions. *Saccharomyces cerevisiae* strain EBY100 [MATa AGA1::GAL1-AGA1::URA3 ura3-52 trp1 leu2-1 his3-200 pep4::HIS3 prb1-1.6R can1 GAL] was used for surface display of scaffoldins. All *E. coli* cultures were grown in Luria-Bertani (LB) medium (10.0 g/L tryptone, 5.0 g/L yeast extract, 10.0 g/L NaCl), supplemented with either 100 μg/mL ampicillin or 50 μg/mL karamycin. All yeast cultures were grown in SDC medium (20.0 g/L dextrose, 6.7 g/L yeast nitrogen base without amino acids, 5.0 g/L casamino acids).

To display scaffoldins, a gene fragment coding for a scaffoldin containing three cohesins from *C. cellulolyticum*, *C. thermocellum* and *R. flavefaciens* and one cellulose binding domain was amplified using plasmid pETscaf6 (Fierobe et al., 2005) as the template with the forward primer F1NdeI (5'– TATAGCTAGCGGCGATTCTCTTAAAGTTACAGT -3') and the reverse primer R1SalI (5'– ATATGTCGACGTGGTGGTG-GTGGTG -3'). The PCR product was then digested and ligated into the surface display vector pCTCON2 (Boder and Wittrup, 1997) to form pScaf-ctf. Similar procedures, except for changing the reverse primers to RASalI (5'– ATATGTCGACATCTGACGGCGGTATTGTTGTTG -3') and RBSalI (5'– ATATGTCGACTATATCTCCAACAT-TTACTCCAC -3'), were used for the construction of pScaf-c and pScaf-ct.

Plasmids pETec (Gaudin et al., 2000) and pETGf (Fierobe et al., 2005), encoding the exoglucanase CelE and endoglucanase CelG of *C. cellulolyticum* fused to the dockerin from *C. cellulolyticum* and *C. thermocellum*, respectively, were kindly given by H.-P. Fierobe (CNRS, France). Plasmid pETAf encoding a His6-tagged endoglucanase CelA and a dockerin from *C. thermocellum* was obtained by PCR from pCelA using the forward primer F2NdeI (5'- ATATCATATGGCAGGTGTGCCTTTTAACACAAA -3') and the reverse primer R2XhoI (5'- ATATCTCGAGCTAATAAGGTAGGTGGGG -3'). The amplified fragment was cloned in to NdeI-XhoI linearized plasmid pET24a to form pETAf. Plasmid pBglAf encoding a His6-tagged dockerin from *R. flavefaciens* fused to a β -glucosidase BglA from *C. thermocellum* was obtained by two-step cloning. First, a gene fragment coding for the His6-tagged dockerin of *R. flavefaciens* was obtained from pETGf by digesting with BamHI and XhoI and ligated into pET24a to form pETDf. The gene fragment of BglA was amplified by PCR from pBglA using the forward primer F3NdeI (5'- ATATCATATGTCAAAGATAACTTTCCCAAAA -3') and the reverse primer R3BglIII (5'- ATATAGATCTTTAAAAACCGTTGTTTTTGATTACT -3'), and inserted into a NdeI-BamHI linearized pETDf to form pBglAf. A summary of all of the scaffoldins and dockerin-tagged cellulases used in this study is listed in Table 2.1.

Display of scaffoldins on the yeast cell surface

For the display of scaffoldins on the yeast surface, yeast cells harboring pScaf#3, pScaf#2, or pScaf#1 were precultured in SDC medium for 18 h at 30°C. These precultures were sub-inoculated into 200 mL SGC medium (20.0 g/L galactose, 6.7 g/L

yeast nitrogen base without amino acids, 5.0 g/L casamino acids) at an optical density (OD₆₀₀) of 0.1 and grown for 48 h at 20°C.

Expression and purification of dockerin-tagged cellulases

E. coli strains expressing At, Ec, and Gf were pre-cultured overnight at 37°C in LB medium supplemented with appropriate antibiotics. The pre-cultures were sub-inoculated in 200 mL LB medium supplemented with 1.5% glycerol and appropriate antibiotics at an initial OD of 0.01 and incubated at 37°C until the O.D. reached 1.5. The cultures were then cooled to 20°C, and isopropyl thio-β-D-galactoside (IPTG) was added to a final concentration of 200 μM. After 16 h, cells were harvested by centrifugation (3000Xg, 10 min) at 4°C, resuspended in buffer A (50 mM Tris-HCl pH 8.0, 100 mM NaCl, and 10 mM CaCl₂), and lysed with a sonicator. The different cellulases were purified using a His-Binding Resin (Novagen) at 4°C.

Minicellulosome Assembly on the yeast cell surface

To assemble the mini-cellulosomes, either cell lysates containing dockerin-tagged cellulases or purified cellulases were incubated with yeast cells displaying the scaffoldin for 1 h at 4°C in buffer A. After incubation, cells were washed and harvested by centrifugation (3000Xg, 10 mins) at 4°C and resuspended in the same buffer for further use.

Immunofluorescence microscopy

Yeast cells displaying scaffoldins or the mini-cellulosomes on the surface were harvested by centrifugation, washed with PBS buffer (8 g/L NaCl, 0.2 g/L KCl, 1.44 g/L Na₂HPO₄, 0.24 g/L KH₂PO₄), and resuspended in 250 μ L of PBS buffer containing 1 mg/mL BSA, and 0.5 μ g of anti-C-Myc or anti-C-His IgG (Invitrogen) for 4 h with occasional mixing. Cells were then pelleted and washed with PBS before resuspending in PBS buffer plus 1 mg/mL BSA and 0.5 μ g anti-mouse IgG conjugated with Alexa 488 (Molecular Probes). After incubating for 2 h, cells were pelleted and washed twice with PBS, followed by resuspension in PBS buffer to an OD₆₀₀ of 1. For fluorescence microscopy (Olympus BX51), 5-10 μ L of cell suspensions were spotted on slides and a cover slip was added. Images from Alexa 488 were captured using the QCapture Pro6 software. Whole cell fluorescence was measured using a fluorescent microplate reader (Synergy4, BioTek, VT) with an excitation wavelength at 485 nm and an emission wavelength at 535 nm.

Enzyme assays

Carboxymethyl cellulose (CMC) was obtained from Sigma and used as a substrate. Phosphoric acid swollen cellulose (PASC) was prepared from Avicel PH101 (Sigma) according to the method of Walseth (1952). Enzyme activity was assayed in the presence of a 0.3% (wt/vol) concentration of cellulose at 30°C in 20 mM Tris-HCl buffer (pH 6.0). Samples were collected periodically and immediately mixed with 3 mL of DNS reagents (10 g/L dinitrosalicylic acid, 10 g/L sodium hydroxide, 2 g/L phenol, 0.5 g/L sodium sulfite). After incubating at 95°C for 10 minutes, 1 mL of 40% Rochelle salts was

added to fix the color before measuring the absorbance of the supernatants at 575 nm. Glucose concentration was determined using a glucose HK assay kit from Sigma.

Fermentation

Fermentation was conducted anaerobically at 30°C. Briefly, yeast cells were washed once with buffer containing 50 mM Tris-HCl, pH 8.0, 100 mM NaCl, and 10 mM CaCl₂ and resuspended in SDC medium containing 6.7 g/L yeast nitrogen base without amino acids, 20 g/L casamino acids, and 10 g/L PASC as the sole carbon source. Reducing sugars and glucose concentration were measured by the methods described above. The amount of residual cellulose was measured by the phenol-sulfuric acid method as described by Dubois et al. (1956). Ethanol concentration was measured by the gas chromatography (model 6890, Hewlett Packard, USA) using a flame ionization detector and HP-FFTP column.

RESULTS

Functional display of mini-scaffoldins on yeast surface

Previously, several highly synergistic designer mini-cellulosomes that are able to hydrolyze cellulose up to 6-fold faster than free enzymes were created (Fierobe et al., 2005). We reasoned that significant improvements in both cellulose hydrolysis and ethanol production can be achieved if a similar mini-cellulosome can be assembled onto the yeast surface. A plasmid coding for a trifunctional scaffoldin (Scaf-ctf) consisting of an internal CBD flanked by three divergent cohesin domains from *C. thermocellum* (T), *C. cellulolyticum* (C) and *R. flavefaciens* (F) (Figure 2.1) was created for surface display. To further demonstrate the specificity among the different dockerin/cohesion pairs, two smaller scaffoldins, Scaf-c containing a cohesin domain from *C. cellulolyticum* followed by a CBD, and Scaf-ct containing an additional cohesin domain from *C. thermocellum* at the C-terminus of the CBD were generated (Figure 2.1). The different scaffoldins were displayed onto the yeast surface using the glycosylphosphatidylinositol (GPI)-anchor (Boder and Wittrup, 1997) linked at the N-terminal side of the scaffoldins. A c-Myc tag was added to the C-terminus of all the scaffoldins to allow detection using anti-c-Myc serum.

To probe the surface localization of the scaffoldin, immunofluorescent labeling of cells was carried out using anti-c-Myc serum and Alexa 488 conjugated goat anti-mouse IgG. Cells displaying the scaffoldin domains were brightly fluorescence (Figure 2.2A), while no fluorescence was observed for the control yeast cells (EBY100). Since

monoclonal antibodies are not able to penetrate the cell wall, the fluorescence images confirmed that the scaffoldins are displayed on the cell surface.

Functionality of the displayed scaffoldins

To investigate the functionality of the displayed scaffoldins, an exoglucanase (CelE) from *C. cellulolyticum* fused with a dockerin domain from the same species (Ec), an endoglucanase (CelG) from *C. cellulolyticum* fused with a dockerin domain from *R. flavefaciens* (Gf), and an endoglucanase (CelA) fused with a dockerin domain from *C. thermocellum* (At). A His6 tag was added to the C-terminus of all the dockerin domains for detection of the assembly. Cells displaying scaffoldins on the surface were incubated directly with *E. coli* cell lysates containing At, Ec, or Gf for 1 h to form the cellulosome complex. Presence of each cellulase-dockerin pair on cells displaying Scaf-ctf was confirmed by immunofluorescence microscopy using the anti-His6 antibody (Figure 2.2B).

To demonstrate the specificity of different cohesin/dockerin pairs, similar experiments were performed with cells displaying either Scaf-ct or Scaf-c. For Scaf-ct displaying cells, fluorescence was detected only in the presence of Ec or At, whereas incubation with Gf did not result in any detectable fluorescence (Figure 2.2C). Similarly, for Scaf-c displaying cells, fluorescence was only observed in the presence of Ec (Figure 2.2D). These results confirm that the specificity of the cohesins is preserved even when displayed on the surface as only the corresponding dockerin-tagged enzymes are assembled correctly.

Functionality of the displayed mini-cellulosomes

To demonstrate the functionality of the assembled mini-cellulosomes, cells expressing scaf-ctf were first saturated with different combinations of Ec, At, and/or Gf. As depicted in Figure 2.3, a similar level of fluorescence was detected from the c-Myc tag and His6 tag when only one dockerin-tagged enzyme was added indicating the correct 1:1 binding between the cohesin/dockerin pairs. More importantly, a corresponding increase in the fluorescent intensity was observed when an increasing number of enzymes were docked onto scaf-ctf. This result confirms that the correct 1:1 binding ratio between each dockerin/cohesin pair was preserved even when assembled into a three-enzyme mini-cellulosome on the cell surface (Figure 2.3).

Engineered yeast cells docked with different combination of cellulases were used to further examine the functionality for cellulose hydrolysis. Cells were resuspended in Tris buffer containing carboxymethyl cellulose (CMC) and the rate of reducing sugar production was determined. As shown in Figure 2.4, cells with any one of the three cellulases docked on the surface showed visible differences in cellulose hydrolysis than the control. Among them, At had the highest rate of hydrolysis, followed by Gf, and Ec, a trend consistent with the relatively low activity of the exoglucanase CelE on CMC (Gaudinet al., 2000). The rate of CMC hydrolysis increased in an additive fashion when two of the cellulases were docked on the surface, and the fastest rate of hydrolysis was observed when all three cellulases were assembled. The additive effect on CMC

hydrolysis confirms that the recruitment of cellulases into the displayed scaffoldin has very minimum effect on their individual functionality.

Synergistic effect of displayed mini-cellulosomes

The synergistic effect on cellulose hydrolysis is the most intriguing property of naturally occurring cellulosomes. To test whether the synergistic effect of the mini-cellulosome structure was preserved when displayed on the yeast surface, avicel hydrolysis was compared with purified cellulases. In this case, the amount of each cellulase docked onto scaf-ctf was first determined from the binding experiments. These pre-determined amounts of cellulases were then mixed together and the hydrolysis of avicel using the cellulase mixture was compared with whole cells displaying the functional cellulosome containing the same amount of each cellulase. As shown in Table 2.2, the level of reducing sugar production was consistently higher for cells displaying the cellulosome, confirming that synergy was indeed maintained (Fierobe et al., 2005). More importantly, the level of synergy increased from 1.62 to 2.44 when the number of cellulases recruited in the mini-cellulosome system increased from one to three. This result suggests the potential to further enhance cellulose hydrolysis by increasing the number of displayed cellulases.

Incorporation of β -glucosidase into the mini-cellulosome

Since *S. cerevisiae* is unable to transport and utilize oligosaccharides, directing the complete hydrolysis of cellulose to glucose is essential. To achieve this goal, a β -

glucosidase (BglA) from *C. thermocellum* tagged with the dockerin from *R. flavefaciens* was constructed. Figure 2.5 shows the time course of reducing sugar and glucose released from PASC using different enzyme combinations docked onto the cell surface. Although over 40% of the PASC was hydrolyzed in the presence of the endoglucanase At, less than 25% of the reducing sugar was further hydrolyzed to glucose. In comparison, presence of the exoglucanase Ec not only enhanced reducing sugar production but also increased glucose production by 3-fold. The addition of BglA further improved the rate of glucose liberation although no difference in reducing sugar formation was observed. This result is very significant as we demonstrated, for the first time, that a functional mini-cellulosome containing all three exoglucanase, endoglucanase, and β -glucosidase activities can be successfully assembled on the surface of a heterologous host. Our result also confirms the important role of β -glucosidase in achieving a higher conversion of cellulose to glucose. More importantly, the displayed mini-cellulosome exhibited significant synergy in both reducing sugar and glucose liberation when compared to free enzymes. It should be noted that the modest improvement in glucose formation by BglA is the result of glucose inhibition, a known behavior for many β -glucosidase including BglA (Demain et al., 2005, Wong, 1995).

Direct fermentation of amorphous cellulose to ethanol

The ability of ethanol fermentation from PASC was examined by using the scaffoldin-displaying strains docked with different cellulases. As shown in Figure 5.6, the increase in ethanol production was accompanied by a concomitant decrease in the total

sugar concentration. The level of ethanol production and PASC hydrolysis were directly correlated to the number of cellulases docked onto the surface. The maximum ethanol production for cells displaying At, Ec, and BglA was 3.5 g/L after 48 h. This corresponds to 95% of the theoretical ethanol yield at 0.49 g ethanol/g sugar consumed. Moreover, the glucose concentrations during the fermentation were below the detection limit. This indicates all the glucose produced was quickly consumed, resulting in no detectable glucose accumulation in the medium. The level of ethanol production for cells displaying all three cellulases was higher than cells displaying only At and Ec, again confirming the importance of β -glucosidase in the overall cellulose to ethanol conversion. More importantly, the synergistic effect of the mini-cellulosome was also observed as the ethanol production was more than 3-fold lower from a culture using the same amounts of purified At, Ec, and BglA added to the medium.

DISCUSSION

Biomass represents an inexpensive feedstock for sustainable bioethanol production. Among the three biological events occurred during conversion of cellulose to ethanol: enzyme production, polysaccharide hydrolysis and sugars fermentation, cellulose hydrolysis is widely recognized as the key step to make bioconversion economically competitive (Lynd et al., 2008). In addition, it is believed that significant cost reduction can be achieved when two or more steps are combined, such as in CBP (Lynd et al., 2005). To achieve this goal, we demonstrated the functional assembly of a minicellulosome on the yeast surface to render the ethanologenic microbe cellulolytic.

First, a chimeric minicellulosome containing three dockerin/cohesin pairs from different species was assembled on the yeast surface. Although similar minicellulosomes have been shown to hydrolyze cellulose with high synergy *in vitro* (Fierobe et al., 2005), successful demonstration for *in vivo* systems has never been achieved. Immunofluorescence microscopy showed the successful translocation of the mini-scaffoldin on the yeast surface, and the functionality of the cohesin domains were retained by observing the successful assembly of the corresponding dockerin-tagged cellulases. Since the specificity of the dockerin/cohesin pairs is preserved, suggesting that it may be possible to direct any enzymatic subunit to a specified position within a modular scaffoldin by tagging with the designated dockerin.

Another interesting property for using cellulosome is its synergistic effect on cellulose hydrolysis comparing with free enzymes. Recent studies (Fierobe et al., 2002; Bayer et al., 2007) suggest that the close proximity and ordering of the enzyme

components appear to be the key. In the present study, the displayed mini-cellulosome retained this key characteristic. Interestingly, the level of synergy increased with an increasing number of cellulases docked onto the surface. Cha and colleagues tested the effect of multiple copies of cohesin on the cellulase activities of different mini-cellulosomes, and reported an increase in synergy with increasing numbers of cohesins (Cha et al., 2007). This synergistic effect was preserved even when a new mini-cellulosome composed of a β -glucosidase BglA, an endoglucanase At and an exoglucanase Ec was assembled on the yeast surface.

To further demonstrate the superiority of using the displayed cellulosome for ethanol production, cellulose hydrolysis and ethanol production was tested using both free enzymes and displayed minicellulosomes. Independent of the number of cellulases incorporated in the minicellulosome, similar levels of enhancement in cellulose hydrolysis as well as ethanol production were detected. The ethanol production, in particular, was more than 2.6-fold higher than the culture when all three cellulases were added as free enzymes. This when combined with the close to 95% theoretical ethanol yield make this an efficient process for direct fermentation of cellulose to ethanol.

In conclusion, a minicellulosome composed of exoglucanase, endoglucanase, and β -glucosidase activities was successfully assembled on the yeast surface for the first time. The possibility of displaying enzymes based on the interaction between a displayed anchoring domain and secreted enzymes has recently been reported (Ito et al., 2009). We are currently working on secreting all three cellulases into the medium to enable their direct assembly into a functional minicellulosomes on the yeast surface.

REFERENCES

1. **Bayer, E. A., J. P. Belaich, Y. Shoham, and R. Lamed.** 2004. The cellulosomes: Multienzyme machines for degradation of plant cell wall polysaccharides. *Annu Rev Microbiol* **58**:521-554.
2. **Bayer, E. A., R. Lamed, and M. E. Himmel.** 2007. The potential of cellulases and cellulosomes for cellulosic waste management. *Curr Opin Biotechnol* **18**:237-245.
3. **Boder, E. T., and K. D. Wittrup.** 1997. Yeast surface display for screening combinatorial polypeptide libraries. *Nat Biotechnol* **15**:553-557.
4. **Cha, J., S. Matsuoka, H. Chan, H. Yukawa, M. Inui, and R. H. Doi.** 2007. Effect of multiple copies of cohesins on cellulase and hemicellulase activities of *Clostridium cellulovorans* mini-cellulosomes. *J Microbiol Biotechnol* **17**:1782-1788.
5. **Chao, G., W. L. Lau, B. J. Hackel, S. L. Sazinsky, S. M. Lippow and K. D. Wittrup.** 2006. Isolating and engineering human antibodies using yeast surface display. *Nat Protocols* **1**:755 – 768.
6. **Cho, K. M., Y. J. Yoo, and H. S. Kang.** 1999. δ -Integration of endo/exo-glucanase and beta-glucosidase genes into the yeast chromosomes for direct conversion of cellulose to ethanol. *Enzyme Microb Technol* **25**:23-30.
7. **Curry, C., N. Gilkes, G. O'Neill, R. C. Miller, and N. Skipper.** 1988. Expression and secretion of a cellulomonas-fimi exoglucanase in *Saccharomyces cerevisiae*. *Appl Environ Microbiol* **54**:476-484.

8. **Demain, A. L., M. Newcomb, and J. H. D. Wu.** 2005. Cellulase, clostridia, and ethanol. *Microbiol Mol Biol Rev* **69**:124-154.
9. **Doi, R. H., and A. Kosugi.** 2004. Cellulosomes: Plant-cell-wall-degrading enzyme complexes. *Nat Rev Microbiol* **2**:541-551.
10. **Dubois, M., K. A. Gilles, J. K. Hamilton, P. A. Rebers and F. Smith.** 1956. Colorimetric method for determination of sugars and related substances, *Anal Chem* **28**: 350–356.
11. **Fierobe, H. P., E. A. Bayer, C. Tardif, M. Czjzek, A. Mechaly, A. Belaich, R. Lamed, Y. Shoham, and J. P. Belaich.** 2002. Degradation of cellulose substrates by cellulosome chimeras - Substrate targeting versus proximity of enzyme components. *J Biol Chem* **277**:49621-49630.
12. **Fierobe, H. P., F. Mingardon, A. Mechaly, A. Belaich, M. T. Rincon, S. Pages, R. Lamed, C. Tardif, J. P. Belaich, and E. A. Bayer.** 2005. Action of designer cellulosomes on homogeneous versus complex substrates - Controlled incorporation of three distinct enzymes into a defined trifunctional scaffoldin. *Biol Chem* **280**:16325-16334.
13. **Fujita, Y., S. Takahashi, M. Ueda, A. Tanaka, H. Okada, Y. Morikawa, T. Kawaguchi, M. Arai, H. Fukuda, and A. Kondo.** 2002. Direct and efficient production of ethanol from cellulosic material with a yeast strain displaying cellulolytic enzymes. *Appl Environ Microbiol* **68**:5136-5141.
14. **Fujita Y, I. Junji, M. Ueda, H. Fukuda, and A. Kondo.** 2004. Synergistic saccharification, and direct fermentation to ethanol, of amorphous cellulose by

use of an engineered yeast strain codisplaying three types of cellulolytic enzyme. *Appl Environ Microbiol* **70**: 1207-1212.

15. **Gaudin, C., A. Belaich, S. Champ, and J. P. Belaich.** 2000. CelE, a multidomain cellulase from *Clostridium cellulolyticum*: a key enzyme in the cellulosome. *J Bacteriol* **182**:1910–1915.
16. **Haan, R. D., S.H. Rose, L.R. Lynd, and W.H. van Zyl.** 2007. Hydrolysis and fermentation of amorphous cellulose by recombinant *Saccharomyces cerevisiae*. *Metab Eng* **9**: 87-94.
17. **Haimovitz R., Y. Barak, E. Morag, M. Voronov-Goldman, Y. Shoham, R. Lamed, and E. A. Bayer.** 2008. Cohesin-dockerin microarray: Diverse specificities between two complementary families of interacting protein modules. *Proteomics* **8**: 968-979.
18. **Ito, J., A. Kosugi, T. Tanaka, K.i Kuroda, S. Shibasaki, C. Ogino, M. Ueda, H. Fukuda, R. H. Doi, and A. Kondo.** 2009. Regulation of the Display Ratio of Enzymes on the *Saccharomyces cerevisiae* Cell Surface by the Immunoglobulin G and Cellulosomal Enzyme Binding Domains. *Appl Environ Microbiol* **75**: 4149-415.
19. **Lee, J. S., B. Parameswaran, J. P. Lee, and S. C. Park.** 2008. Recent developments of key technologies on cellulosic ethanol production. *J Sci Ind Res* **67**:865-873.

20. **Lu, Y. P., Y. H. P. Zhang, and L. R. Lynd.** 2006. Enzyme-microbe synergy during cellulose hydrolysis by *Clostridium thermocellum*. *Proc Natl Acad Sci USA* **103**:16165-16169.
21. **Lynd, L. R., M. S. Laser, D. Bransby, B. E. Dale, B. Davison, R. Hamilton, M. Himmel, M. Keller, J. D. McMillan, J. Sheehan, and C. E. Wyman.** 2008. How biotech can transform biofuels. *Nat. Biotechnol.* **26**:169-172.
22. **Lynd, L. R., W. H. van Zyl, J. E. McBride, and M. Laser.** 2005. Consolidated bioprocessing of cellulosic biomass: an update. *Curr Opin Biotechnol* **16**:577-583.
23. **Lynd, L. R., C. E. Wyman, and T. U. Gerngross.** 1999. Biocommodity engineering. *Biotechnol Prog* **15**:777-793.
24. **Nevoigt, E.** 2008. Progress in metabolic engineering of *Saccharomyces cerevisiae*. *Microbiol Mol Biol Rev* **72**:379-412.
25. **Pages, S., A. Belaich, J. P. Belaich, E. Morag, R. Lamed, Y. Shoham, and E. A. Bayer.** 1997. Species-specificity of the cohesin-dockerin interaction between *Clostridium thermocellum* and *Clostridium cellulolyticum*: Prediction of specificity determinants of the dockerin domain. *Proteins-Structure Function and Genet* **29**:517-527.
26. **Shoham, Y., R. Lamed, and E. A. Bayer.** 1999. The cellulosome concept as an efficient microbial strategy for the degradation of insoluble polysaccharides. *Trends Microbiol* **7**:275-281.

27. **Walseth, C. S.** 1952. Occurrence of cellulases in enzyme preparations from microorganisms, *TAPPI J.* **35**: 228–233.
28. **Wong, D. W. S.** 1995. *Food Enzymes- Structure and Mechanisms*, 1st ed. Springer.
29. **Zaldivar, J., J. Nielsen, and L. Olsson.** 2001. Fuel ethanol production from lignocellulose: a challenge for metabolic engineering and process integration. *Appl Microbiol Biotechnol* **56**:17-34.

Table 2.1. Scaffoldins and dockerin-tagged cellulases used in this study

Protein name	Description (from N terminus to C terminus)	Host cell	Tag
Scaf-c	Scaffoldin containing a cohesin from <i>C. cellulolyticum</i> followed by a CBD	<i>S. cerevisiae</i>	c-Myc
Scaf-ct	Scaffoldin containing a cohesin from <i>C. cellulolyticum</i> followed by a CBD followed by a second cohesin from <i>C. thermocellum</i>	<i>S. cerevisiae</i>	c-Myc
Scaf-ctf	Scaffoldin containing a cohesin from <i>C. cellulolyticum</i> followed by a CBD followed by a second cohesin from <i>C. thermocellum</i> and a third cohesin from <i>R. flavefaciens</i>	<i>S. cerevisiae</i>	c-Myc
At	Endoglucanase CelA from <i>C. thermocellum</i> fused with its native dockerin	<i>E. coli</i>	c-His6
Ec	Exoglucanase CelE from <i>C. cellulolyticum</i> fused with its native dockerin	<i>E. coli</i>	c-His6
Gf	Endoglucanase CelG from <i>C. cellulolyticum</i> fused with a dockerin from <i>R. flavefaciens</i>	<i>E. coli</i>	c-His6
BglA	β -Glucosidase BglA from <i>C. thermocellum</i> fused with a dockerin from <i>R. flavefaciens</i>	<i>E. coli</i>	c-His6

Table 2.2. Amount of reducing sugars released from Avicel after 24 h of incubation at 30°C either by cells displaying cellulosomes or by the same amount of free enzymes^a.

Cellulase (s)	Reducing sugars (mg/liter) released from:		Degree of synergy
	cellulosome	Free enzymes	
At	46.1	28.3	1.62
At+Ec	80.1	37.6	2.13
At+Ec+Gf	132.3	54.2	2.44

^a Reactions were conducted either with different cellulase pairs (CelE-Dc [Ec], CelA-Dt [At], or CelG-Df [Gf]) docked on the displayed Scaf-ctf or with the corresponding purified cellulases. The degree of synergy is defined as the amount of sugar released from the cellulosome over the amount of sugar released from free enzymes.

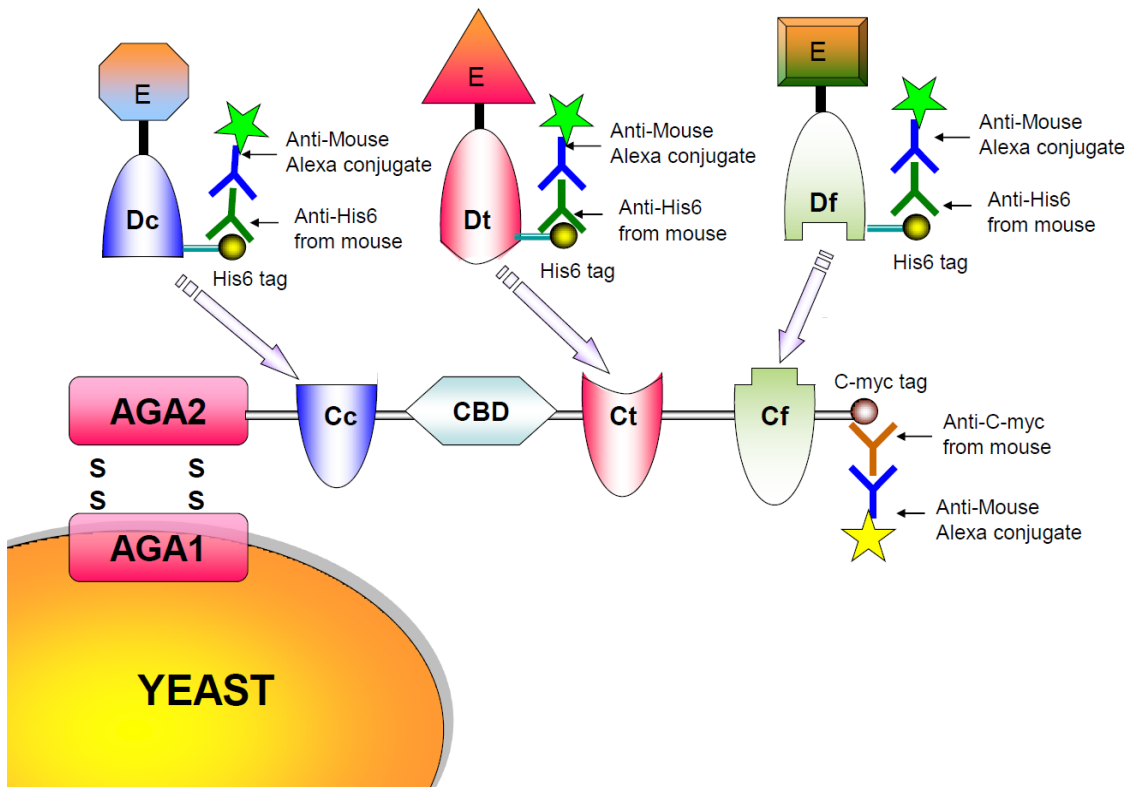


Figure 2.1. Functional assembly of minicellulosomes on the yeast cell surface. A trifunctional scaffoldin (Scaf-ctf) consisting of an internal CBD flanked by three divergent cohesin (C) domains from *C. thermocellum* (t), *C. cellulolyticum* (c), and *R. flavefaciens* (f) was displayed on the yeast cell surface. Three different cellulases (E1, E2, and E3) fused with the corresponding dockerin domain (either Dt, Dc, or Df) were expressed in *E. coli*. Cell lysates containing these cellulases were mixed with yeast cells displaying Scaf-ctf for the functional assembly of the minicellulosome.

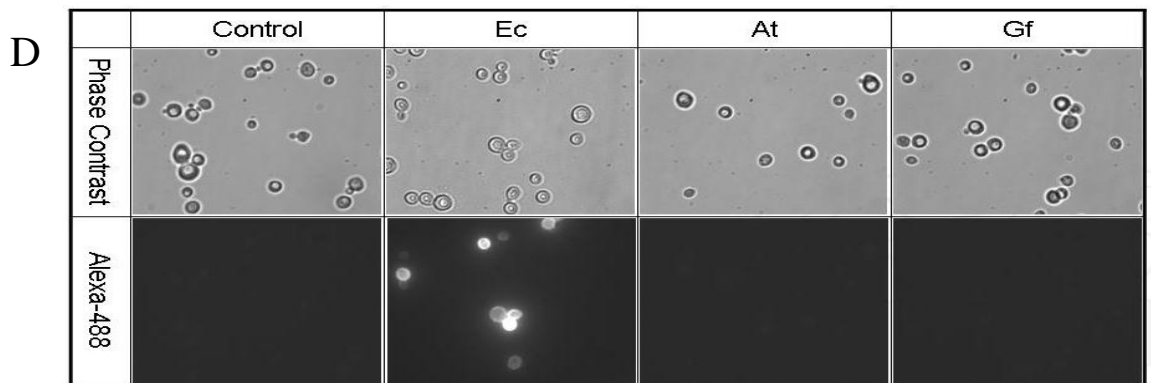
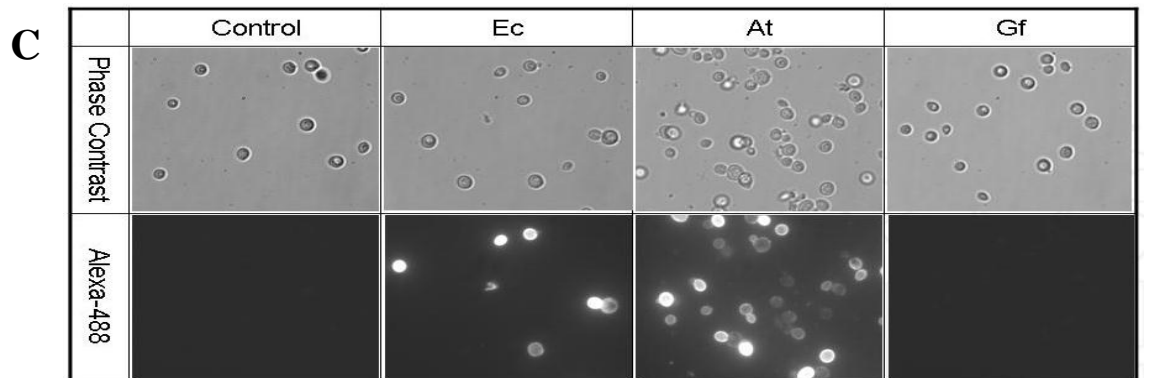
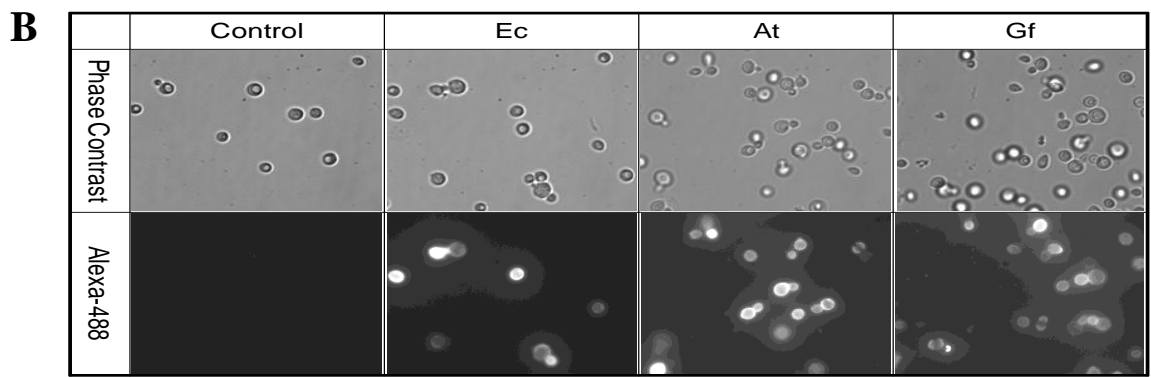
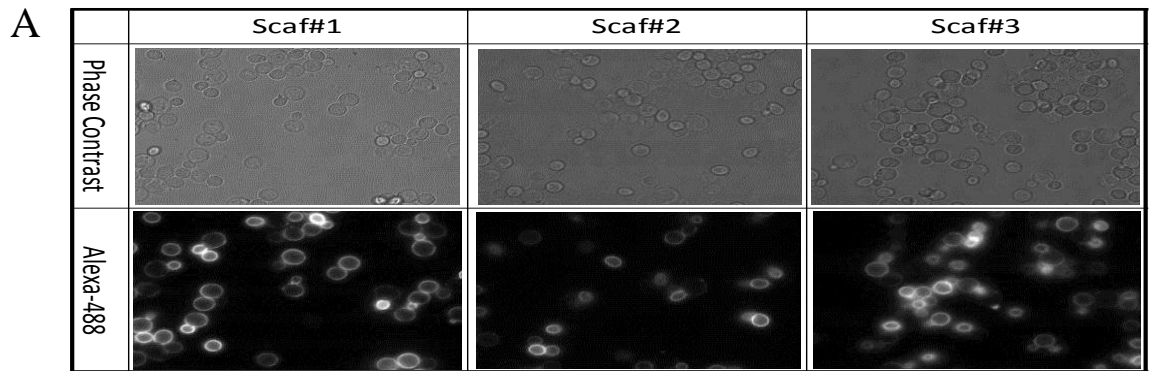


Figure 2.2. Phase-contrast and immunofluorescence micrographs of yeast cells displaying minicellulosomes. (A) Cells displaying either scaffoldin Scaf-c, Sacf-ct, or Sacf-ctf. Functional assembly of three dockerin-tagged cellulases (CelE-Dc [Ec], CelA-Dt [At], or CelG-Df [Gf]) on cells displaying (B) Sacf-ctf, (C) Sacf-ct, or (D) Scaf-c. Cells were probed with either anti-c-Myc or anti-c-His6 serum and fluorescently stained with a goat anti-mouse IgG conjugated with Alexa Fluor 488. Cells displaying only the scaffoldins were used as controls.

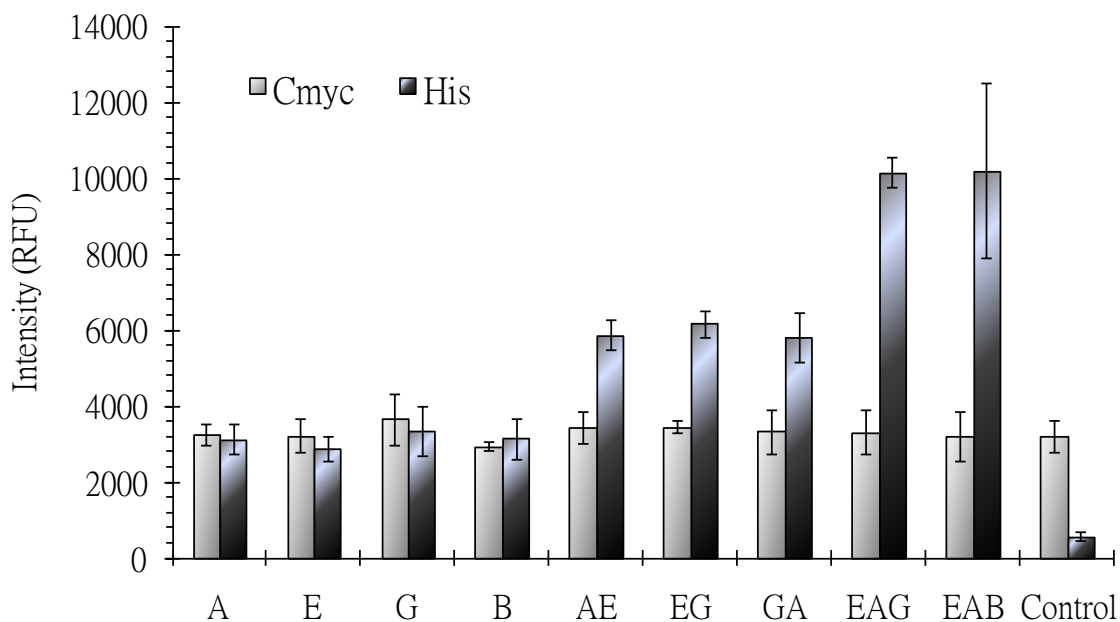


Figure 2.3. Fluorescence intensity of cells either displaying scaffoldin Sacf-ctf or with different combinations of dockerin-tagged cellulases (At [A], Ec [E], and Gf [G]) docked on the displayed Sacf-ctf. Cells were probed with either anti-c-Myc or anti-c-His6 serum and fluorescently stained with goat anti-mouse IgG conjugated with Alexa Fluor 488. Whole-cell fluorescence was determined with a fluorescence microplate reader. Cells displaying only Scaf-ctf were used as controls. RFU, relative fluorescence units.

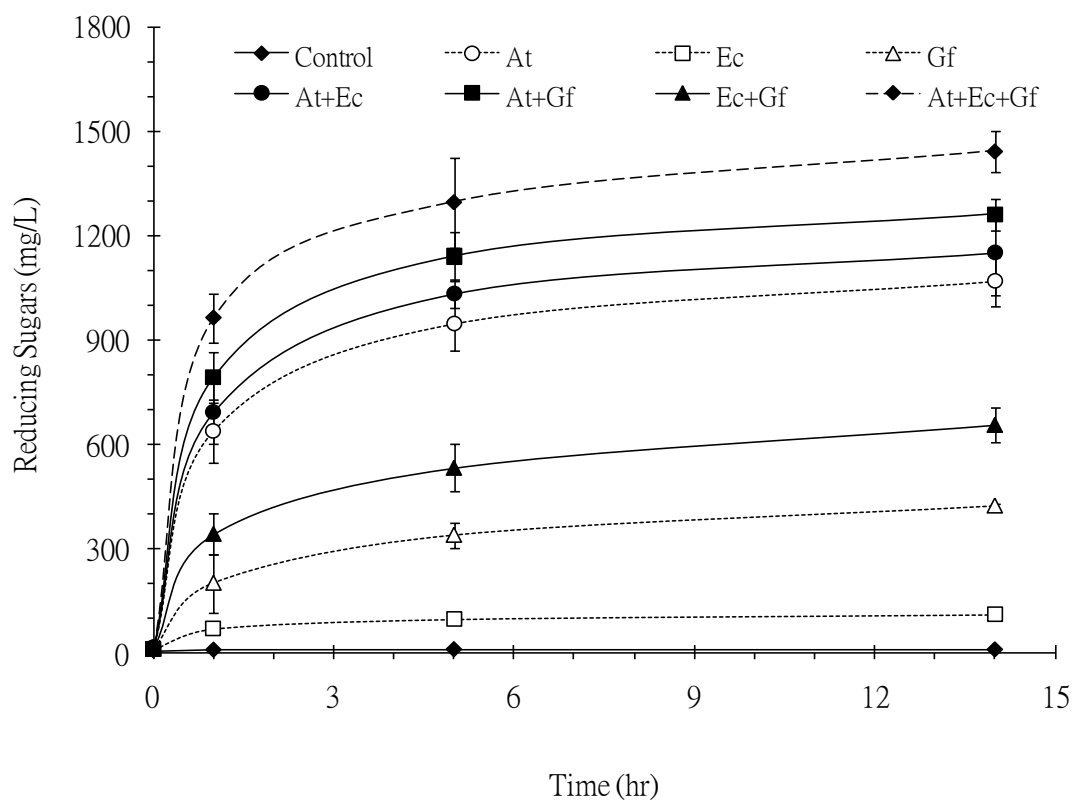


Figure 2.4. Whole-cell hydrolysis of CMC by different cellulase pairs (CelE-Dc [Ec], CelA-Dt [At], or CelG-Df [Gf]) docked on the displayed Scaf-ctf protein. Cells displaying only Scaf-ctf were used as controls.

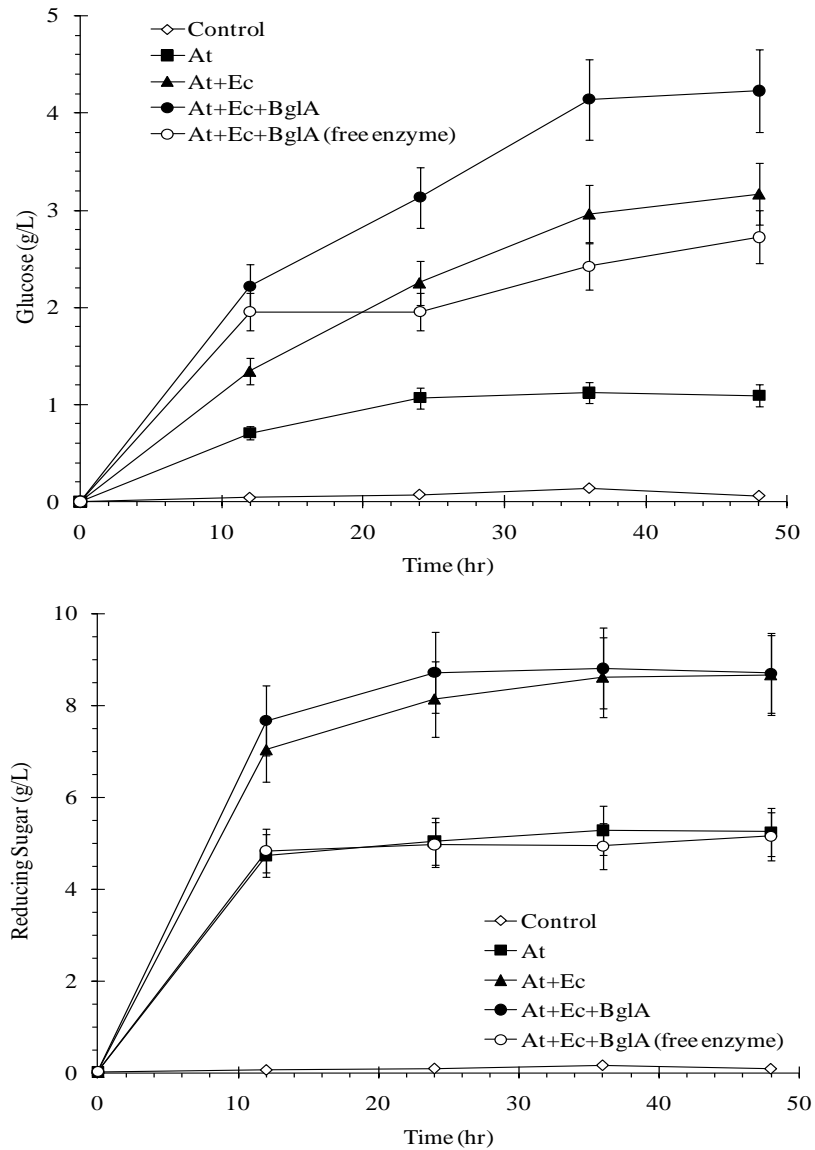


Figure 2.5. Production of glucose (A) and reducing sugars (B) from the hydrolysis of PASC by free enzymes and by surface-displayed cellulosomes. Reactions were conducted either with different cellulase pairs (CelE-Dc [Ec], CelA-Dt [At], or β -glucosidase-Df [BglA]) docked on the displayed Scaf-ctf protein or with the corresponding purified cellulases. Cells displaying only Scaf-ctf were used as controls.

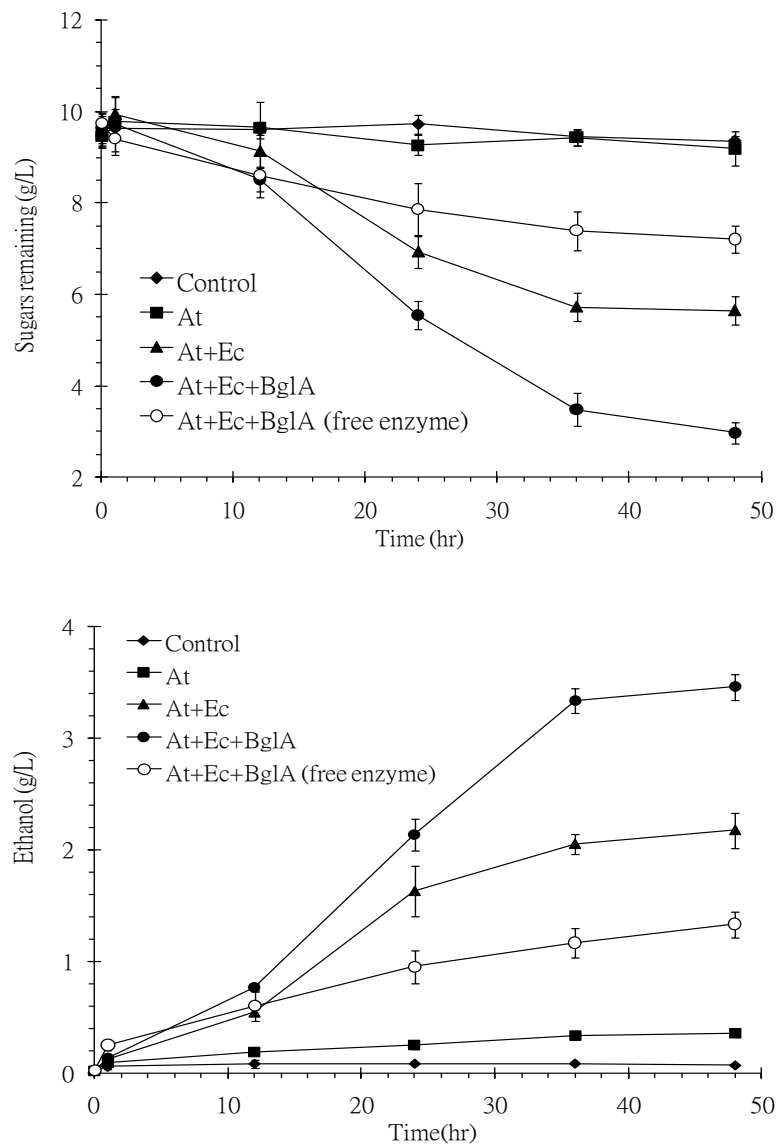


Figure 2.6. Time profiles of ethanol production (A) and cellulose hydrolysis (B) from PASC by control strain EBY100 plus free enzymes and yeast cells displaying functional cellulosomes. Fermentations were conducted either with different cellulase pairs (CelE-Dc [Ec], CelA-Dt [At], or β -glucosidase-Df [BglA]) docked on cells displaying Scaf-ctf or with control strain EBY100 plus the corresponding purified cellulases.

CHAPTER 3

**Surface display of a functional mini-cellulosome by intracellular complementation
using a synthetic yeast consortium:
Application for cellulose hydrolysis and ethanol production**

ABSTRACT

In this chapter, we report the surface assembly of a functional minicellulosome by using a synthetic yeast consortium. The basic design of the consortium consisted of four different engineered yeast strains capable of either displaying a trifunctional scaffoldin, Scaf-ctf (SC), carrying three divergent cohesin domains from *Clostridium thermocellum* (t), *Clostridium cellulolyticum* (c), and *Ruminococcus flavefaciens* (f), or secreting one of the three corresponding dockerin-tagged cellulases (endoglucanase [AT], exoglucanase [EC/CB], or β -glucosidase [BF]). The secreted cellulases were docked onto the displayed Scaf-ctf in a highly organized manner based on the specific interaction of the three cohesin-dockerin pairs employed, resulting in the assembly of a functional minicellulosome on the yeast surface. The results obtained from resting cell assay gave the final ethanol yield of 0.43 g of ethanol/g of cellulose consumed, which is corresponded to 83% of the theoretical value. We further tested the capability of the synthetic consortium for simultaneous growth and ethanol production from cellulose hydrolysis in an anaerobic setting. The final ethanol production of 1.4 g/L corresponded to 80% of the theoretical value and was 1.8-fold higher than a similar yeast consortium secreting only the three cellulases. This result confirms the use of a synthetic biology approach for the synergistic saccharification and fermentation of cellulose to ethanol by using a yeast consortium displaying a functional minicellulosome.

INTRODUCTION

According to the new Energy Policy Act, several billion gallons of renewable fuel must be produced by 2012, with most of that volume produced as biofuels from renewable biomass. Cellulosic biomass is the most abundant and sustainable material for biofuel production because of its high sugar content. It has been estimated that 1.4 billion tons of cellulosic biomass can be produced annually in the United States without affecting the food supply, animal feed, and fiber use (Perlack et al., 2005). Ethanol is useful as an alternative transportation fuel and could lessen the nation's dependence on foreign oil (Lynd et al., 2005).

Unfortunately, cost-effective production of ethanol from cellulosic biomass remains a major challenge, primarily due to its highly recalcitrant nature (Himmel et al., 2007). Typically, the synergistic actions of endoglucanase, exoglucanase, and β -glucosidase are required for the complete hydrolysis of cellulose to glucose. The high cost associated with the use of a large quantity of enzymes required for efficient biomass conversion to fermentable sugars is a primary impeding factor. While the cost of ethanol production has become more competitive by combining cellulose saccharification and fermentation (SSCF), a new method known as consolidated bioprocessing (CBP), which further combines enzyme production with SSCF into a single process, has gained increasing recognition as a potential solution for the low-cost production of ethanol (Lynd et al., 2008). However, a natural microorganism that possesses the capability for efficient enzyme production, cellulose saccharification, and ethanol fermentation remains elusive (Zhang et al., 2005). In recent years, efforts have been made in engineering

microorganisms toward the goal of consolidated bioprocessing (Den Haan et al., 2007). In particular, *Saccharomyces cerevisiae* is an attractive engineering candidate due to its high ethanol productivity and high inherent ethanol tolerance (Nevoigt, 2008). However, many past attempts based on either secretion of cellulases or surface display of cellulases have resulted in relative low ethanol productivity (Cho et al., 1999; Curry et al., 1988; Fujita et al., 2002 and 2004).

In nature, anaerobic microorganisms have developed an elaborate enzyme complex known as cellulosome for efficient hydrolysis of cellulose. This highly ordered structure allows the assembly of multiple enzymes in close proximity to the substrate, resulting in a high level of enzyme-substrate-microbe synergy (Fierobe et al., 2005). Our group reported recently the functional assembly of minicellulosomes on the yeast surface and demonstrated an up-to-3-fold increase in ethanol production from phosphoric acid-swollen cellulose (PASC) compared with free enzymes (Tsai et al., 2009). A similar enhancement in ethanol production has also been reported by the Zhao group, who used an engineered yeast strain coexpressing a displayed miniscaffoldin and three different cellulases (Wen et al., 2010). However, coexpression of all four components in a single strain resulted in relatively low levels of exoglucanase and β -glucosidase, probably due to the heavy metabolic burden and potential jamming of the secretion machinery. To address these issues, we report here the use of a synthetic yeast consortium composed of one strain displaying the miniscaffoldin and three strains secreting dockerin-tagged cellulases for the functional presentation of minicellulosomes on the yeast surface (Figure

3.1) and investigate the capability of the synthetic consortium toward direct ethanol production and cell growth under anaerobic fermentation.

MATERIALS AND METHODS

Strains and media

Escherichia coli strain JM109 [recA1 endA1 supE44 hsdR17 gyrA96 thi relA1 λ - Δ (lac-proAB) (F' traD36 proAB lacIq lacZ Δ M15)] was used as a host for recombinant DNA manipulation. *S. cerevisiae* strain EBY100 (MATa AGA1::GAL1-AGA1::URA3 ura3-52 trp1 leu2 Δ 1 his3 Δ 200 pep4::HIS3 prb1 Δ 1.6R can1 GAL) was used for displaying the scaffoldin and the secretion of β -glucosidase. *S. cerevisiae* strain BY4742 (MAT α his3 Δ 1 leu2 Δ 0 lys2 Δ 0 ura3 Δ 0) was used for secretion of the remaining enzymes and constitutively displaying of the scaffoldin. *E. coli* strains were grown in LB medium (1% tryptone, 0.5% yeast extract, 1% NaCl) with 100 μ g/liter of ampicillin when required. Except for the consortium experiments, yeast strains were either grown in YPD medium (2% dextrose, 1% yeast extract, 2% peptone) or SDC medium (2% glucose, 0.67% yeast nitrogen base, 0.5% Casamino Acids). The filamentous fungus *Trichoderma reesei* used for mRNA extraction was cultured in potato dextrose agar medium (Difco Laboratories) containing 0.4% potato starch, 2% glucose, and 2% agar at 25°C.

Plasmid construction and transformation

Primers used for plasmid construction are provided in Table 3.1 of the supplemental material. Construction of the surface display vector pSctf was previously described (Tsai et al., 2009). To construct the secretion plasmid pAt, a 1,338-bp fragment of the *Clostridium thermocellum* endoglucanase CelA gene was amplified by PCR using FAt and RAt as primers and the vector pETAt as the template. The amplified fragment

was cloned into the ClaI and XhoI sites of plasmid pCEL15 (Moses et al., 2005) under the control of a constitutive PGK promoter. Plasmid pEc, encoding a His6-tagged exoglucanase (CelE) from *Clostridium cellulolyticum*, was generated by PCR from pETEc (Gaudin et al., 2000) using primers FEc and REc. The amplified fragment was cloned into ClaI-XhoI-linearized plasmid pCEL15 to obtain pEc. The secretion vector pCBH2c was constructed using a two-step procedure. First, the dockerin domain of *C. cellulolyticum* was amplified by PCR using primers FDc and RDc and ligated into the BglII and XhoI sites of pCEL15 to form pDc. The gene coding for the cellobiohydrolase CBHII was amplified from the total RNA extracted from *T. reesei* by reverse transcription-PCR using primers FCBH2 and RCBH2. The resulting product was digested and ligated into the ClaI and BamHI sites of pDc to form pCBH2c. To generate plasmid pBGLf, the *Ruminococcus flavefaciens* dockerin domain amplified from pETGf (Fierobe et al., 2005) using primers FDf and RDF was ligated into pBGL encoding a β -glucosidase gene from *Thermoascus aurantiacus* (Hong et al., 2007).

Plasmid pAG α -Sctf used for constitutively displaying the trifunctional miniscaffoldin the yeast cell surface was constructed as described below. The Scaf-ctf fragment, consisting of three different cohesins from *C. cellulolyticum*, *C. thermocellum* and *R. flavefaciens* and a cellulose binding module (CBM), was amplified from the plasmid pSctf (Tsai et al., 2009) by PCR using primers FSctf and RSctf. The resulting fragment (2046 bps) was digested with XbaI and SalI and cloned into the XbaI and SalI sites of a multiple copy surface-display vector pSSAG α , which consisted of the yeast 3-phosphoglycerate kinase (PGK1) promoter, the secretion signal of *Rhizopus oryzae*

amylase, a C-myc tag, the C-terminus α -agglutinin gene AG α 1 and the PGK1 terminator. All yeast transformations were performed according to the standard lithium acetate procedure as described elsewhere (Ausubel et al., 1994). All the recombinant strains used in this research are summarized in Table 3.2.

Development of synthetic consortia

Yeast strains EBY100 harboring either pSctf or pBGLf (carrying a Trp1 marker) and BY4742 harboring either pCEL15, pAt, pCBH2c, or pEc (carrying a URA3 marker) were first precultured in SDC medium at 30°C for 18 h. For coculturing of the synthetic consortia, the initial strains were mixed to the desired ratio into 200 ml SGC medium (20.0 g/liter galactose, 6.7 g/liter yeast nitrogen base without amino acids, 5.0 g/liter Casamino Acids) supplemented with 10 mM CaCl₂ to an optical density at 600 nm (OD₆₀₀) of 1 and grown for 48 h at 20°C.

Resting cell assays

For the resting cell assays, PASC was prepared from Avicel PH101 (Sigma) according to the method of Walseth (Walseth, 1952) and used as the substrate. Cells from the different consortia were first washed once with buffer containing 50 mM Tris-HCl (pH 8.0), 100 mM NaCl, and 10 mM CaCl₂ and resuspended in 20 mM Tris-HCl buffer (pH 6.0) supplemented with 10 mM CaCl₂ and 10 g/liter PASC to a final OD of 50. Samples were collected periodically and immediately mixed with 3 ml of DNS reagent (10 g/liter dinitrosalicylic acid, 10 g/liter sodium hydroxide, 2 g/liter phenol, 0.5 g/liter

sodium sulfite) to determine the level of reducing sugar. After incubating at 95°C for 10 min, 1 ml of 40% Rochelle salts was added to fix the color before measuring the absorbance of the supernatants at 575 nm. The glucose concentration was determined using a glucose HK assay kit from Sigma.

Fermentation by pregrown cells

Cells from the different consortia were washed and resuspended in 10 ml SDC medium containing 6.7 g/liter yeast nitrogen base without amino acids, 20 g/liter Casamino Acids, and 10 g/liter PASC as the sole carbon source to a final OD of 50 or 15 mg (cell dry weight)/ml deducing sugars, and glucose concentrations were measured by the methods described above. The amount of residual cellulose was measured by the phenol-sulfuric acid method as described by Dubois et al. (1956). The ethanol concentration was measured by gas chromatography (model 6890; Hewlett Packard) using a flame ionization detector and an HP-FFTP column.

Simultaneous ethanol production and cell growth under anaerobic fermentation

Different consortia were grown in rubber stoppered glass serum bottles containing SC-PASC medium (6.7 g/l yeast nitrogen base w/o amino acids, 20 g/l casamino acids, and 10 g/l PASC supplemented with 10 mM CaCl₂, 0.01 g/l ergosterol and 0.42 g/l tween 80). Precultures of each yeast population were grown separately in SDC media (20 g/l glucose, 6.7 g/l yeast nitrogen base, 5 g/l casamino acids), harvested, and washed with sterilized water to prevent media carry over. For co-culturing of the synthetic consortia,

each strain was mixed equally to a total optical density of 0.5. Samples were collected periodically through a capped syringe needle pierced through the bottle stopper (Tsai et al., 2009). Yeast cells in fermentation media were counted in triplicate on SDC plates by the plate count method.

Immunofluorescence microscopy

Immunofluorescence microscopy was performed as described previously (Tsai et al., 2009). Briefly, cells were washed with phosphate-buffered saline (PBS) and resuspended in PBS containing 1 mg/ml of bovine serum albumin (BSA). Either anti-His6 or anti-Myc antibody was added and incubated for 1 h with occasional mixing. Alexa Fluor 488-conjugated anti-mouse IgG was added after washing and resuspending in PBS with 1 mg/ml of BSA. Images were acquired by using a fluorescence microscope (Olympus BX51) after washing with PBS three times. Whole-cell fluorescence was measured using a fluorescence microplate reader (Synergy4; BioTek, VT) with an excitation wavelength at 485 nm and an emission wavelength at 535 nm.

Enzyme activity assay

To assay the functional secretion of β -glucosidase, 100 μ l of a 10 mM concentration of the fluorescent substrate p-4-methylumbellifery- β -d-glucopyranoside was added to 100 μ l of culture medium and incubated at 37°C for 1 h. The activity was confirmed by detecting the fluorescence under UV light. To test the successful secretion of functional AT, EC, and CBHC in the medium, a modified Congo red staining method

was employed (Thu et al., 2008). Briefly, carboxymethyl cellulose (CMC) was added to 100 μ l of culture medium to a concentration of 1% and incubated at 37°C for 2 h. Thereafter, 20 μ l of Congo red solution (0.1% Congo red in 50 mM potassium phosphate buffer [pH 6.5]) was used for staining. The culture medium from BY4742/pCEL15 was used as a negative control in all cases.

RESULTS

Secretion of dockerin-tagged endoglucanase, exoglucanase, and β -glucosidase.

To enable the complete hydrolysis of cellulose to glucose, three different yeast strains were engineered to secrete either an endoglucanase CelA from *C. thermocellum* (A), an exoglucanase CelE from *C. cellulolyticum* (E), or β -glucosidase BglI from *Thermoascus aurantiacus* (Bgl). For specific docking of secreted enzymes onto the surface display miniscaffoldin (Scaf-ctf), three different dockerins from *C. thermocellum* (t), *C. cellulolyticum* (c), and *R. flavefaciens* (f) were used to generate dockerin-tagged enzymes, resulting in At, Ec, and Bglf, respectively. All three dockerin-tagged enzymes were secreted using an α -factor secretion peptide and flanked by a His6 tag.

To examine the functional secretion of At, the culture medium for BY4742/pAt was introduced into a 1% CMC solution for 2 h and stained with Congo red. A clear color change from red to yellow confirmed At activity (Figure 3.2A), while no color change was observed with the culture medium of cells displaying Scaf-ctf. In addition, functionality of the dockerin domain in At was confirmed by incubating the culture medium with cells displaying Scaf-ctf, followed by immunofluorescence microscopy using the anti-His6 antibody (Figure 3.2B). Similarly, the activity of secreted Ec was confirmed by observing a color change from red to orange with the Congo red assay (Figure 3.2C). Secretion of Bglf was confirmed by detecting a strong fluorescence signal upon addition of the fluorescent substrate p-4-methylumbellifery- β -d-glucopyranoside to the culture medium of EBY100/pBGLf (Figure 3.2E). Moreover, detectable fluorescence was observed on the Scaf-ctf-displaying cells only after incubation with the culture

medium of either BY4742/pEc or EBY100/pBGLf, again confirming the functionality of the dockerin domains of the two secreted enzymes (Figure 3.2D and 3.2F). Collectively, these results confirmed the successful secretion of functional dockerin-tagged enzymes from the three engineered yeast strains.

Functional assembly of each enzyme onto the surface-displayed scaffoldin. With the successful secretion of all dockerin-tagged enzymes, the feasibility of recruiting these engineered yeast strains into a synthetic consortium system was examined. For the initial experiments, four different consortia with different cell populations—a strain displaying Scaf-ctf (SC), a strain carrying pCEL15 (CE) as a nonsecretion control, an At-secreting strain (AT), an Ec-secreting strain (EC), and a Bglf-secreting strain (BF)—were created to test the ability of the consortia to hydrolyze PASC and to produce ethanol. By exploiting the specific interactions of the different dockerin-cohesin pairs, we expected the spontaneous self-assembly of a functional minicellulosome onto the displayed Scaf-ctf. All consortia developed are listed in Table 3.3.

Different populations of cells were cocultured, washed, and resuspended in SDC medium to a final OD of 50. As shown in Figure 3.3A, the consortium composed of SC, CE, and AT (C2) showed a noticeable increase in ethanol production compared to the control consortium (SC and CE) secreting no enzyme (C1). This result clearly suggests the functional assembly of secreted At onto the displayed Scaf-ctf, as demonstrated by the ability to hydrolyze PACS and subsequent ethanol production. The surface assembly of At was further verified by immunofluorescence microscopy using both anti-C-myc and anti-His antibodies (Figure 3.4B). While the fluorescent intensity detected for the C-myc

tag was similar between the two consortia (C1 and C2), only the consortium containing AT (C2) showed an appreciable level of His tag fluorescence, confirming the docking of secreted At onto the surface-displayed Scaf-ctf.

Consistent with the expected enhancement in glucose liberation by the addition of exoglucanase, ethanol production (Figure 3.3A) was slightly increased for the consortium containing both AT and EC (C3). However, a further 3-fold increase in ethanol production was observed for the consortium (C4) containing all the functional populations (SC, AT, EC, and BF) required to assemble the trifunctional minicellulosome (Figure 3.3A). This increase in ethanol production was expected, as the presence of β -glucosidase is essential for complete hydrolysis of cellulose into glucose. By probing the His tag from each secreted cellulase, the level of enzyme incorporation onto the surface for different consortia could be directly assessed using whole-cell fluorescence measurements. Although the incorporation of secreted Ec (C3) and Bglf (C4) was confirmed by an increase in the His tag fluorescence intensity, the level of Ec incorporation was substantially lower than that of At or Bglf (Figure 3.3B). This low level of Ec incorporation is consistent with the modest increase in ethanol production, suggesting that the efficiency of the consortium could be further improved by increasing the exoglucanase activity.

One major benefit of the consortium system is our ability to modulate any given population without affecting the other cell populations. To test this hypothesis, a cellobiohydrolase/exoglucanase CBHIII from *T. reesei* (CBH), which has been shown to have high-level secretion in *S. cerevisiae* (Penttilä et al., 1988), was tagged with the C.

cellulolyticum dockerin domain (CBHc) and functionally secreted from strain BY4742 (CB). As shown in Figure 3.3B, compared to the consortium with EC (C4), the new consortia (C5 and C6) using CB showed a higher level of His tag fluorescence intensity, indicating the improved docking level of CBHc. This enhanced level of CBHc docking was accompanied by a corresponding increase in PASC hydrolysis and ethanol production (Figure 3.3C). An ethanol level of 930 mg/liter was achieved after 50 h, which corresponds to 83% of the theoretical value (0.43 g of ethanol/g of cellulose). These results confirm the cooperative action between each population in the consortium and the capabilities of the surface-assembled minicellulosomes for cellulosic ethanol production.

Simultaneous ethanol production and cell growth under anaerobic fermentation

To enable the direct growth and ethanol production on PASC by the synthetic yeast consortium, the Aga1-Aga2 anchor system used in the previous study (Tsai et al., 2009) which required galactose for induced expression was replaced by a constitutively expressed Aga1 anchor system using a strong PGK promoter (Figure 3.4A). To demonstrate the display of Scaf-ctf, immunofluorescence assays were carried out using the anti C-myc antibody (Fig. 3.4B). The fluorescence signal detected on the yeast cell surface confirmed the correct expression and translocation of the miniscaffoldin.

The ability of the consortium to grow and produce ethanol directly from PASC was investigated. In addition to the newly constructed strain displaying Scaf-ctf (SCC) under a constitutive promoter, the three strains secreting either an endoglucanase (AT),

an exoglucanase (CB) or a β -glucosidase (BF) tagged with a different dockerin domain and flanked by a His6 tag were used in the consortium. Different yeast strains were initially grown separately in SDC medium overnight and then mixed equally to a total initial cell density of $\sim 5 \times 10^6$ cell/ml to form the functional consortium (C7). A strain carrying the plasmid pCEL15 (CE) with no heterogenous protein expression was used as a control population. To compare the performance, another consortium composed of cellulase secreting cells (AT/CB/BF) and CE (C8) was used.

An initial glucose concentration of 1 g/L was added to allow the synthesis and assembly of the cellulosome structure. For the consortium C1 containing only SC, no appreciable level of cell growth and PASC degradation was observed; only the added glucose was converted to ethanol (Figure 3. 5A and 3.5B). In comparison, a significant level of cell growth was observed for the consortium C7 containing the functionally displayed cellulosome, and only minimum growth was detected for the consortium C8 secreting only cellulases (Figure 3.5A). The enhancement in cell growth was also reflected in both PASC degradation and ethanol production; the final ethanol level of ~ 1.4 g/L is 1.8-fold higher than the consortium secreting only cellulases (Figure 3. 5B and 3.5C). The final ethanol yield of 0.39 g ethanol/g PASC is equivalent to 80% of the theoretical value.

DISCUSSION

Cellulose, a major component of the plant cell wall, is the most abundant renewable carbon source in nature that can be enzymatically degraded for ethanol production. However, the high cost of cellulases needed for complete hydrolysis is still one of the major obstacles in the quest for an economically feasible cellulose-based ethanol process (McBride et al., 2005). Cellulosome is a multicomponent enzyme complex that has been extensively investigated in recent years because of its intriguing potential in providing synergistic and highly efficient degradation of cellulose. Progress has been made in engineering yeast cells to display minicellulosome structures, toward the goal of CBP (Tsai et al., 2009; Wen et al., 2010). However, the two previous studies based on either in vitro loading of enzymes or simultaneous display of scaffoldin and secretion of cellulases in a single host cell presented problems. In the case of in vitro enzyme loading, the process cannot truly be CBP because separate *E. coli* cultivations are necessary. For the single host cell system, the inability to fine-tune levels of the three cellulases resulted in a highly uneven distribution toward endoglucanase. As a result, a substantially lower theoretical yield of 62% cellulose-to-ethanol conversion was obtained, compared to over 95% in the case of in vitro enzyme loading.

To address these problems, we engineered a synthetic yeast consortium capable of surface assembly of a functional minicellulosome via intracellular complementation. The basic design consisted of four different engineered yeast strains capable of either displaying the miniscaffoldin or secretion of one of the three required dockerin-tagged enzymes (endoglucanase, exoglucanase, or β -glucosidase). There are several unique

features of our consortium system. First, the dockerin-cohesin pairs used in the present study are from three different species, which enable specific interactions between each dockerin-tagged enzyme and the displayed miniscaffoldin, resulting in highly controllable ordering of each enzyme in the minicellulosome structure. Second, by exploiting the modular nature of each population to provide a unique building block for the minicellulosome structure, the overall cellulosome assembly, cellulose hydrolysis, and ethanol production can be easily improved simply by the replacement of populations in the consortium. As a result, the improved consortium consisting of the population secreting the cellobiohydrolase CBHII produced almost twice the level of ethanol as the consortium barely secreting the exoglucanase Ec.

To accomplish the goal of simultaneous cell growth and ethanol production on cellulose, the yeast consortium was further manipulated to enable the constitutive assembly of the minicellulosome on the yeast cell surface. The resulting consortium can grow on cellulose and produce ethanol more efficiently than a similar consortium secreting only cellulases because of the synergistic action on cellulose hydrolysis by the mini-cellulosome structure.

To our knowledge, this is the first successful report of the site-specific display of a multifunctional enzyme complex on the yeast surface through cooperative intracellular complementation using a synthetic consortium. Even though the ethanol productivity obtained in this research is much lower than required in practice (Zaldivar et al., 2001), our results successfully demonstrated the concept of using a microbial consortium for the simultaneous growth and ethanol production from cellulose. However, further

improvements of the consortium system are required to significantly improve the overall productivity. Furthermore, since our current study demonstrates the feasibility of assembling a functional minicellulosome consisting of only three enzymes on the yeast surface, there is no reason why other designer cellulosome structures cannot be similarly assembled by coordinating the required intracellular complementation within the consortium population.

REFERENCES

1. **Ausubel, F. M., R. Brent, R. E. Kingston, D. D. Moore, J. G. Seidman, J. A. Smith, and K. Struhl.** 1994. Current protocols in molecular biology, vol. 2. John Wiley & Sons, New York, NY.
2. **Cho, K. M., Y. J. Yoo, and H. S. Kang.** 1999. δ -Integration of endo/exo-glucanase and β -glucosidase genes into the yeast chromosomes for direct conversion of cellulose to ethanol. *Enzyme Microb Technol* **25**:23-30.
3. **Curry, C., N. Gilkes, G. Oneill, R. C. Miller, and N. Skipper.** 1988. Expression and secretion of a *Cellulomonas fimi* exoglucanase in *Saccharomyces cerevisiae*. *Appl Environ Microbiol* **54**:476-484.
4. **Den Haan, R., S. H. Rose, L. R. Lynd, and W. H. van Zyl.** 2007. Hydrolysis and fermentation of amorphous cellulose by recombinant *Saccharomyces cerevisiae*. *Metab Eng* **9**:87-94.
5. **Dubois, M., K. A. Gilles, J. K. Hamilton, P. A. Rebers, and F. Smith.** 1956. Colorimetric method for determination of sugars and related substances. *Anal Chem* **28**:350-356.
6. **Fierobe, H. P., F. Mingardon, A. Mechaly, A. Belaich, M. T. Rincon, S. Pages, R. Lamed, C. Tardif, J. P. Belaich, and E. A. Bayer.** 2005. Action of designer cellulosomes on homogeneous versus complex substrates: controlled incorporation of three distinct enzymes into a defined trifunctional scaffoldin. *J Biol Chem* **280**:16325-16334.

7. **Fujita, Y., J. Ito, M. Ueda, H. Fukuda, and A. Kondo.** 2004. Synergistic saccharification, and direct fermentation to ethanol, of amorphous cellulose by use of an engineered yeast strain codisplaying three types of cellulolytic enzyme. *Appl Environ Microbiol* **70**:1207-1212.
8. **Fujita, Y., S. Takahashi, M. Ueda, A. Tanaka, H. Okada, Y. Morikawa, T. Kawaguchi, M. Arai, H. Fukuda, and A. Kondo.** 2002. Direct and efficient production of ethanol from cellulosic material with a yeast strain displaying cellulolytic enzymes. *Appl Environ Microbiol* **68**:5136-5141.
9. **Gaudin, C., A. Belaich, S. Champ, and J. P. Belaich.** 2000. CelE, a multidomain cellulase from *Clostridium cellulolyticum*: a key enzyme in the cellulosome. *J Bacteriol* **182**:1910-1915.
10. **Himmel, M. E., S. Y. Ding, D. K. Johnson, W. S. Adney, M. R. Nimlos, J. W. Brady, and T. D. Foust.** 2007. Biomass recalcitrance: engineering plants and enzymes for biofuels production. *Science* **315**:804-807.
11. **Hong, J., H. Tamaki, and H. Kumagai.** 2007. Cloning and functional expression of thermostable beta-glucosidase gene from *Thermoascus aurantiacus*. *Appl Microbiol Biotechnol* **73**:1331-1339.
12. **Lynd, L. R., M. S. Laser, D. Brandsby, B. E. Dale, B. Davison, R. Hamilton, M. Himmel, M. Keller, J. D. McMillan, J. Sheehan, and C. E. Wyman.** 2008. How biotech can transform biofuels. *Nat Biotechnol* **26**:169-172.
13. **Lynd, L. R., W. H. van Zyl, J. E. McBride, and M. Laser.** 2005. Consolidated bioprocessing of cellulosic biomass: an update. *Curr Opin Biotechnol* **16**:577-583.

14. **McBride, J. E., J. J. Zietsman, W. H. Van Zyl, and L. R. Lynd.** 2005. Utilization of cellobiose by recombinant β -glucosidase-expressing strains of *Saccharomyces cerevisiae*: characterization and evaluation of the sufficiency of expression. *Enzyme Microb Technol* **37**:93-101.
15. **Moses, G., R. R. Otero, and I. S. Pretorius.** 2005. Domain engineering of *Saccharomyces cerevisiae* exoglucanases. *Biotechnol Lett* **27**:355-362.
16. **Nevoigt, E.** 2008. Progress in metabolic engineering of *Saccharomyces cerevisiae*. *Microbiol Mol Biol Rev* **72**:379-412.
17. **Penttilä, M. E., L. André, P. Lehtovaara, M. Bailey, T. T. Teeri, and J. K. C. Knowles.** 1988. Efficient secretion of two fungal cellobiohydrolases by *Saccharomyces cerevisiae*. *Gene* **63**:103-112.
18. **Perlack, R. D., L. L. Wright, A. F. Turhollow, R. L. Graham, B. J. Stokes, and D. C. Erbach.** 2005. Biomass as feedstock for bioenergy and bioproducts industry: the technical feasibility of a billion-ton annual supply. U.S. Department of Energy, Oak Ridge, TN.
19. **Thu, M., M. M. Oo, M. Myint, and S. S. Maw.** 2008. Screening on cellulase enzyme activity of *Aspergillus niger* strains on cellulosic biomass for bioethanol production, p. 12-14. GMSARN International Conference on Sustainable Development: issues and prospects for the GMS. Greater Mekong Subregion Academic and Research Network, Pathumthani, Thailand.

20. **Tsai, S. L., J. Oh, S. Singh, R. Z. Chen, and W. Chen.** 2009. Functional assembly of minicellulosomes on the *Saccharomyces cerevisiae* cell surface for cellulose hydrolysis and ethanol production. *Appl Environ Microbiol* **75**:6087-6093.
21. **Walseth, C. S.** 1952. Occurrence of cellulases in enzyme preparations from microorganisms. *TAPPI J* **35**:228-233.
22. **Wen, F., J. Sun, and H. M. Zhao.** 2010. Yeast surface display of trifunctional minicellulosomes for simultaneous saccharification and fermentation of cellulose to ethanol. *Appl Environ Microbiol* **76**:1251-1260.
23. **Zaldivar, J., J. Nielsen, and L. Olsson.** 2001. Fuel ethanol production from lignocellulose: a challenge for metabolic engineering and process integration. *Appl Microbiol Biotechnol* **56**: 17-34.
24. **Zhang, Y. H. P., and L. R. Lynd.** 2005. Cellulose utilization by *Clostridium thermocellum*: bioenergetics and hydrolysis product assimilation. *Proc Natl Acad Sci USA* **102**:7321-7325.

Table 3.1. Primers used in this study

Primer	Sequence (Restriction sites are bold)
FAt	GCATAT TCGAT GCAGGTGTGCCTTTTAAACACAAAATACCCC
RAt	ATAT CTCGAG CTAGTGGTGGTGGTGGTGGTGATAAGGTAGGTG GGGTATGC
FEc	GCATAT TCGAT CCTTGTTGGGGCAGGAGATTTGATTTCGAAACC
REc	GCAT CTCGAG CTAGTGGTGGTGGTGGTGGTGCTGTGTGATTTTT CCTAACAAGAATGAT
FCBH2	ATATAT TCGAT CAAGCATGCTCAAGCGTCTGGGG
RCHB2	ATAT GGATC CTGCAGGAACGATGGGTTTGCGTTTGTG
FDc	ATATAGAT CTGGATC CTTGGGTTAAGGGTTCAGGCTGG
RDc	ATAT CTCGAG TTAATGATGATGATGATGATGCTGTGTGATTTTT CCTAACAAGAATGAT
FDf	ATATT CTAGAG ATGTTTCAAATAATGTTTACTATGTAAATGT
RDf	TAAT GGATC CTCAATGATGATGATGATGATGTTGAGGAAGTGT GATGAGTTC
FSctf	GCG CTCTAGAG GCGATTCTCTTAAAGTTACAGT
RSctf	GCGCG TCGAC CTTAACAATGATAGCGCCAT

Table 3.2. Strains and plasmids used in this study

Strain	Host Plasmid	Promoter Marker Tag	Description
CE	BY4742 pCEL15	PGK URA HIS ₆	Secretes a small peptide (negative control)
AT	BY4742 pAt	PGK URA HIS ₆	Secretes endoglucanase At (CelA from <i>C. thermocellum</i> with its native dockerin)
EC	BY4742 pEc	PGK URA HIS ₆	Secretes exoglucanase Ec (CelE from <i>C. cellulolyticum</i> with its native dockerin)
CB	BY4742 pCBH2c	PGK URA HIS ₆	Secretes cellobiohydrolase CBHc (CBHII from <i>T. reesei</i> fused with a dockerin from <i>C. cellulolyticum</i>)
BF	EBY100 pBGLf	GAP TRP HIS ₆	Secretes β -glucosidase Bglf (Bg1I from <i>T. aurantiacus</i> fused with a dockerin from <i>R. flavefaciens</i>)
SC	EBY100 pScaf3	GAL TRP C-myc	Displays the mini-scaffoldin Sacf-ctf (Galactose induced expression)
SCC	BY4742 pAG α -Sctf	PGK URA C-myc	Displays the mini-scaffoldin Sacf-ctf (Constitutive expression)

Table 3.3. Consortia generated in this study

Consortium	Populations	Description
C1	SC,CE,CE,CE	A consortium without secreting any enzymes (negative control)
C2	SC,AT,CE,CE	A consortium forming a cellulosome structure containing only endoglucanases
C3	SC,AT,EC,CE	A consortium forming a cellulosome structure containing endoglucanases, and exoglucanases
C4	SC,AT,EC,BF	A consortium forming a cellulosome structure containing endoglucanases, and exoglucanases and β -glucosidase
C5	SC,AT,CB,CE	A consortium forming a cellulosome structure containing endoglucanases, and cellobiohydrolases
C6	SC,AT,CB,BF	A consortium forming a cellulosome structure containing endoglucanases, and cellobiohydrolases and β -glucosidase
C7	SCC,AT,CB,BF	A consortium forming a cellulosome structure containing endoglucanases, and cellobiohydrolases and β -glucosidase (Constitutive expression)
C8	CE, AT,CB,BF	A consortium only secreting the three enzymes: endoglucanases, and cellobiohydrolases and β -glucosidase

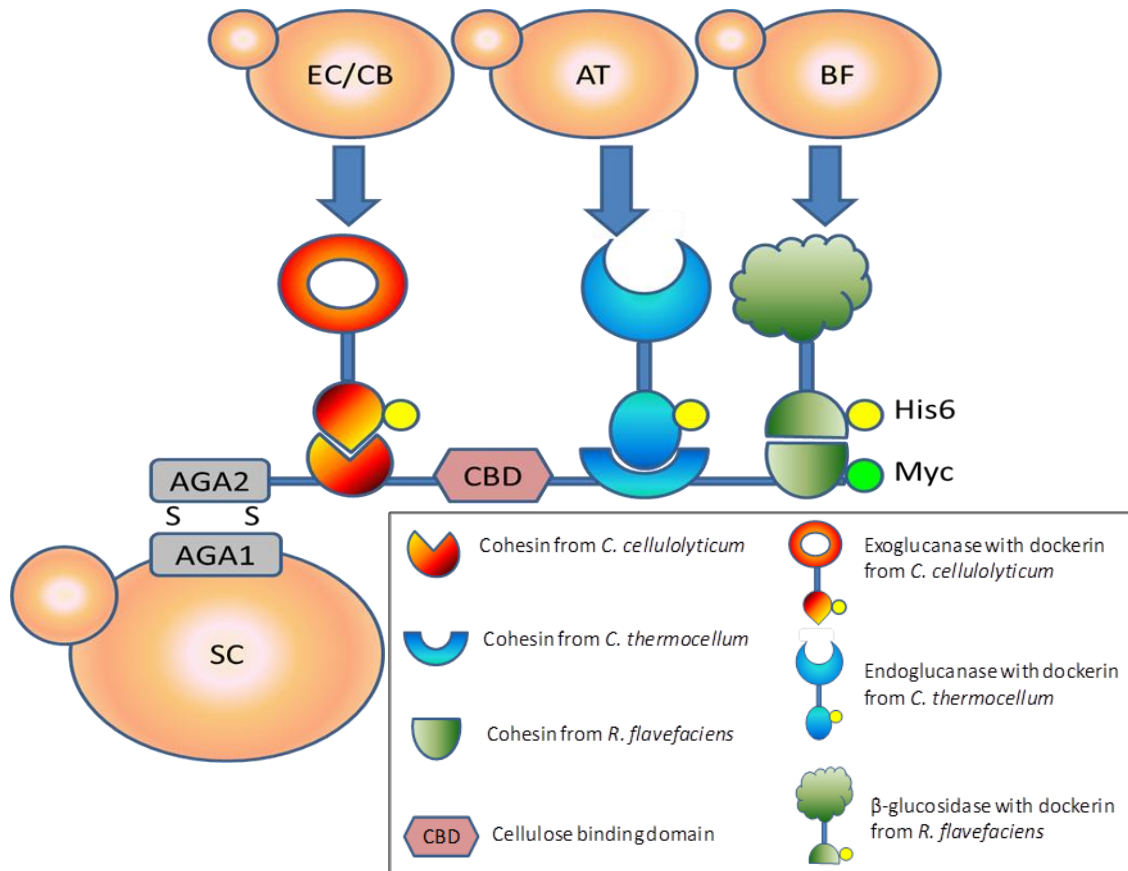


Figure 3.1. Surface assembly of a functional mini-cellulosome through intracellular complementation using a synthetic yeast consortium. The basic design consisted of four different engineered yeast strains capable of either displaying a trifunctional scaffoldin Scaf-ctf (SC) or secreting one of the three corresponding dockerin-tagged enzymes (endoglucanase [AT], exoglucanase [EC/CB] or β -glucosidase [BF]).

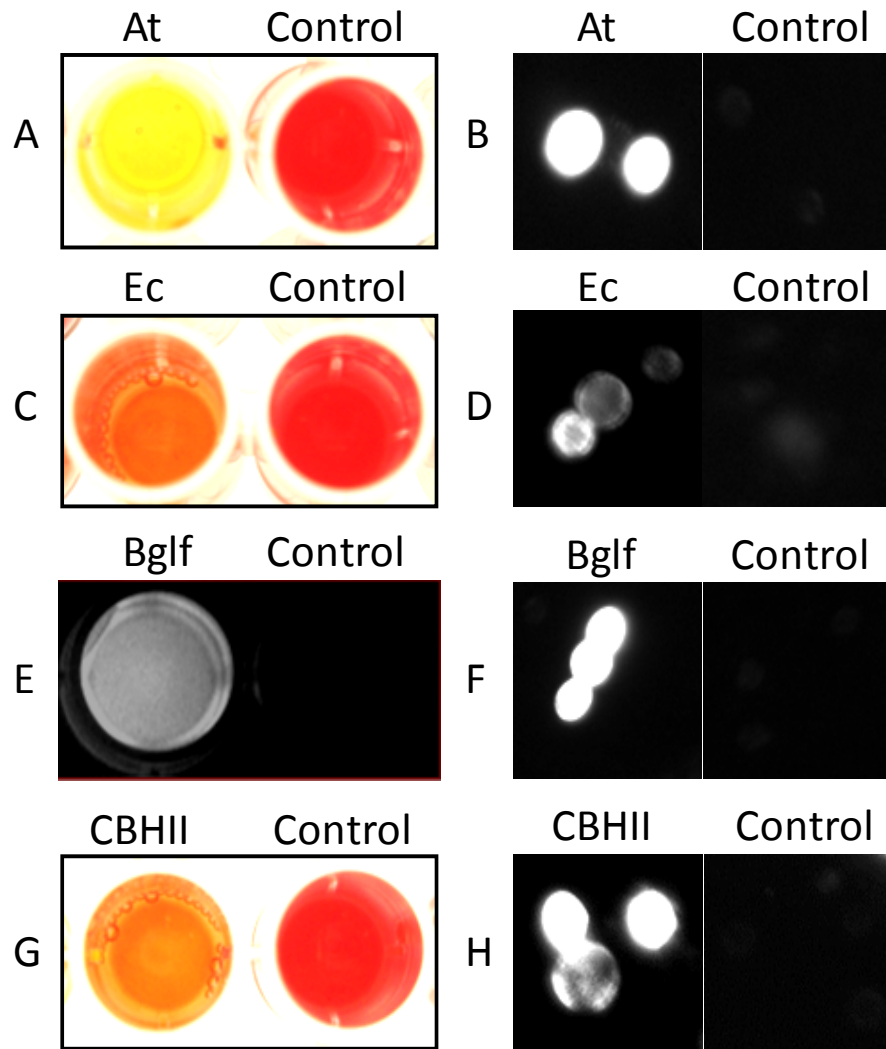


Figure 3.2. Secretion of dockerin-tagged enzymes. (A-D) Enzyme activities in the growth medium of different secretion strains were examined by using either CMC (A-C) or p-4-methylumbellifery- β -D-glucopyranoside (D) as the substrate. For the CMC assay, Congo Red was added as an indicator. (E-G) Binding of secreted enzymes onto surface displayed Scaf-ctf was confirmed by immunofluorescence microscopy. Cells were probed with anti-C-His6 sera and fluorescently stained with a goat anti-mouse IgG conjugated with Alexa Fluor 488. Growth medium was used as control in all cases.

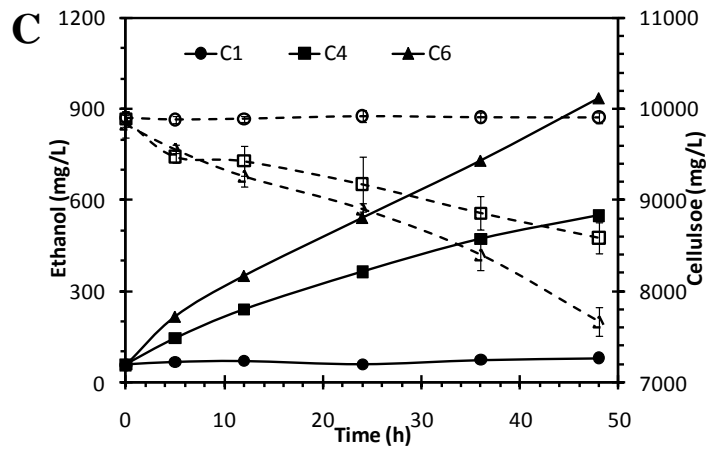
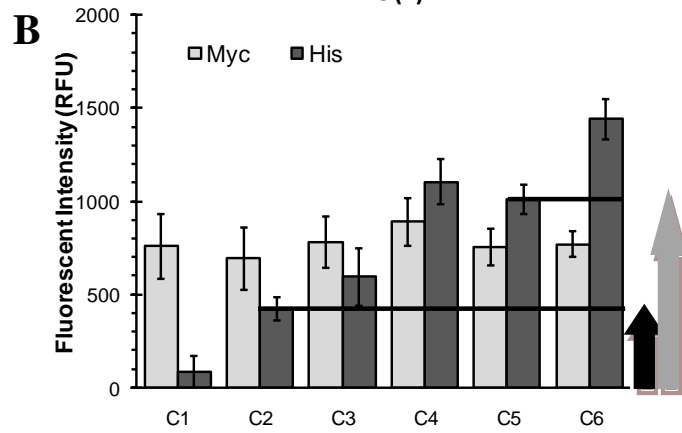
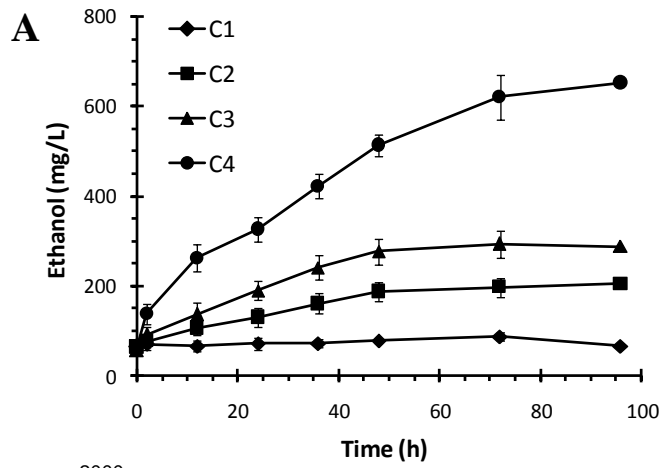


Figure 3.3. Cellulose hydrolysis and ethanol production by different synthetic consortia (See Table 3.3). Different consortia were established using a strain displaying Scaf-ctf (SC), a strain carrying pCEL15 (CE) as a control, an At-secreting strain (AT), an Ec-secreting strain (EC), a CHBc-secreting strain (CB), and/or a Bglf-secreting strain (BF). (A) Ethanol production from PASC by different synthetic consortia. (B) Docking of At, Ec, and/or BglF onto Scaf-ctf-displaying cells in different consortia. Cells were probed with either anti-C-myc or anti-C-His6 sera and fluorescently stained with a goat anti-mouse IgG conjugated with Alexa Fluor 488. Whole cell fluorescence was determined using a fluorescent microplate reader. The dark arrow and gray arrow on the right hand side showed the increase in fluorescent intensity after At and CBHII docking. (C) Cellulose hydrolysis (dashed line) and ethanol production (solid line) from PASC by a consortium composed of SC, AT, CB, and BF.

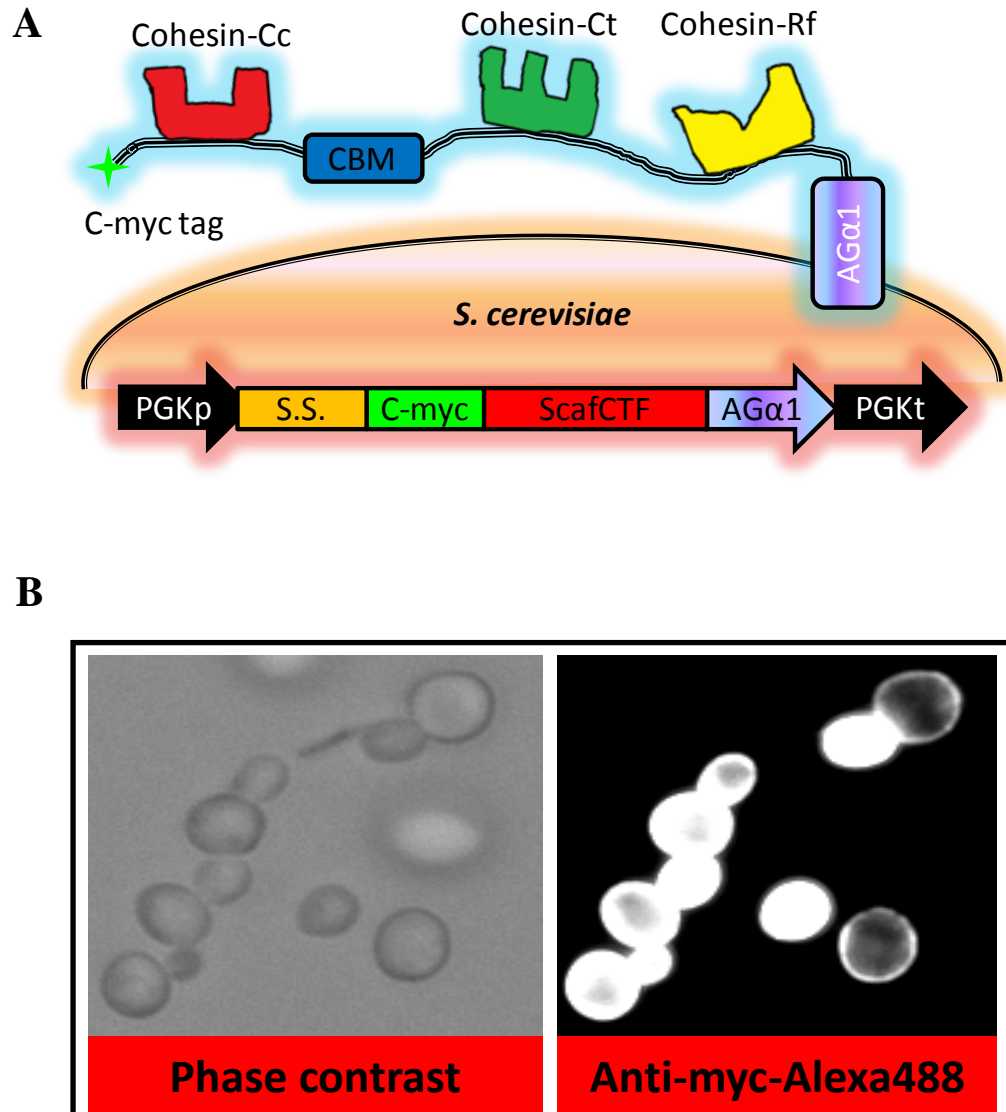


Figure 3.4. Constitutive surface display of scaffoldin Scaf-ctf using the Agα1 anchor and the constitutive PGK promoter. (A) Schematic representation of the surface display approach. (B) Confirmation of surface displayed Scaf-ctf by immunofluorescence microscopy. Cells were probed with anti-Cmyc sera and fluorescently stained with a goat anti-mouse IgG conjugated with Alexa Fluor 488.

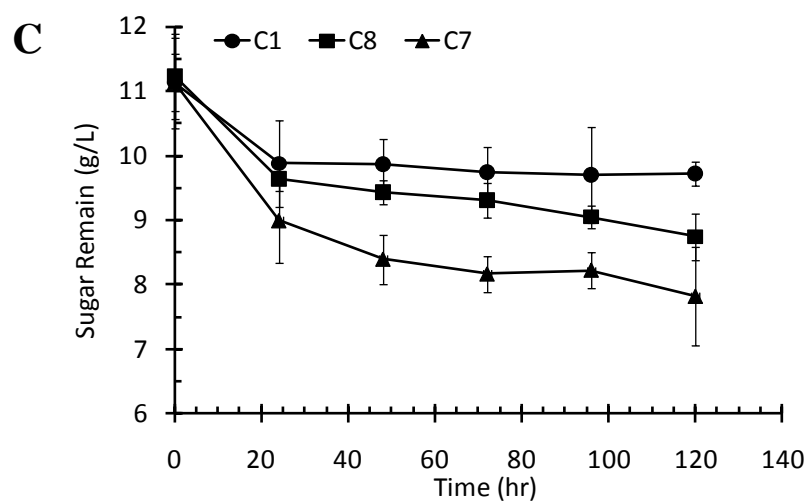
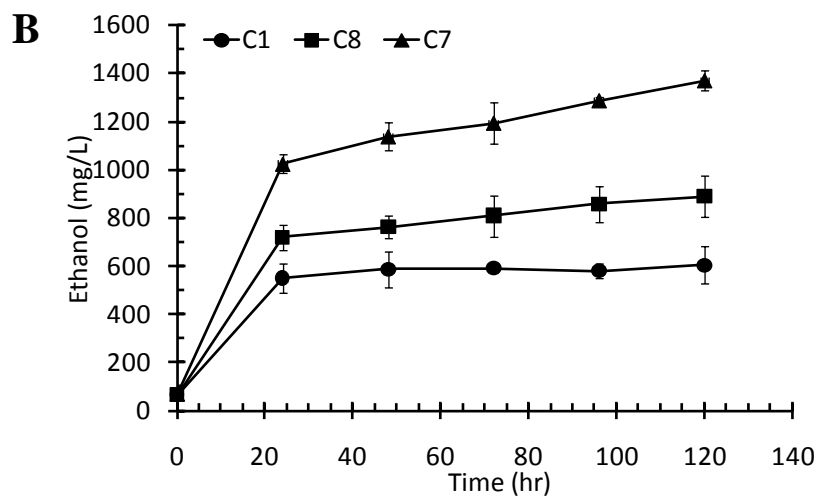
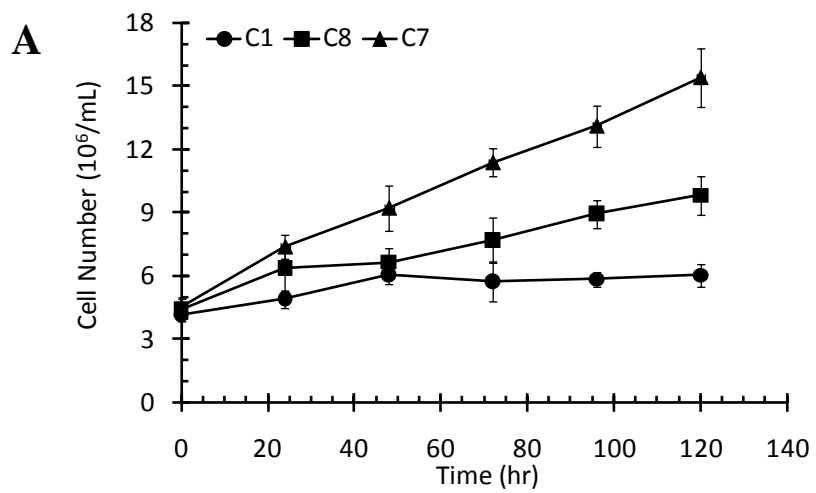


Figure 3.5. (A) Cell growth and (B) ethanol production and (C) PASC hydrolysis by the different yeast consortia, i.e., consortium C1 without secreting enzymes (●), consortium C8 only secreting enzymes (■) and consortium C1 forming cellulosome structure (▲). Samples were collected periodically through a capped syringe needle pierced through the bottle stopper. Yeast cells in fermentation media were counted in triplicate on SDC plates by the plate count method.

CHAPTER 4

Functional assembly of complexly structured cellusomes on the *Saccharomyces cerevisiae* surface for enhanced cellulose hydrolysis and ethanol production

ABSTRACT

Improvements on overall efficiency and yield of hydrolyzed sugars from lignocellulosic biomass are being chased for several decades in order to reduce the cost for making biofuels. We demonstrated the functional assembly of a complex cellulosome on the yeast cell surface, consisting of (1) a surface bound anchoring scaffoldin, (2) an adaptor scaffoldin to amplify the enzyme loading, and (3) an enzymatic subunit for cellulose hydrolysis. The displayed complex cellulosome retained the ability for glucose liberation from cellulose hydrolysis. When a tetravalent complex cellulosome containing two adaptor scaffoldins that bore 4 enzymatic subunits was assembled on the yeast surface, the recombinant cellulolytic yeast exhibited significantly enhanced glucose liberation and ethanol production from phosphoric acid swollen cellulose (PASC). The final ethanol concentration of 1.9 g/L was 4-fold higher than that of a divalent cellulosome structure. This result confirms that creating a more complex cellulosome system bearing higher enzyme loading would be a promising way to further increase the efficiency for cellulose hydrolysis rather than just simply increase the cell densities. This result can perhaps also help us to explain why a native cellulosome system is so elaborate for cellulose hydrolysis.

INTRODUCTION

Biofuels derived from lignocellulosic biomass, the most abundant renewable organic material on Earth, are attractive alternatives to current petroleum-based fuels due to their sustainable and environment-friendly nature. However, the main technological obstacle to more widespread usages of this resource is the lack of low-cost technologies to overcome their recalcitrant nature, especially the hydrolysis of the highly ordered cellulose structure (Lynd et al., 2002). As plants have evolved mechanisms to protect their cell wall's polysaccharides, only a small fraction of natural microorganisms can efficiently degrade cellulose (Himmel et al., 2010).

Improvements on the overall efficiency and yield of hydrolyzed sugars from lignocellulosic biomass are being pursued for several decades, including genetic engineering of crops for better sugar accessibility (Hosano et al., 2009), reformation and improvement of pretreatment technologies (Studer et al., 2010), and directed evolution of cellulases for enhanced activity and stability (Hardiman et al., 2010; Li et al., 2010). All these efforts have shown improved sugar liberation from lignocellulosic biomass, but the costs for making lignocellulosic biofuel still cannot compete with the petroleum-based fuels, mainly due to the high cost of cellulases added extraneously.

With the problems stated above, one obvious way to reduce the cost is to have the hydrolytic enzymes produced simultaneously by the solvengenic microorganism. Recently, it has been shown that the overall cost can be even further reduced by four-fold using a one-step consolidated bioprocessing (CBP) of lignocellulose to ethanol, where

cellulase production, cellulose hydrolysis, and sugar fermentation all occur in one reactor (Lynd et al., 2005).

Numerous attempts have been made to create recombinant organisms for CBP. One way is to create recombinant cellulolytic microorganisms that naturally give high product yields, such as the historical ethanol producer, *Saccharomyces cerevisiae*, but into which cellulolytic systems were engineered. Since in a CBP setting, energies are intensively limited due to the anaerobic condition that favors product formation, a cellulolytic system that can maximize the catalytic efficiency of cellulose hydrolysis using only a limited amount of enzymes would be of great interest.

Many anaerobic bacteria have developed an elaborately structured multienzyme complex on the cell surface for efficient cellulose hydrolysis, called the cellulosome. The main feature of this nanomachine is a structural scaffoldin consisting of at least one cellulose-binding domain (CBD) and repeating cohesin domains, which are docked individually with a different cellulases tagged with a corresponding dockerin domain. This highly ordered structure allows the assembly of multiple enzymes in close proximity, mediated by the high-affinity protein-protein interaction ($>10^{-9}$ M) between the dockerin and cohesin modules, resulting in a high level of enzyme-substrate-microbe synergy.

Our group has functionally displayed different mini-cellulosomes on the yeast surface either by *in vitro* assembly or by intercellular complementation (Tsai et al., 2009; Tsai et al., 2010). In resting-cell cultures, these engineered yeast strains were able to hydrolyze phosphoric acid swollen cellulose (PASC) and produced up to 3-fold higher level of ethanol than using free enzymes. Recently, we demonstrated the ability of this

consortium for simultaneous growth and ethanol production using PASC as the sole carbon source (Goyal et al., In Press). Again, a 3-fold higher ethanol production was observed using the consortium displaying the mini-cellulosome than a similar yeast consortium secreting only the three cellulases.

Even though the ethanol production level is relative modest using our existing yeast consortium, this is due to the low enzyme density on the displayed mini-cellulosome. As natural cellulosomes contain up to 20 or more enzymes, we believe that the use of more complex cellulosome structures is the key to increasing the overall ethanol production level. In nature, an exquisitely diverse set of cellulosome structures is employed. Instead of just using a single scaffoldin and numerous dockerin-carrying enzymes as in the case of *Clostridium cellulovorans* (Shoseyov and Doi, 1990) and *Clostridium cellulolyticum* (Faure et al., 1989), some bacteria, such as *Acetivibrio cellulolyticus* (Xu et al., 2003) and *Bacteroids cellulosolvans* (Ding et al., 2000), exhibit a more complex cellulosome structure, in which several adaptor scaffoldins were found in addition to the surface-anchored scaffoldin. These adaptor scaffoldins serve to amplify the number of enzymatic subunits that can be incorporated into the cellulosome complex and thereby effectively increasing the overall enzyme density.

Taking a cue from nature, a four-enzyme or tetravalent cellulosome structure was created in the present study by mimicking the adaptor scaffoldin-mediated assembly strategy (Fig. 1). The resulting four-enzyme cellulosome produced 3-fold more reducing sugars and ethanol when compared to a two-enzyme cellulosome. This type of adaptive

strategy is particularly well suited for our consortium design because of the flexibility in producing different components required for the complex assembly.

MATERIALS AND METHODS

Strains, plasmids and Media

Escherichia coli strain JM109 [*endA1*, *recA1*, *gyrA96*, *thi*, *hsdR17* (r_k^- , m_k^+), *relA1*, *supE44*, Δ (*lac-proAB*)] was used as the host for genetic manipulations. *E. coli* BL21 (DE3) [F^- *ompT gal hsdS_B* ($rB^- mB^-$) *dcm lon* λ DE3] and *E. coli* BL21-Gold (DE3) [F^- *ompT gal hsdS_B* ($rB^- mB^-$) *dcm lon* λ DE3] *E. coli* BL21 (DE3) [F^- *ompT gal hsdS_B* ($rB^- mB^-$) *dcm*⁺ Tet^r λ DE3 *endA Hte*] were used as production host for cellulases and adapters expressions. *Saccharomyces cerevisiae* strain EBY100 [*MATa AGA1::GAL1-AGA1::URA3 ura3-52 trp1 leu2_1 his3_200 pep4::HIS3 prb1_1.6R can1 GAL*] was used for surface display of anchor protein. All *E. coli* cultures were grown in Luria-Bertani (LB) medium (10.0 g/L tryptone, 5.0 g/L yeast extract, 10.0 g/L NaCl), supplemented with either 100 μ g/mL ampicillin or 50 μ g/mL karamycin. All yeast cultures were grown in SDC medium (20.0 g/L dextrose, 6.7 g/L yeast nitrogen base without amino acids, 5.0 g/L casamino acids).

Plasmid pCTCON2 (Boder and Wittrup, 1997) was used to construct the surface displayed anchoring scaffoldin containing two cohesins from *A. cellulolyticus* (Genebank Accession No. AF155197) and *B. cellulosolvans* (Genebank Accession No. AF224509). Synthetic genes encoding sequences of a pair of cohesion and dockerin from *A. cellulolyticus*, and another pair of cohesion and dockerin from *B. cellulosolvans* were purchased from GenScript (Piscataway, New Jersey, USA). After digesting with restriction enzymes *NdeI* and *SallI*, the cohesins coding fragment was ligated into plasmid pCTCON2 to create an in-frame fusion C-terminal to the AGA2 gene. The resulting

plasmid pCohAcBc was under the control of a galactose inducible promoter and flanked with a *C-myc* tag at the c-terminus of the anchor protein, which facilitates the confirmation of protein translocation via immunofluorescence.

The construction of adaptor scaffoldin which contain a dockerin of *A. cellulolyticus* or *B. cellulosolvans*, a cohesin of *R. flavesfaciens*, a cohesin of *C. thermocellum* and a cellulose binding module (CBM) is described as follows. The dockerins of *A. cellulolyticus* and *B. cellulosolvans* were obtained from the synthetic genes by digesting with restriction enzymes *SacI* and *NotI*. The resulting fragments were then cloned into the same sites of expression vector pET24a to generate pDockAc and pDockBc. The sequence encoding a dockerin of *R. flavesfaciens*, a dockerin of *C. thermocellum* and a CBM was obtained using plasmid pScaf-ctf (Tsai et al., 2009) as template by PCR using forward primer F2Coh1CBM (5'-GCTAGCTAGCGCTACGGCTACGCCC-3') and reverse primer R2Coh1CBM (5'-GCTAGAGCTCCTTAACAATGATAGCGCCAT-3'). The PCR product was further digested and ligated into the *NheI* and *SacI* sites of vectors pDockAc and pDockBc to form pETAdpA and pETAdpB.

Recombinant endoglucanase was constructed by fusion the endoglucanase CelG from *C. cellulolyticum* with the dockerin from *C. thermocellum* as described below. The catalytic domain of CelG was amplified by PCR using pETGt (Fierobe et al., 2005) as template with primers FCelG (5'-GCTAGCTAGCGGAACATATAACTATGGAGAAGCATTACAG-3') and RCelG (5'-GCATGCGGCCGCAGGAACGAGCTTTGTGC-3'). The PCR product was then digested with *NheI* and *NotI* and ligated into

the same restriction sites of plasmid pET24a to generate pETCelGΔDock. The dockerin from *C. thermocellum* was obtained by PCR using pETAt (Tsai et al., 2009) as template with primers FDockCt (5'-GCTAGCGGCCGCAACTTCCCGAATCCTTTGAGTGAC-3') and RDockCt (5'-GCTACTCGAGATAAGGTAGGTGGGGTATGC -3'). The resulting fragment was further digested with *NotI* and *XhoI* and then cloned into pETCelGΔDock to form pETGt. The construction of plasmid pBglAf encoding a β -glucosidase from *C. thermocellum* and a dockerin of *R. flavesfaciens* was described elsewhere (Tsai et al., 2009).

Display of anchor protein on yeast surface

For the display of anchoring scaffoldin on the yeast surface, yeast cells harboring pCohAcBc were pre-cultured in SDC medium for 18 h at 30°C. These pre-cultures were further washed with SDC medium (20.0 g/L galactose, 6.7 g/L yeast nitrogen base without amino acids, 5.0 g/L casamino acids) once and then sub-inoculated into 200 mL SGC medium at an optical density (OD₆₀₀) of 0.5 and grown for 48 h at 20°C.

Expression of adaptor scaffoldins and dockerin-tagged cellulases

E. coli strains BL21 (DE3) expressing the adaptor scaffoldins AdpA and AdpB, and the recombinant β -glucosidase BglAf were pre-cultured overnight at 37°C in LB medium supplemented with appropriate antibiotics. The pre-cultures were sub-inoculated in 200 mL LB medium supplemented with 1.5% glycerol and appropriate antibiotics at an initial OD of 0.01 and incubated at 37°C until the O.D. reached 1.5. The cultures were

then cooled to 20°C, and isopropyl thio- β -D-galactoside (IPTG) was added to a final concentration of 100 μ M. After 16 h, cells were harvested by centrifugation (3000Xg, 10 min) at 4°C, resuspended in buffer A (50 mM Tris-HCl pH 8.0, 100 mM NaCl, and 10 mM CaCl₂), and lysed with a sonicator.

For the expression the recombinant endoglucanase CelGt, *E. coli* strains BL21-Gold (DE3) harboring pCelGt were pre-cultured overnight at 37°C in LB medium supplemented with appropriate antibiotics. The pre-cultures were sub-inoculated in 200 mL LB medium supplemented with 1.5% glycerol and appropriate antibiotics at an initial OD of 0.01 and incubated at 37°C until the O.D. reached 1.5. The cultures were then put in ice for 30 min and then 15°C for another 30min without shacking, IPTG was added to a final concentration of 100 μ M and the cell culture was kept at 15°C with shacking for 18 h. The cells were harvested by centrifugation (3000Xg, 10 min) at 4°C, resuspended in buffer A, and lysed with a sonicator.

Assembly of complex cellulosome of the yeast surface

To assemble the cellulosomes, cell lysates containing one or both of the adaptor scaffoldin were incubated with yeast cells displaying the anchor for 1 h at 4°C in buffer A. After incubation, cells were washed and harvested by centrifugation (3000Xg, 10 mins) at 4°C and resuspended in the same buffer with higher adapter concentration. Similar procedure with increased adapter concentrations was repeated trice in order to saturate all the cohesins on the anchoring protein. Thereafter, the yeast cells displaying the anchoring scaffoldin saturated with adapters were than incubated with cell lysates containing CelGt

or BglAf for 1 h at 4°C in buffer A. Similarly, three repeats with increased protein concentration were conducted to force the saturation.

Immunofluorescence microscopy

The procedure of immunofluorescence assay for checking the translocation of the anchoring scaffoldin and the assembly of the adaptor scaffoldins and enzymes was similar to that described by Tsai and colleagues (Tsai et al., 2009). Yeast cells displaying anchoring proteins or the cellulosomes on the surface were harvested by centrifugation, washed with PBS buffer (8 g/L NaCl, 0.2 g/L KCl, 1.44 g/L Na₂HPO₄, 0.24 g/L KH₂PO₄), and resuspended in 250 µL of PBS buffer containing 1 mg/mL BSA, and 0.5 µg of anti-C-Myc or anti-C-His IgG (Applied Biological Materials Inc) for 2 h with occasional mixing. Cells were then pelleted and washed with PBS before resuspending in PBS buffer plus 1 mg/mL BSA and 0.5 µg anti-mouse IgG conjugated with Alexa 488 (Molecular Probes). After incubating for 1 h, cells were pelleted and washed twice with PBS, followed by resuspension in PBS buffer to an OD₆₀₀ of 1. For fluorescence microscopy (Olympus BX51), 5-10 µL of cell suspensions were spotted on slides and a cover slip was added. Images from Alexa 488 were captured using the QCapture Pro6 software. Whole cell fluorescence was measured using a fluorescent microplate reader (Synergy4, BioTek, VT) with an excitation wavelength at 485 nm and an emission wavelength at 535 nm.

Enzyme assays

Carboxymethyl cellulose (CMC) was obtained from Sigma and used as a substrate. Phosphoric acid swollen cellulose (PASC) was prepared from Avicel PH101 (Sigma) according to the method of Walseth (27). Enzyme activity was assayed in the presence of a 0.3% (wt/vol) concentration of cellulose at 30°C in 20 mM Tris-HCl buffer (pH 6.0). Samples were collected periodically and immediately mixed with 3 mL of DNS reagents (10 g/L dinitrosalicylic acid, 10 g/L sodium hydroxide, 2 g/L phenol, 0.5 g/L sodium sulfite). After incubating at 95°C for 10 minutes, 1 mL of 40% Rochelle salts was added to fix the color before measuring the absorbance of the supernatants at 575 nm. Glucose concentration was determined using a glucose HK assay kit from Teco Diagnostic (Anaheim, California, USA).

Fermentation

Fermentation was conducted anaerobically at 30°C. Briefly, yeast cells were washed once with buffer containing 50 mM Tris-HCl, pH 8.0, 100 mM NaCl, and 10 mM CaCl₂ and resuspended in SDC medium containing 6.7 g/L yeast nitrogen base without amino acids, 20 g/L casamino acids, and 10 g/L PASC as the sole carbon source. Reducing sugars and glucose concentration were measured by the methods described above. The amount of residual cellulose was measured by the phenol-sulfuric acid method as described by Dubois et al (10). Ethanol concentration was measured by the gas chromatography (model 7890, Agilent, USA) using a flame ionization detector and HP-5 column.

RESULTS AND DISCUSSION

Design strategy of adaptive assembly

Previously we have developed a synthetic yeast consortium for cellulosic ethanol production. Even though the resulting consortium showed the ability to grow and produce ethanol by hydrolyzing PASC, the final ethanol level of 1.2 g/L was relatively modest. To further elevate the production rate, we sought to create a designer cellulosome with a higher enzyme density. Rather than simply extending the number of cohesin domains on the displayed scaffoldin, our design is based on an adaptive assembly strategy. This adaptive strategy was chosen primarily based on the improper folding problems encountered during the display of more complex scaffoldin structures containing more than three cohesin domains and the flexibility in synthesizing the different components for the assembly using the yeast consortium system. The initial design is composed of an anchoring scaffoldin (AnScf) containing the two cohesin domains from *A. cellulolyticus* and *B. cellulosolvans* that is functionally displayed on the yeast surface using the glycosylphosphatidylinositol (GPI)-anchor (Boder and Wittrup, 1997). A c-Myc tag is added to the C-terminus of the anchoring scaffoldin to allow for immuno-probing. To enable the display of a larger number of cohesin domains, two adaptor scaffoldins (AdpA and AdpB) containing either the dockerin domain of *A. cellulolyticus* or *B. cellulosolvans*, a cohesin domain of *R. flavesfaciens* (f), a cohesin domain of *C. thermocellum* (t) and a cellulose-binding module (CBM) can then associate with the surface bound Anscf to extend the structure. A hexahistidine tag (his-tag) is added at the C-terminus of each adaptor scaffoldin for immuno-probing. Finally, a recombinant endoglucanase CelG

tagged with a dockerin domain from *C. thermocellum* (Gt) and a β -glucosidase BglA tagged with a dockerin domain from *C. thermocellum* (Bglf) can be loaded onto the extended structure to form a four-enzyme or tetravalent cellulosome structure on the yeast surface.

Functional display of the anchoring scaffoldin on the yeast surface

To display the anchoring scaffoldin Anscf, the entire scaffold was fused to the Aga2p subunit of a-agglutinin (Shen et al. 2001) in a fashion similar to that used in our prior yeast display studies (Tsai et al., 2009). The correct translocation of Anscf on the yeast surface was confirmed by immunofluorescent labeling using the anti c-Myc sera and Alexa 488 conjugated goat anti-mouse IgG. As shown in Figure 4.2, bright fluorescence was observed with cells displaying Anscf, while no significant fluorescence was detected on the control cells. Typically, a detectable fluorescence signal could be observed for 60-75% of the cells after induction, indicating around 60-75% of the cells displaying Anscf on the surface. This is consistent with other reports when the Aga1-Aga2 anchor system was used for surface display. (Boder and Wittrup, 1997; Kieke et al., 1997; Goyal et al., 2011)

Expression of the adaptor scaffoldins and their functional docking onto the anchoring scaffoldin

The two adaptor scaffoldins were expressed in *E. coli* strain BL21 Gold under control of a strong T7 promoter. Production of both adaptors was confirmed through

SDS-PAGE by detecting the presence of a protein band of the appropriate size (Figure 4.3A). To confirm the expression of full length proteins, the existence of the His tag at the C-terminus of both adaptor scaffoldins was examined by Western-blot analysis (Figure 4.3B). For both adaptors, only one band, located at the expected molecular weight, was presented after blotting, indicating the successful expression of full length proteins.

To confirm the proper folding of both adaptors, we further investigated the amenability of the resultant hybrid proteins for affinity- purification on cellulose via their CBM (Barak et al., 2005). This purification procedure could be accomplished by batch adsorption to and desorption from cellulose matrices. Although several partially degraded products were observed after purification during SDS-PAGE analysis, the only band detected by Western-blotting was located at the calculated molecular weight for both adaptors (Figure 4.3A and 4.3B). Collectively, these results indicated that (1) both adaptors appeared to be properly folded as they retained the ability to bind to Avicels via the CBM, and (2) the only portion that could bind onto the surface-displayed anchoring scaffoldin were full length proteins.

To test whether the adaptor scaffoldins can correctly associate with the surface displayed anchoring scaffoldin, additional immunofluorescence studies were performed. A monoclonal anti-His tag antibody, which recognizes the hexa-histidine epitope at the C-terminus of the adaptor scaffoldins, was labeled with Alexa 488 conjugated goat anti-mouse IgG for immunofluorescence staining. As can be seen in Figure 4.4, yeast cells incubated with either one of the two adaptors showed a significant increase in the whole-

cell fluorescence, indicative of adaptor binding. More importantly, a similar level of fluorescence was detected from the c-Myc tag and His tag indicating the correct 1:1 binding between the anchoring and adaptor scaffoldin pairs. When these yeast cells were further incubated with the other adaptor scaffoldin, an additive amount of fluorescence was detected. Taken together, these results indicated several important facts: (1) the two adaptor scaffoldins successfully associated with the surface-displayed anchoring scaffoldin, (2) no cross association occurred for the two different dockerin-cohesin pairs since a comparable level of fluorescence was detected when only one adaptor was added, and (3) the steric hindrance between the two adaptor scaffoldins was negligible since a two-fold increase in fluorescence was detected in the presence of a second adaptor scaffoldin.

Functional assembly of the complex cellulosome

After proving the functionality of the anchoring scaffoldin and the dockerin domains on the adaptors, another important aspect of the adaptor scaffoldins is their ability to recruit cellulases into the cellulosome structure through the specific dockerin-cohesin interaction. Cells displaying the anchoring scaffoldin were first saturated with either one or both adaptor scaffoldins as described above. *E. coli* lysates containing either Gt or Bglf were then used for the enzyme assembly. Again, quantitative assessment of enzyme docking was performed by whole-cell immunofluorescence measurements by probing the His tag fused to the C-terminus of the enzymes. As shown in Figure 4.5A, binding of Gt was confirmed by a 2-fold increase in the whole-cell fluorescence when

cells saturated with only one adaptor scaffoldin was incubated with Gt. More importantly, an approximate 4-fold increase in fluorescence intensity was observed when Gt was bound onto the cells possessing both adaptor scaffoldins on their surface, indicating the docking of two Gt per cell. Similarly, the functionality of *R. flavefaciens* cohesin in the two adaptors was confirmed by detecting the binding of Bglf. A two- or four-fold increase in fluorescence intensity was detected, respectively, when yeast cells possessing either one adaptor or two adaptors were used for Bglf docking (Figure 4.5B). Collectively, these results confirm the correct docking of both enzymes onto the adaptor scaffoldins.

With the successful docking of both enzymes individually onto the adaptor scaffoldins, the feasibility of docking both enzymes side by side onto both adaptors was further examined. For this purpose, immunofluorescence assay probing the recognition tags in several combinations was performed, including (1) the anchoring scaffoldin Anscaf displayed cells, (2) Anscaf displayed cells incubated with *E. coli* lysate containing the adaptor scaffoldin AdpA, (3) Anscaf displayed cells incubated with *E. coli* lysate containing both adaptor scaffoldins AdpA and AdpB, (4) Anscaf displayed cells incubated with *E. coli* lysate containing the adaptor scaffoldin AdpA and the two enzymes Gt and Bglf, and (5) Anscaf displayed cells incubated with *E. coli* lysate containing both adaptor scaffoldins AdpA and AdpB and the two enzymes Gt and Bglf. As is evident from Figure 4.5C, a 2-fold increase in the whole-cell fluorescence when cells possessing the two adaptor scaffoldins were saturated with the two enzymes compared to the one possessing only one enzyme-saturated adaptor scaffoldin,

demonstrating the correct side-by-side docking of both enzymes onto the adaptor scaffoldins.

Synergistic effect of the complex cellulosome

The synergistic effect on cellulose hydrolysis is the most intriguing property of naturally occurring cellulosomes and artificial cellulosome. (Lu et al., 2006; Fierobe et al., 2005; Tsai et al., 2009). This can be attributed to either direct substrate channeling, substrate targeting, and/or enzyme proximity (Bayer et al., 2007). In nature, a heterogeneous subpopulation of cellulosomes that is morphologically and functionally different is detected even during growth on a single substrate (Doi et al., 2003; Han et al., 2005; Fendri et al., 2009). This observation suggests that the ability to maintain enzyme proximity may be more important than the precise enzyme ordering in the overall enzyme synergy. In the present study, the effect of enzyme density and proximity on the synergism of cellulose hydrolysis and ethanol production was further investigated using our adaptive cellulosomal structures.

Initially, PASC hydrolysis by resting cells was compared using different cellulosomal structures (Figure 4.6). In the first setup (S1), 50% of the yeast cells were docked with the two adaptor scaffoldins but no enzymes. The second setup (S2) contained 50% of the yeast cells displaying a defective divalent cellulosome in which enzymes were recruited only to one adaptor (AdpA). In the third setup (S3), all cells displayed a defective divalent cellulosome, effectively doubling the bulk enzyme density than in S2. The last setup (S4) contained 50% of the yeast cells displaying a complete

tetravalent cellulosome in which enzymes were recruited into both adaptors (AdpA and AdpB); this setup provides the same enzyme density as in S3 except that all enzymes are presented in close proximity in the tetravalent cellulosome. Other than S3, the rest of the population was composed of cells displaying only the anchoring scaffoldin.

Figure 4.7 shows the time course of reducing sugars and glucose released from PASC hydrolysis using different setups. A possessive endoglucanase CelG was used in concert with β -glucosidase in order to convert more than 50% of the released sugar oligomers to glucose as reported (Gal et al., 1997). As depicted in Figure 4.7A and 4.7B, cells displaying the divalent cellulosome (S2) exhibited a significantly higher rate of reducing sugars and glucose released from PASC hydrolysis than the control cells (S1). When the number of yeast cells displaying the divalent cellulosome was increased from 50% (S2) to 100% (S3), which corresponds to a 2-fold increase in the bulk enzyme density, a two-fold increase in reducing sugar and glucose liberation was also observed. In comparison, cells displaying the tetravalent cellulosome (S4) exhibited a 1.5-fold increase in both the reducing sugars and glucose production compared to S3. Since the same amount of enzymes was maintained in S3 and S4, this further increase by S4 clearly demonstrates the importance of enzyme proximity in improving cellulose hydrolysis.

Direct fermentation of amorphous cellulose to ethanol

The level of ethanol production from PASC was compared for the different setups in resting cell fermentation. While glucose inhibition of β -glucosidase is well documented in a resting cell experiments (Wong, 1995; Demain et al., 2005; Tsai et al.,

2009), this inhibition can be eliminated by the quick glucose uptake during fermentation. As shown in Fig 6, the increase in ethanol production was accompanied by a concomitant decrease in the total sugar concentration. The level of ethanol production and PASC hydrolysis were directly correlated to the trend observed in the resting cell experiment. The maximum ethanol production for S4 was 1.9 g/L after 72 h. This corresponds to ~90% of the theoretical ethanol yield. Moreover, no detectable glucose accumulation in the medium was observed, indicating the quick uptake of glucose by the cells. The level of ethanol production for S3 was two-fold lower than S4, consistent with the resting-cell hydrolysis experiment. More importantly, the higher level of enzyme synergy afforded by the tetravalent cellulosomal design resulted in more than 4-fold improvement in the ethanol production when compared to the divalent structure in S2. This non-linear scaling in enzyme synergy provided by enzyme clustering is perhaps the main reason why natural cellulosomes are all multivalent in nature. It is clear that the more practical utility of synthetic cellulosomes is not to simply increase the overall enzyme loading but to harness the non-linear nature of synergy by increase the overall enzyme density and proximity.

In conclusion, a complex tetravalent cellulosome was developed for enhanced cellulose hydrolysis and ethanol production using an adaptive assembly strategy. The engineered yeasts possessing a complete tetravalent cellulosome on the surface exhibited a 4-fold increase in ethanol production than those displaying a defective divalent cellulosome, indicating the crucial role of enzyme proximity on the cellulosomal synergy. The unique feature of the anchoring and the adaptor scaffoldin strategy to amplify the number of enzymatic subunits can be easily extended into more complex cellulosomal

structures in order to achieve the higher level of enzyme synergy. Although this is a proof-of concept study, to our best knowledge, it is the first report that manifested the benefit of increasing local enzyme density over bulk enzyme density in cellulosome systems for cellulose hydrolysis.

REFERENCES

1. **Barak, Y., T. Handelsman, D. Nakar, A. Mechaly, R. Lamed, Y. Shoham, and E. A. Bayer.** 2005. Matching fusion protein systems for affinity analysis of two interacting families of protein: the cohesin-dockerin interaction. *J Mol Recognit* **18**:491-501.
2. **Bayer, E. A., R. Lamed, and M. E. Himmel.** 2007. The potential of cellulases and cellulosomes for cellulosic waste management. *Curr Opin Biotechnol* **18**:1-9.
3. **Boder, E. T., and K. D. Wittrup.** 1997. Yeast surface display for screening combinatorial polypeptide libraries. *Nat Biotechnol* **15**:553-557.
4. **Demain, A. L., M. Newcomb, and J. H. D. Wu.** 2005. Cellulase, clostridia, and ethanol. *Microbiol Mol Biol Rev* **69**:124-154.
5. **Ding, S.-Y., E. A. Bayer, D. Steiner, Y. Shoham, and R. Lamed.** 2000. A scaffoldin of the *Bacteroides cellulosolvens* cellulosome that contains 11 type II cohesins. *J Bacteriol* **182**:4915-4925.
6. **Doi, R. H., A Kosugi, K. Murashima, Y. Tamaru, and S. O. Han.** 2003. Cellulosomes from mesophilic bacteria. *J Bacteriol* **185**:5907–5914.
7. **Faure, E., A. Belaich, C. Bagnara, C. Gaudin, J. -P. Belaich.** 1989. Sequence analysis of the *Clostridium cellulolyticum* endoglucanase-A-encoding gene, *celCCA*. *Gene* **84**:39-46.
8. **Fendri, I., C. Tardif, H. -P. Fierobe, S. Lignon, O. Valette, S. Pagès, and S. Perret.** 2009. The cellulosomes from *Clostridium cellulolyticum*- Identification of new components and synergies between complexes. *FEBS J* **276**:3076-3086.

9. **Fierobe, H. P., F. Mingardon, A. Mechaly, A. Belaich, M. T. Rincon, S. Pages, R. Lamed, C. Tardif, J. P. Belaich, and E. A. Bayer.** 2005. Action of designer cellulosomes on homogeneous versus complex substrates - Controlled incorporation of three distinct enzymes into a defined trifunctional scaffoldin. *Biol Chem* **280**:16325-16334.
10. **Goyal, G., S. -L. Tsai, N. Da Silva, and W. Chen.** 2011. Simultaneous cell growth and ethanol production from cellulose by an engineered yeast consortium displaying a functional mini-cellulosome. *Microb Cell Factories* **10**:89.
11. **Gal, L., C. Gaudin, A. Belaich, S. Pages, C. Tardif, and J. -P. Belaich.** 1997. CelG from *Clostridium cellulolyticum*: a multidomain endoglucanase acting efficiently on crystalline cellulose. *J Bacteriol* **179**:6595-6601.
12. **Han S. O., H. Yukawa, M. Inui, and R. H. Doi,** 2005. Effect of carbon source on the cellulosomal subpopulations of *Clostridium cellulovorans*. *Microbiol* **5**:1491-1497.
13. **Hardiman E., M. Gibbs, R. Reeves, and P. Bergquist.** 2010. Directed evolution of a thermophilic beta-glucosidase for cellulosic bioethanol production. *Appl Biochem Biotechnol* **161**:301-312.
14. **Himmel, M. E., Q. Xu, Y. Luo, S. Y. Ding, R. Lamed, and E. A. Bayer.** 2010. Microbial enzyme systems for biomass conversion: emerging paradigms. *Biofuels* **1**:323-341.
15. **Hisano, H., R. Nandakumar, and Z. Y. Wang.** 2009. Genetic modification of lignin biosynthesis for improved biofuel production. *In Vitro Cell Dev Biol-Plant* **45**:306-313.

16. **Keike, M. C., B. K. Cho, E. T. Boder, D. M. Kranz, and K. D. Wittrup.** 1997. Isolation of anti-T cell receptor scFv mutants by yeast surface display. *Protein Eng* **10**:1303-1310.
17. **Li, Y. C., D. C. Irwin, D. B. Wilson.** 2010. Increased crystalline cellulose activity via combinations of amino acid changes in the family 9 catalytic domains and family 3c cellulose binding module of *Thermobifida fusca* Cel9A. *Appl Environ Microbiol* **76**:2582-2588.
18. **Lu, Y. P., Y. H. P. Zhang, and L. R. Lynd.** 2006. Enzyme-microbe synergy during cellulose hydrolysis by *Clostridium thermocellum*. *Proc Natl Acad Sci USA* **103**:16165-16169.
19. **Lynd, L. R., P. J. Weimer, W. H. van Zyl, and I. S. Pretorius.** 2002. Microbial cellulose utilization: fundamentals and biotechnology. *Microbiol Mol Biol Rev* **66**:506-577.
20. **Lynd, L. R., W. H. van Zyl, J. E. McBride, and M. Laser.** 2005. Consolidated bioprocessing of cellulosic biomass: an update. *Curr Opin Biotechnol* **16**:577-583.
21. **Shen, Z. M., L. Wang, J. Pike, C. K. Jue, H. Zhao, H. de Nobel, J. Kurjan, and P. N. Lipke.** 2001. Delineation of functional regions within the subunits of the *Saccharomyces cerevisiae* cell adhesion molecule a-agglutinin. *J Biol Chem* **276**:15768-75.
22. **Shoseyov, O., and R. H. Doi.** 1990. Essential 170-kDa subunit for degradation of crystalline cellulose by *Clostridium cellulovorans* cellulose. *Proc Natl Acad Sci USA* **87**:2192-2195.

23. **Studer, M. H., J. D. DeMartini, S. Brethauer, H. L. McKenzie, and C. E. Wyman.** 2010. Engineering of a high-throughput screening system to identify cellulosic biomass, pretreatments, and enzyme formulations that enhance sugar release. *Biotechnol Bioeng* **105**:231-238.
24. **Tsai, S. L., G. Goyal, and W. Chen.** 2010. Surface Display of a Functional Minicellulosome by Intracellular Complementation Using a Synthetic Yeast Consortium and Its Application to Cellulose Hydrolysis and Ethanol Production. *Appl Environ Microbiol* **76**:7514-7520.
25. **Tsai, S. L., J. Oh, S. Singh, R. Z. Chen, and W. Chen.** 2009. Functional assembly of minicellulosomes on the *Saccharomyces cerevisiae* cell surface for cellulose hydrolysis and ethanol production. *Appl Environ Microbiol* **75**:6087-6093.
26. **Wong, D. W. S.** 1995. *Food Enzymes- Structure and Mechanisms*, 1st ed. Springer.
27. **Xu, Q., W. Gao, S. -Y. Ding, R. Kenig, Y. Shoham, and E. A. Bayer.** 2003. The cellulosome system of *Acetivibrio cellulolyticus* includes a novel type of adaptor protein and a cell-surface anchoring protein. *J Bacteriol* **185**:4548-4557.

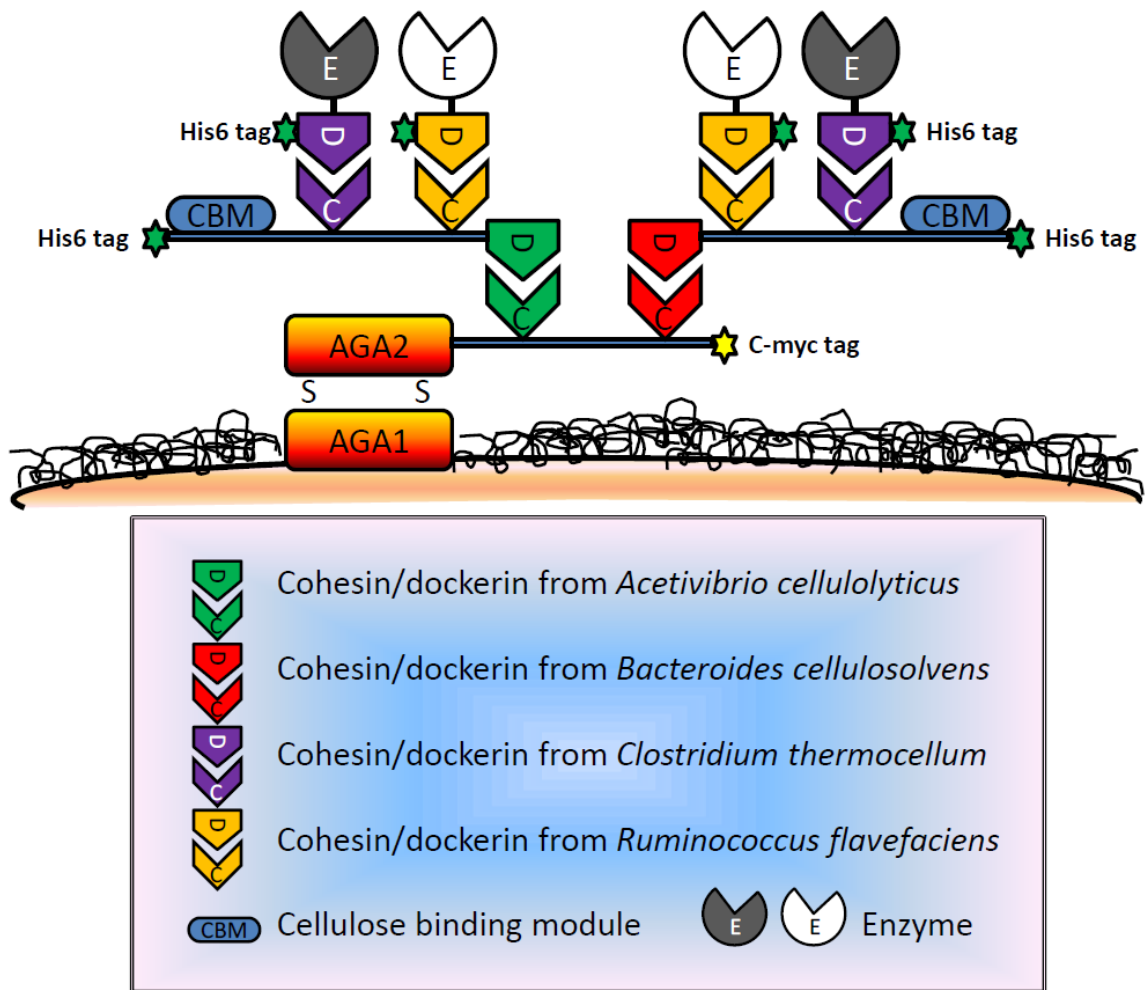


Figure 4.1. A schematic diagram of the complex cellulosome assembled on the yeast surface. Adaptor scaffoldins served as templates for enzyme recruitment are tightly attached to the yeast surface via the surface-displayed anchoring scaffoldin.

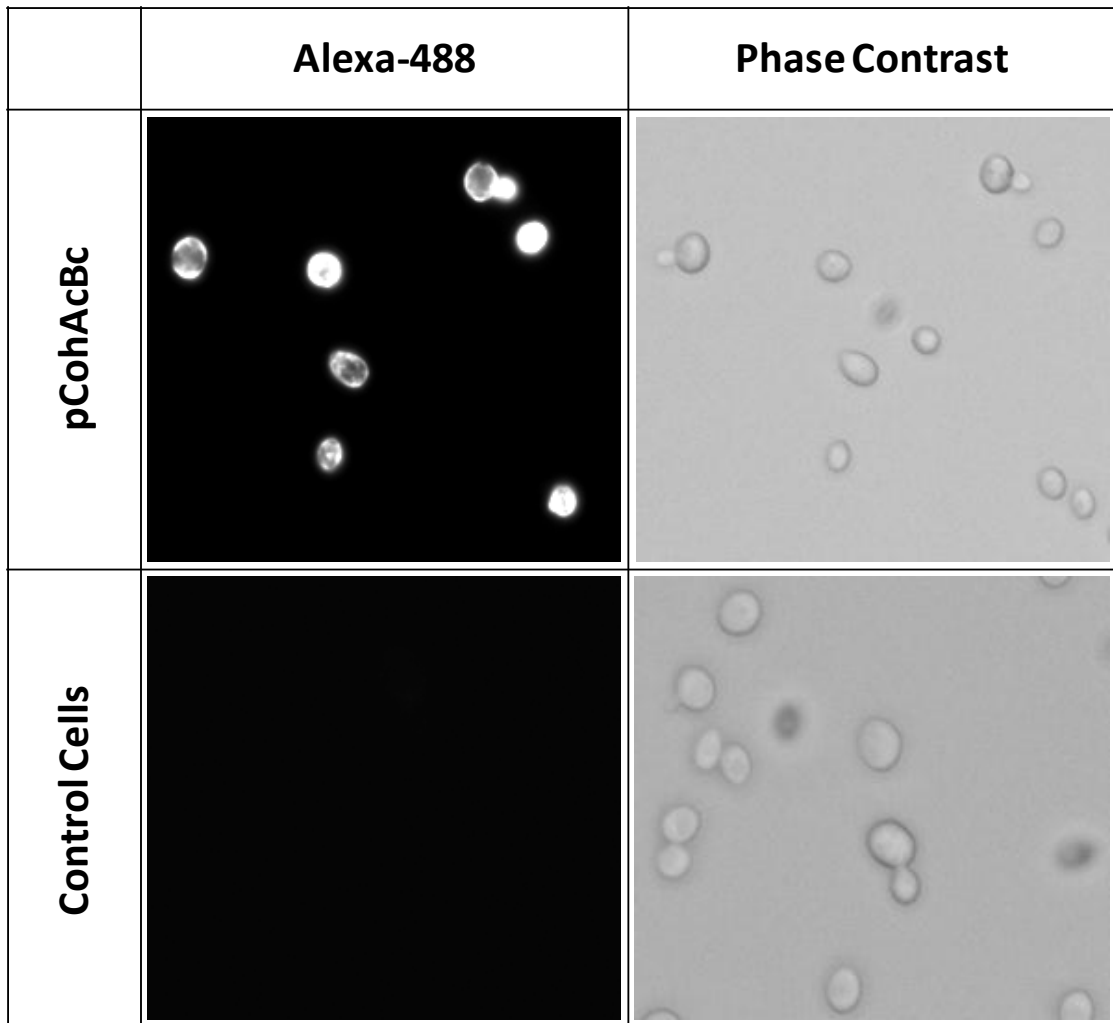


Figure 4.2. Phase-contrast micrographs and immunofluorescence micrographs of the yeast displaying the anchoring scaffoldin pCohAcBc and the control yeast. Cells were probed with anti-C-myc sera and fluorescently stained with a goat anti-mouse IgG conjugated with Alexa Fluor 488. *S. cerevisiae* EBY100 was used as control.

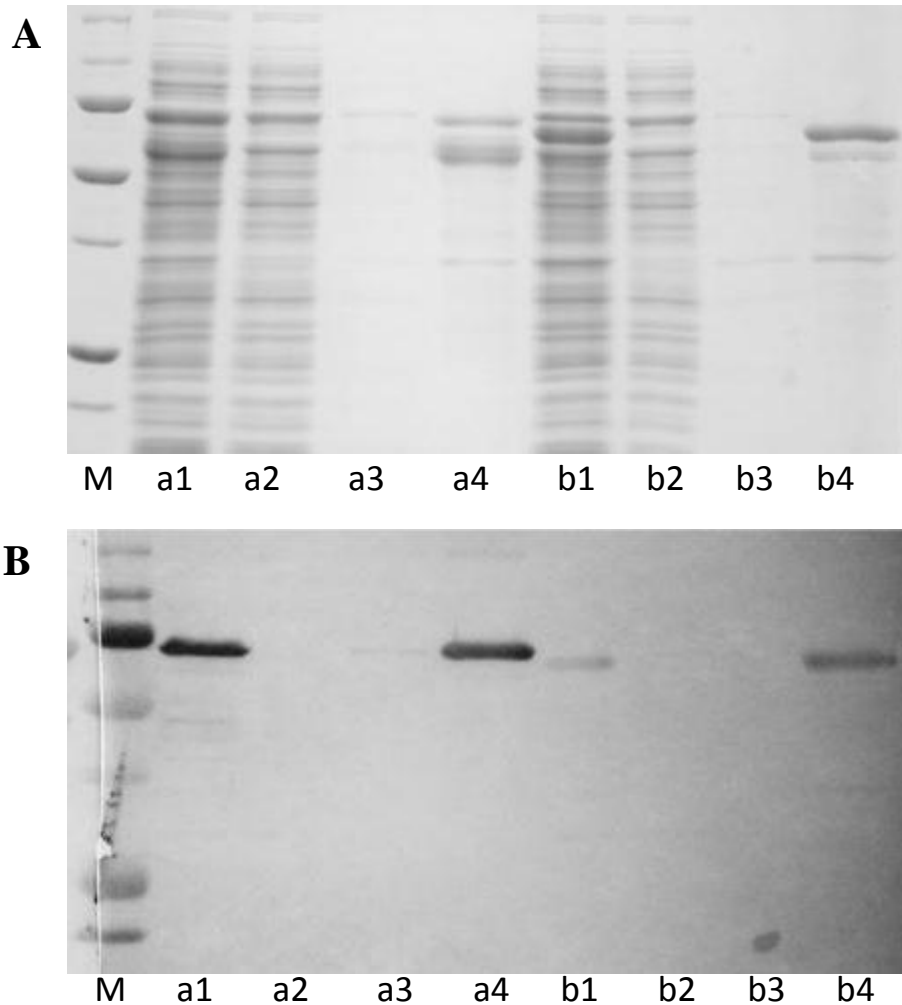


Figure 4.3. Expression and Avicel purification of adaptor scaffoldins analyzed by (A) 10% SDS-PAGE gel and (B) western-blot analysis with goat IgG-alkaline phosphatase conjugate. M, protein marker; a1, cell lysate of AdpA; a2, unbound fraction of adpA; a3, wash fraction of AdpA; a4, bound fraction of AdpA; b1, cell lysate of AdpB; b2, unbound fraction of AdpB; b3, wash fraction of AdpB; b4, bound fraction of AdpB.

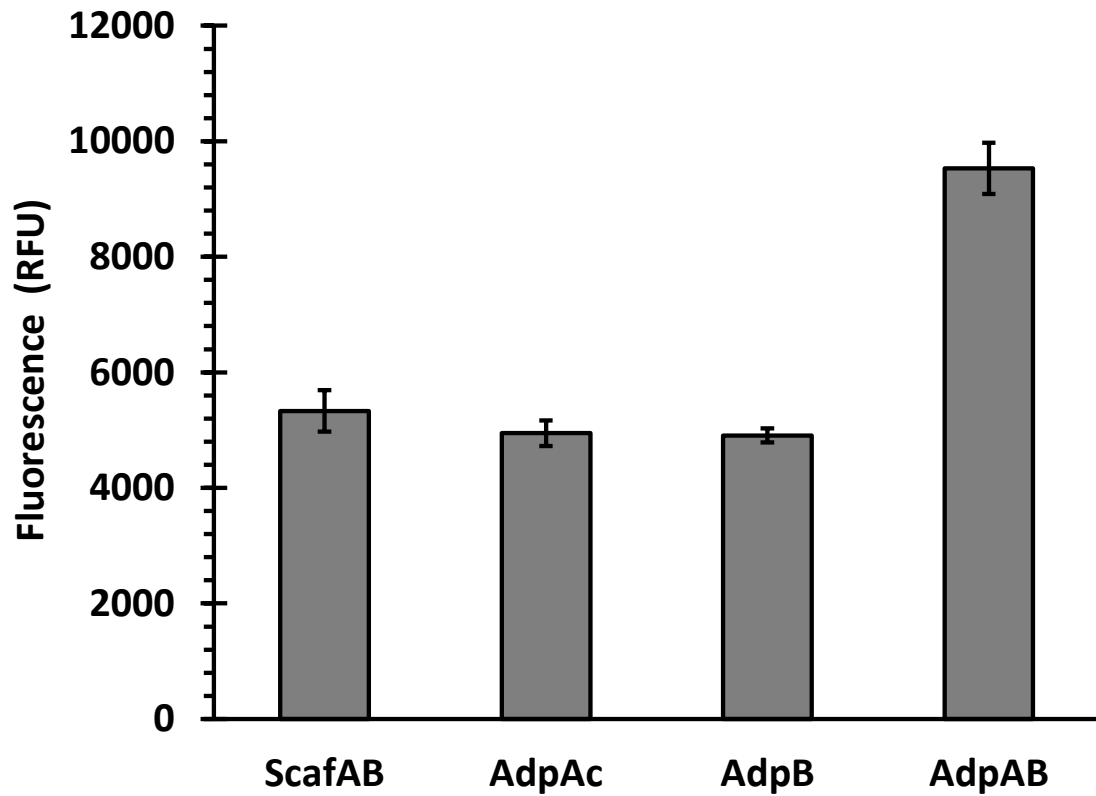


Figure 4.4. Fluorescent intensity of the anchoring scaffoldin displayed yeast after incubated with one and two adaptor scaffoldins. Cells were probed with anti-C-His6 sera and fluorescently stained with a goat anti-mouse IgG conjugated with Alexa Fluor 488. Whole cell fluorescence was determined using a fluorescent microplate reader.

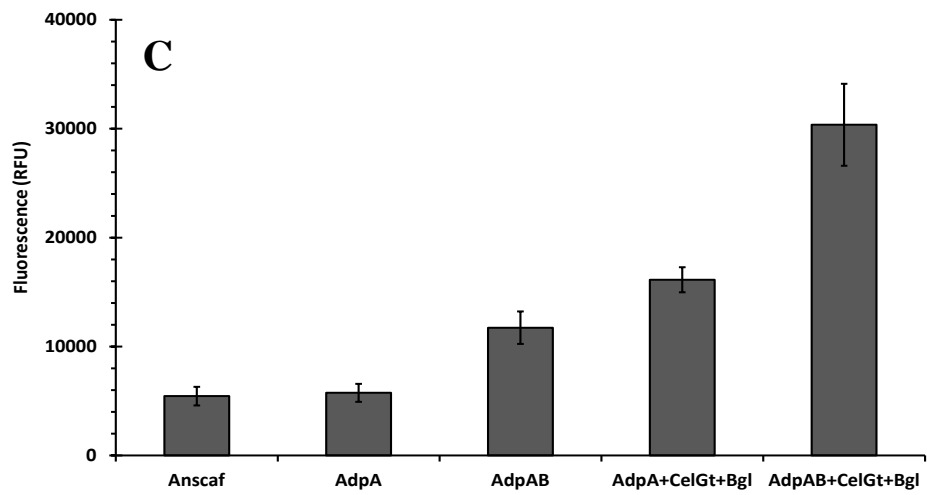
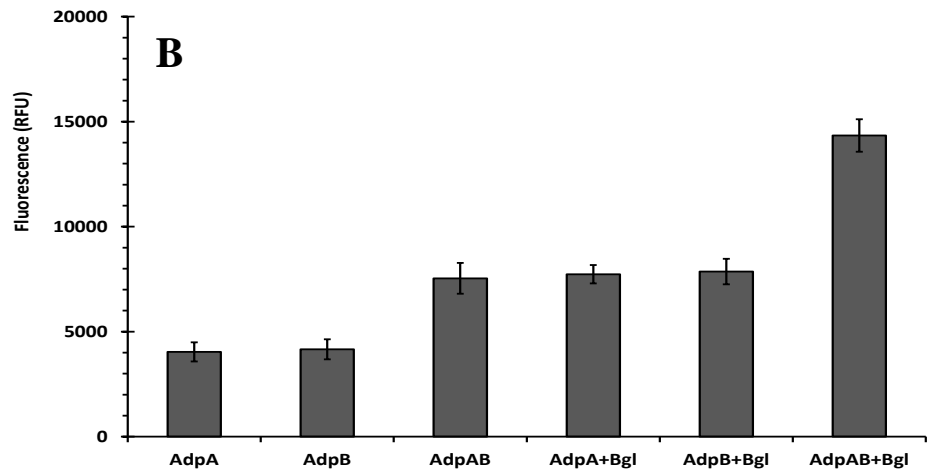
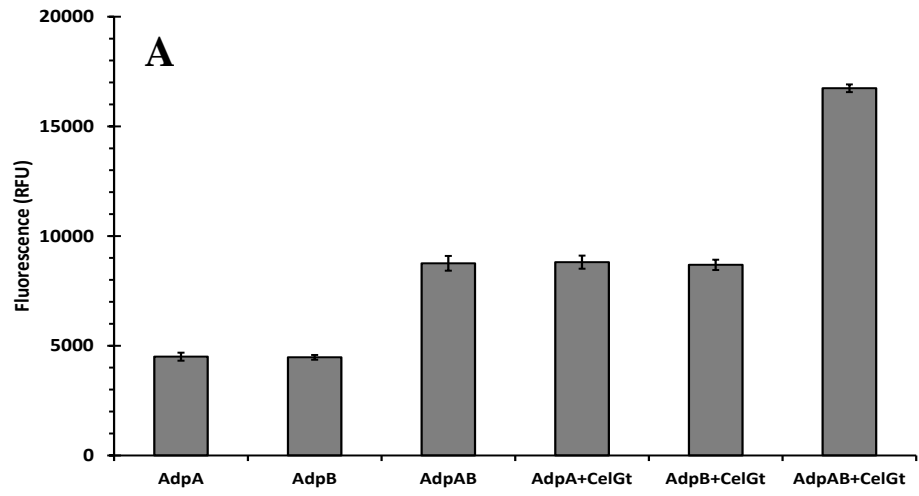


Figure 4.5. Fluorescent intensity of the anchoring scaffoldin displayed yeast after incubated with adaptor scaffoldins and (A) endoglucanase CelGt, (B) β -glucosidase BglAf or (C) both enzymes. Cells displaying Anscaf were probed with anti-C-myc sera and fluorescently stained with a goat IgG Alexa Fluor 488 conjugated. Cells after incubating with *E. coli* lysates were probed with anti-C-His6 sera and fluorescently stained with a goat anti-mouse IgG conjugated with Alexa Fluor 488. Whole cell fluorescence was determined using a fluorescent microplate reader.

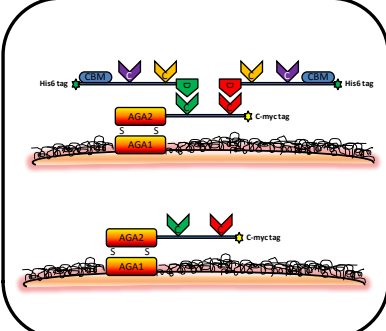
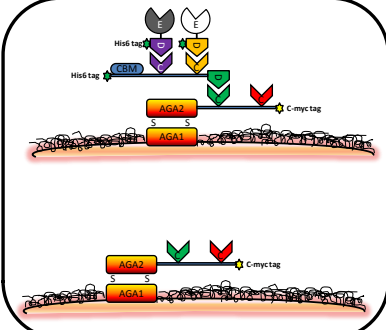
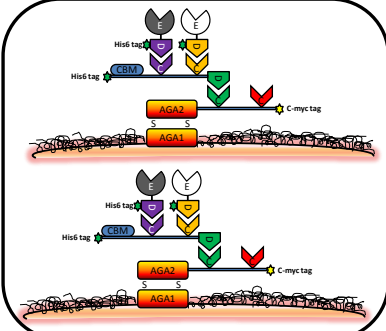
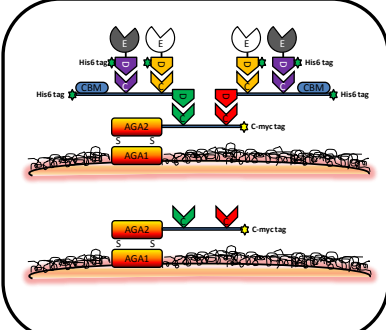
Abbreviation	Scheme	Description
S1		<p><i>Control yeast system:</i> 50% of the yeast cells were docked with the two adaptor scaffoldins but no enzymes; the rest part of the cells displayed only the anchoring scaffoldin.</p>
S2		<p><i>Defective complex-cellulosome system:</i> 50% of the yeast cells displaying a cellulosome in which only two enzymes could be recruited into the structure via the only adaptor scaffoldin (AdpA); the rest part of the cells displayed only the anchoring scaffoldin.</p>
S3		<p><i>Defective complex-cellulosome system:</i> 100% cells displayed a defective complex-cellulosome containing only one adaptor scaffoldin. In this system, the bulk enzyme density was twice of that in the S2 system.</p>
S4		<p><i>Complete complex-cellulosome system:</i> 50% of the yeast cells displaying a cellulosome in which enzymes were recruited into the structure via both of the two adaptor scaffoldins (AdpA and AdpB); the rest part of the cells displayed only the anchoring scaffoldin.</p>

Figure 4.6. Illustration of the different cellulosome systems used in this research.

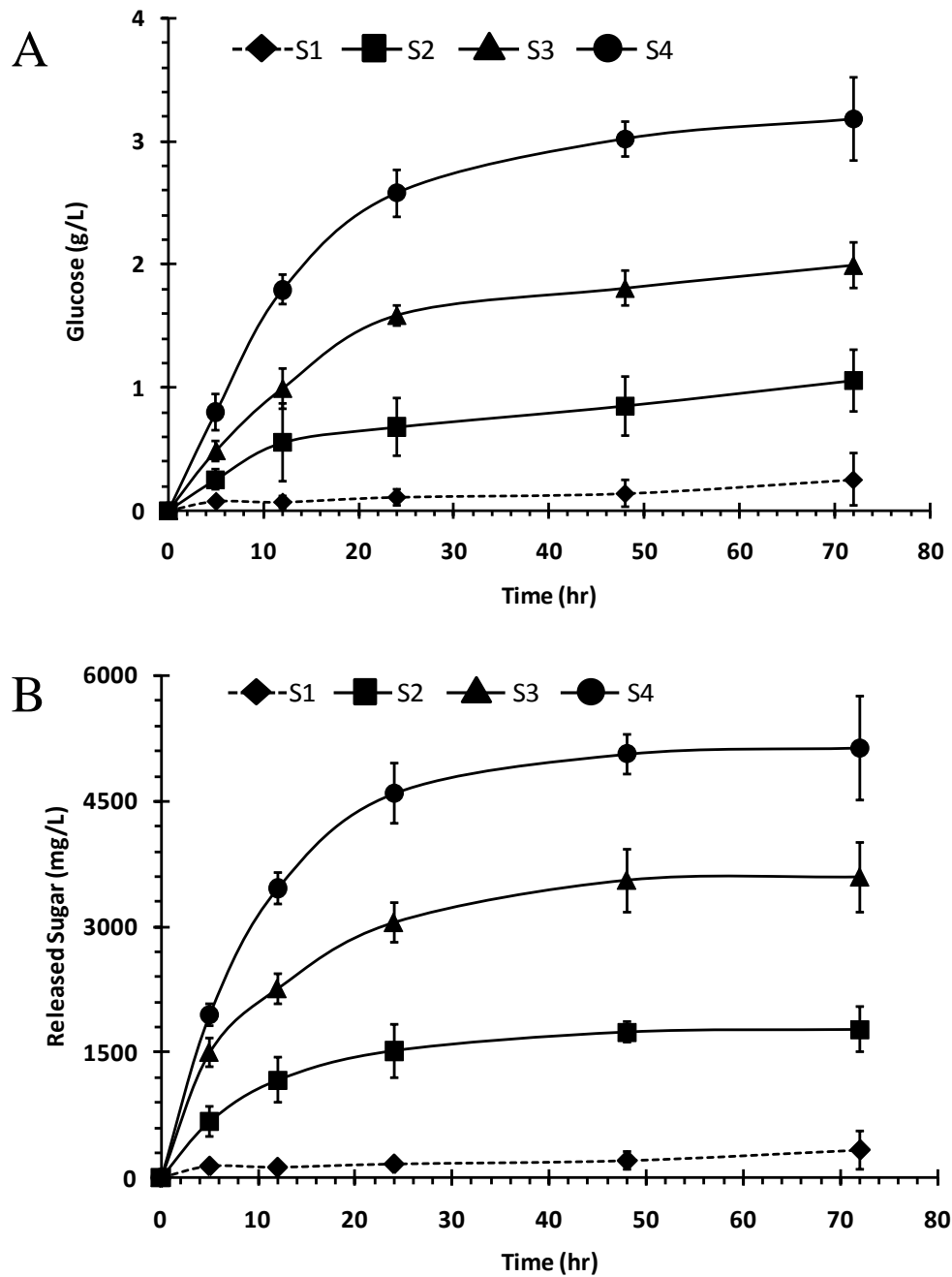


Figure 4.7. Production of glucose (A) and reducing sugars (B) from the hydrolysis of PASC by the yeasts displaying different cellulosomes.

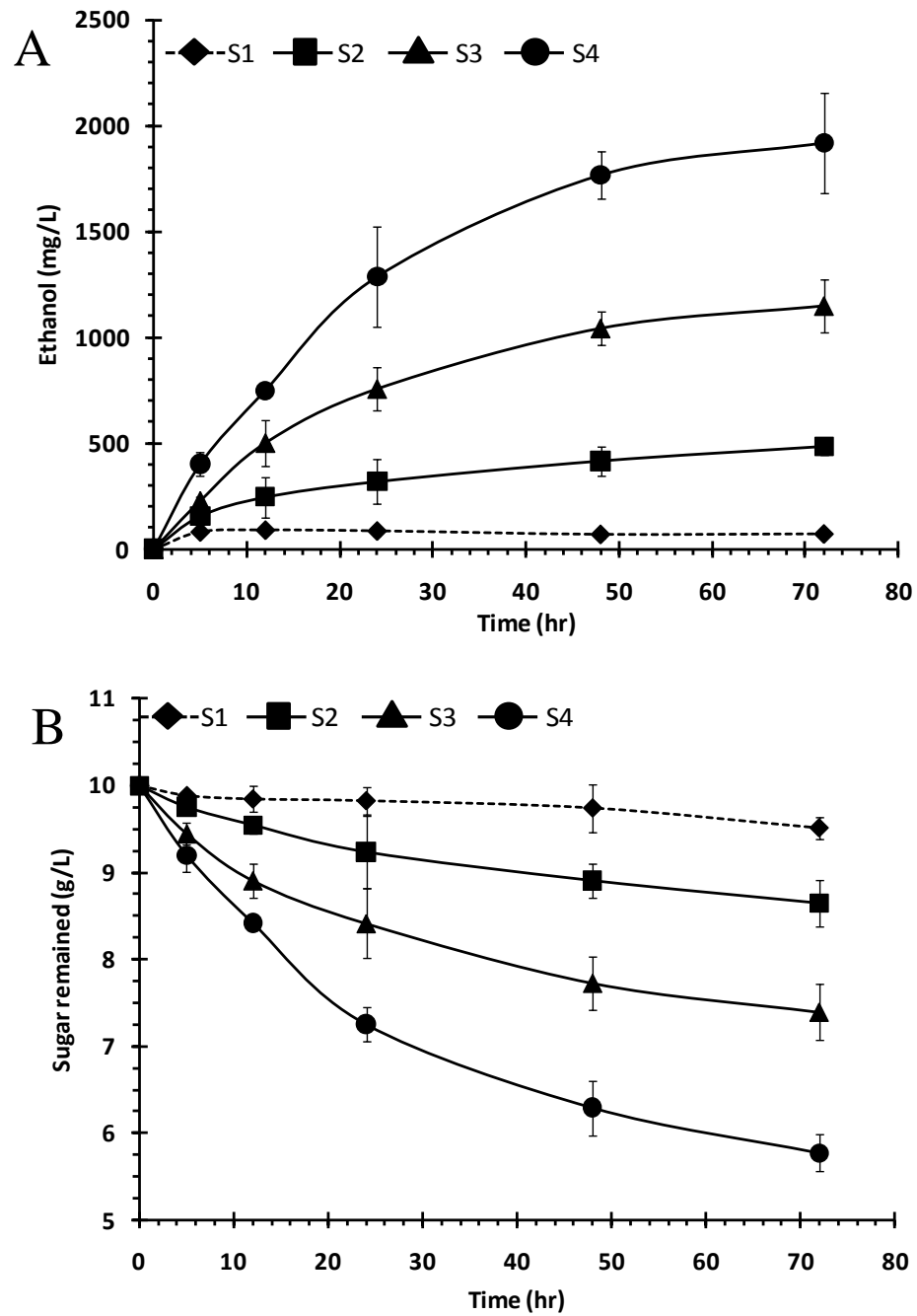


Figure 4.8. Time profiles of ethanol production (A) and cellulose hydrolysis (B) from PASC by the yeasts displaying different cellulosomes.

CHAPTER 5

Co-expression of *Arabidopsis thaliana* phytochelatin synthase and *Treponema denticola* cysteine desulfhydrase for enhanced arsenic accumulation

ABSTRACT

Arsenic is one of the most hazardous pollutants found in aqueous environments and has been shown to be a carcinogen. Phytochelatins (PCs), which are cysteine-rich and thio-reactive peptides, have high binding affinities for various metals including arsenic. Previously, we demonstrated that genetically engineered *Saccharomyces cerevisiae* strains expressing phytochelatin synthase (AtPCS) produced PCs and accumulated arsenic. In an effort to further improve the overall accumulation of arsenic, cysteine desulfhydrase, an aminotransferase that converts cysteine into hydrogen sulfide under aerobic condition, was co-expressed in order to promote the formation of larger AsS complexes. Yeast cells producing both AtPCS and cysteine desulfhydrase showed a higher level of arsenic accumulation than a simple cumulative effect of expressing both enzymes, confirming the coordinated action of hydrogen sulfide and PCs in the overall bioaccumulation of arsenic.

INTRODUCTION

Arsenic is one of the most hazardous pollutants found in the aqueous environment, and has been shown to be a carcinogen, affecting the health of millions throughout the world (Smedley and Kinniburgh, 2002). Due to its extreme toxicity, the US Environmental Protection Agency reduced the maximum contaminant level for arsenic in drinking water from 50 to 10 ppb in 2006 (U.S.EPA, 2001).

Arsenic occurs in several oxidation states. Among them As(III) is generally considered to be more mobile and more toxic than As(V) (Liu et al., 2001). Several treatment technologies have been applied in laboratory- and/or field-scale testing for the removal of arsenic from drinking water including coagulation, filtration, ion exchange, adsorption, and reverse osmosis (DeMarco et al., 2003; Martin et al., 1995; Zouboulis and Katsoyiannis, 2002). However, these technologies are either too expensive, due to the need to oxidize As(III) to As(V), or ineffective for As(III) treatment especially at low arsenic concentration. Therefore, technologies showing economic competitiveness, environmental amenability, and high selectivity are need for effective removal of arsenite.

Bioremediation processes are considered to be cost-effective and environmental-friendly way for heavy metals removal (Singh et al., 2008). In nature, microorganisms have developed several strategies for detoxification of heavy metals such as biotransformation, biomineralization, or biosorption (Barkay and Schaefer, 2001). These different microbial detoxifying mechanisms can potentially be combined to design an efficient bioremediation process (Tsai et al., 2009).

Phytochelatin (PCs) are small enzymatically synthesized cysteine-rich peptides widely found in plants and yeasts, and have been shown to efficiently bind heavy metals such as cadmium, mercury, lead, and arsenite (Kim et al., 2005; Maitani et al., 1996; Schmoger et al., 2000). We have reported enhanced accumulation of arsenite by an engineered *S. cerevisiae* strain expressing the *Arabidopsis thaliana* phytochelatin synthase (AtPCS) due to complexation with PCs (Singh et al., 2008).

Sulfide plays an important role in many metal detoxification mechanisms such as mineralization, which reduces the toxicity of heavy metals by forming insoluble metal precipitates (Barkay and Schaefer, 2001). However, most of the naturally occurring sulfate-reducing bacteria produce hydrogen sulfide only under strictly anaerobic condition (White and Gadd, 1998) and therefore they are not suitable for applications under aerobic conditions. Wang et al. (2001) functionally expressed a cysteine desulfhydrase (CysDes) from *Treponema denticola* in *E. coli* for the aerobic sulfide production and heavy metal precipitation using cysteine as the substrate. Apart from the formation of insoluble arsenic trisulfide (Newman et al., 1997), the formation of soluble arsenic sulfide complexes (thioarsenics) is also a well-known phenomenon (Hollibaugh et al., 2005; Stauder et al., 2005). Although little is known about the bioavailability of thioarsenics, they are reported to be less toxic than arsenite (Rader et al., 2004). In some eukaryotes, incorporation of sulfide to form a more stable high molecular weight PC–metal–sulfide complex in the vacuole has also been demonstrated (Mendoza-Cozatl et al., 2005, 2006).

Given these studies, the goal of this work was to co-express cysteine desulfhydrase and AtPCS in *S. cerevisiae* to elevate the intracellular accumulation of arsenic via the formation of PC–arsenic–sulfide complexes.

MATERIALS AND METHODS

Strains, media and plasmid construction

Plasmid pYES3-atPCS1::FLAG was kindly donated by Dr. Rea at University of Pennsylvania, Philadelphia (Vatamaniuk et al., 1999). The *AtPCS* gene was under the control of a constitutive yeast promoter PGK and flanked by a FLAG tag. The gene coding for cysteine desulfhydrase was amplified from the plasmid pCysdesulf/LacI2/Rock, a gift from Dr. Keasling at University of California, Berkeley (Wang et al., 2001), by PCR and cloned into the *Not1* and *BamH1* restriction sites of the multiple copy yeast shuttle vector pYES3 (Vatamaniuk et al., 1999). The entire cassette (PGKp-CysDes::His-PGKt) of cysteine desulfhydrase gene was then amplified by PCR and further bluntly inserted into the *Sma1* site of plasmid YEplac181 (Gietz and Sugino, 1988) containing a *LEU2* selection marker to form p181CysDes in order to co-transform with pYES3-atPCS1::FLAG carrying a *URA3* selection marker. The gene for cysteine desulfhydrase was under the control of strong yeast promoter PGK and flanked by a His tag. Plasmid maps of the two constructs are given in Figure 5.1. *S. cerevisia* strain BY4742 (MAT α *his3* Δ 1 *leu2* Δ 0 *lys2* Δ 0 *ura3* Δ 0) (Singh et al., 2008) was used for study and plasmid transformation was carried out by the lithium acetate method (Ito et al., 1983).

Cells were grown in 200 mL defined medium containing 6.7 g/L of yeast nitrogen base without amino acids, 20 g/L of galactose, 20 mg/L of adenine sulfate, L-tryptophan, L-histidine-HCl, L-arginine-HCl and L-methionine, 30 mg/L of L-tyrosine, L-isoleucine, L-lysine-HCl and L-phenylalanine, 100 mg/L of L-glutamic acid and L-aspartic acid, 150

mg/L of L-valine, 200 mg/L of threonine and 400 mg/L of serine at 30 °C. 20mg/L of uracil and/or 30 mg/L of L-leucine was also added if required. DCW = dry cell weight.

Phytochelatin measurement

To measure the levels of PC, samples were taken periodically from growing cultures (arsenite enriched media), and PCs were extracted and analyzed by HPLC (Agilent Tech., Palo Alto, CA). Briefly cells were pelleted down from the samples, washed with 5 mM HEPES buffer containing 0.8% NaCl twice before freezing at -80°C for 24 h. PCs were extracted with diethylenetriamine pentaacetic acid (DTPA) with 0.1% TFA and derivatized by reacting with 4-(2-hydroxy-ethyl)-piperazine-1-propane-sulfonic acid buffer (pH 8.2) containing DTPA and monobromobimane (mBrB). The PC content was measured using an excitation wavelength at 380 nm and an emission wavelength at 470 nm.

Arsenic measurement

For arsenic measurements, cells were harvested, washed with 5 mM HEPES buffer containing 0.8% NaCl three times before drying at 65°C for 24 h. The dried cell pellets were digested with 100 μL of concentrated nitric acid for 2 days (modified from Sriprang et al., 2003). The total internal arsenic content was measured using atomic adsorption spectroscopy (Perkin Elmer, Inc., Waltham, MA). Arsenic was determined at 193.7 nm in a graphite furnace.

Sulfide content measurement

The sulfide content was determined by a colorimetric assay as described by Aiking et al. (1982). Briefly, culture samples were centrifuged and the cell pellet was resuspended in 1 mL of 0.75 M NaOH after washing twice with 5 mM HEPES buffer containing 0.8% NaCl. This suspension was transferred to a microcentrifuge tube and incubated at 95°C for 15 min. The suspension was then mixed with 375 µL of 0.75 M NaOH and 250 µL of 2.6% zinc acetate dihydrate, 125 µL of 0.1% *N,N*-dimethyl-*p*-phenylenediamine dihydrochloride in 5 M HCl (freshly prepared) was added, and the solution was vortexed until clear. Next, 50 µL of 11.5 mM FeCl₃ in 6 M HCl was added and the solution was vortexed and incubated at room temperature for 30 min. After appropriate dilution and centrifugation, the OD of the sample was determined at 670 nm.

RESULTS AND DISCUSSION

Cysteine desulphydrase expression

We first investigated whether cysteine desulphydrase expression (BY4742/CysDes) could result in enhanced sulfide formation in yeast as this has not been previously demonstrated. Samples were taken after 15 h to determine the cell density (OD) and the intracellular levels of sulfide and As(III). As clearly shown in Figure 5.2A, expression of cysteine desulphydrase resulted in elevated production of sulfide and the level of enhancement increased with the amount of cysteine added. The enhanced sulfide production also resulted in higher levels of arsenite sequestration in a sulfide-dependent manner (Fig. 5.2B). Unfortunately, a significant growth inhibition was observed in the presence of cysteine (Table 5.1), even though the presence of cysteine desulphydrase partially reduced the level of growth inhibition. While cells expressing cysteine desulphydrase accumulated 25% more arsenite than the wild-type strain BY4742 even in the absence of any added cysteine, this is likely the most desirable condition in practice when combined with the expression of AtPCS as it saves the additional cost of adding cysteine into the medium.

***Arabidopsis thaliana* phytochelatins synthase expression**

Although expression of AtPCS has been shown to enhance arsenite accumulation in *S. cerevisiae* when grown in a rich medium (6.7 g/L yeast nitrogen base without amino acid, 5 g/L casamino acids, 20 g/L of galactose) (Singh et al., 2008), we tested whether a similar enhancement in arsenite accumulation could be obtained using a defined medium

without cysteine supplementation as cysteine is one of the precursors for PC synthesis. As shown in Figure 5.3, cells producing PC showed up to a threefold increase in the intracellular arsenite content over the control BY4742 strain. The level of As accumulation correlated well with the increasing intracellular PC content, confirming again PC is solely responsible for the enhanced As accumulation.

Co-expression of cysteine desulfhydrase and AtPCS

Since the separate expression of cysteine desulfhydrase or AtPCS could both elevate the intracellular arsenic content, it is interesting to explore whether co-expression of both enzymes could further improve As(III) accumulation in an additive manner. Cells co-expressing both enzymes showed the highest intracellular As content, and the overall level of enhancement was 25% higher than a simple addition of the two individual contributions (Fig. 5.4). This is surprising as the intracellular PC level for the co-expression strain was 10% lower than the AtPCS-expressing strain. This can be attributed to the fact that glutathione, which is a precursor for PC synthesis, is also a good substrate for cysteine desulfhydrase for sulfide synthesis. In addition, the enzyme GSH1, which is responsible for glutathione precursor (γ -EC) synthesis, is known to be inhibited by glutathione (Pócsi et al., 2004). Therefore, the increased consumption of glutathione by both cysteine desulfhydrase and PCS resulted in higher glutathione production and a corresponding 30% higher intracellular sulfide content (Chu et al., 1997). The improved arsenite binding is also likely the result of the formation of high molecular weight PC–

As–S complexes as observed in many plants and fungi (Mendoza-Cozatl et al., 2005, 2006).

Concluding remarks

In conclusion, engineered *S. cerevisiae* strains expressing cysteine desulfhydrase and/or AtPCS were created for enhanced accumulation of arsenic. Cells expressing both AtPCS and cysteine desulfhydrase showed a higher level of arsenic accumulation than a simple cumulative effect of expressing both enzymes, confirming the importance of coordinated action of hydrogen sulfide and PCs in the overall bioaccumulation of arsenic.

REFERENCES

1. **Aiking, H., K. Kok, H. Vanheerikhuizen, and J. Vantriet.** 1982. Adaptation to Cadmium by *Klebsiella-Aerogenes* Growing in Continuous Culture Proceeds Mainly Via Formation of Cadmium-Sulfide. *Appl Environ Microbiol* **44**: 938-944.
2. **Barkay, T., and J. Schaefer.** 2001. Metal and radionuclide bioremediation: issues, considerations and potentials. *Curr Opin Microbiol* **4**: 318-323.
3. **Chu, L., J. L. Ebersole, G. P. Kurzban, and S. C. Holt.** 1997. Cystalysin, a 46-kilodalton cysteine desulfhydrase from *Treponema denticola*, with hemolytic and hemoxidative activities. *Infect Immun* **65**: 3231-3238.
4. **DeMarco, M. J., A. K. Sengupta, and J. E. Greenleaf.** 2003. Arsenic removal using a polymeric/inorganic hybrid sorbent. *Water Res* **37**: 164-176.
5. **Gietz, R. D., and A. Sugino.** 1988. New yeast- *Escherichia coli* shuttle vectors constructed with in vitro mutagenized yeast genes lacking six-base pair restriction sites. *Gene* **74**: 527-534.
6. **Hollibaugh, J. T., S. Carini, H. Gurleyuk, R. Jellison, S. B. Joye, G. LeCleur, C. Meile, L. Vasquez, and D. Wallschlager.** 2005. Arsenic speciation in Mono lake, California: Response to seasonal stratification and anoxia. *Geochim Cosmochim Ac* **69**: 1925-1937.
7. **Ito, H., Y. Fukuda, K. Murata, and A. Kimura.** 1983. Transformation of Intact Yeast-Cells Treated with Alkali Cations. *J Bacteriol* **153**: 163-168.
8. **Kim, Y.J., K. S. Chang, M. R. Lee, J. H. Kim, C. E. Lee, Y. J. Jeon, J. S. Choi, H. S. Shin, and S. B. Hwang.** 2005. Expression of tobacco cDNA encoding

- phytochelatin synthase promotes tolerance to and accumulation of Cd and As in *Saccharomyces cerevisiae*. *J Plant Biol* **48**: 440-447.
9. **Liu, S. X., M. Athar, I. Lippai, C. Waldren, and T. K. Hei.** 2001. Induction of oxyradicals by arsenic: Implication for mechanism of genotoxicity. *P Natl Acad Sci USA* **98**: 1643-1648.
 10. **Maitani, T., H. Kubota, K. Sato, and T. Yamada.** 1996. The composition of metals bound to class III metallothionein (phytochelatin and its desglycyl peptide) induced by various metals in root cultures of *Rubia tinctorum*. *Plant Physiol* **110**: 1145-1150.
 11. **Martin, C. J., E. O. Kartinen, and J. Condon.** 1995. Examination of Processes for Multiple Contaminant Removal from Groundwater. *Desalination* **102**: 35-45.
 12. **Mendoza-Cozatl, D., H. Loza-Tavera, A. Hernandez-Navarro, and R. Moreno-Sanchez.** 2005. Sulfur assimilation and glutathione metabolism under cadmium stress in yeast, protists and plants. *FEMS Microbiol Rev* **29**: 653-671.
 13. **Mendoza-Cozatl, D. G., J. S. Rodriguez-Zavala, S. Rodriguez-Enriquez, G. Mendoza-Hernandez, R. Briones-Gallardo, and R. Moreno-Sanchez.** 2006. Phytochelatin-cadmium-sulfide high-molecular-mass complexes of *Euglena gracilis*. *FEBS J* **273**: 5703-5713.
 14. **Newman, D. K., T. J. Beveridge, and F. M. M. Morel.** 1997. Precipitation of arsenic trisulfide by *Desulfotomaculum auripigmentum*. *Appl Environ Microbiol* **63**: 2022-2028.

15. **Pócsi, I., R. A. Prade, and M. J. Penninckx.** 2004. Glutathione, Altruistic Metabolite in Fungi. *Adv Microb Physiol* **49**: 1-46.
16. **Rader, K. J., P. M. Dombrowski, K. J. Farley, J. D. Mahony, and D. M. Di Toro.** 2004. Effect of thioarsenite formation on arsenic(III) toxicity. *Environ Toxicol Chem* **23**: 1649-1654.
17. **Schmoger, M. E. V., M. Oven, and E. Grill.** 2000. Detoxification of arsenic by phytochelatin in plants. *Plant Physiol* **122**: 793-801.
18. **Singh, S., W. Lee, N. A. DaSilva, A. Mulchandani, and W. Chen.** 2008. Enhanced arsenic accumulation by engineered yeast cells expressing *Arabidopsis thaliana* phytochelatin synthase. *Biotechnol Bioeng* **99**: 333-340.
19. **Smedley, P. L., and D. G. Kinniburgh.** 2002. A review of the source, behavior and distribution of arsenic in natural waters. *Appl Geochem* **17**: 517-568.
20. **Stauder, S., B. Raue, and F. Sacher.** 2005. Thioarsenates in sulfidic waters. *Environ Sci Technol* **39**: 5933-5939.
21. **Tsai, S. L., S. Singh, and W. Chen.** 2009. Arsenic metabolism by microbes in nature and the impact on arsenic remediation. *Curr Opin Biotechnol* **20**: 659-667.
22. **Vatamaniuk, O. K., S. Mari, Y. P. Lu, and P. A. Rea.** 1999. AtPCS1, a phytochelatin synthase from *Arabidopsis*: Isolation and in vitro reconstitution. *P Natl Acad Sci USA* **96**: 7110-7115.
23. **Wang, C. L., A. M. Lum, S. C. Ozuna, D. S. Clark, and J. D. Keasling.** 2001. Aerobic sulfide production and cadmium precipitation by *Escherichia coli*

expressing the *Treponema denticola* cysteine desulfhydrase gene. Appl Microbiol Biotechnol **56**: 425-430.

24. **White, C., and G. M. Gadd.** 1998. Accumulation and effects of cadmium on sulphate-reducing bacterial biofilms. Microbiol-UK **144**: 1407-1415.

25. **Zouboulis, A. I., and I. A. Katsoyiannis.** 2002. Arsenic removal using iron oxide loaded alginate beads. Ind Eng Chem Res **41**: 6149-6155.

Table 5.1. Cell densities (O.D.) of the yeast strain BY4742 with or without cysteine desulfhydrase expression after 15 h cultivation at various cysteine concentrations. Data shown below were the average from three independent experiments.

Cysteine Conc.	Cell Growth		
	μM	BY4742	CysDes
0		0.975±0.05	1.142±0.01
1		0.634±0.05	0.639±0.08
5		0.262±0.02	0.455±0.05

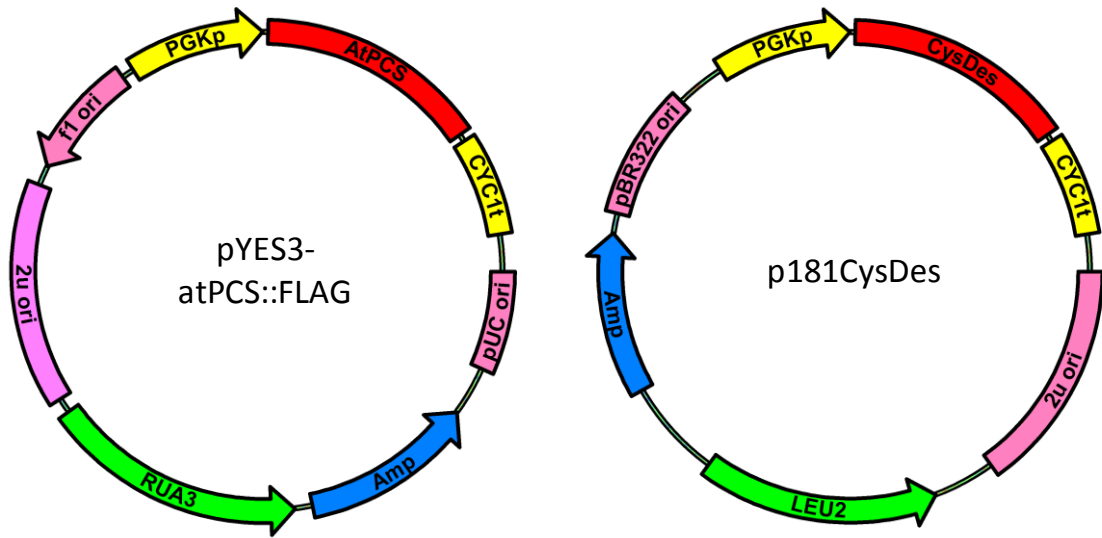


Figure 5.1. Plasmid maps of the construct (A) pYES3-atPCS::FLAG and (B) p181CysDes.

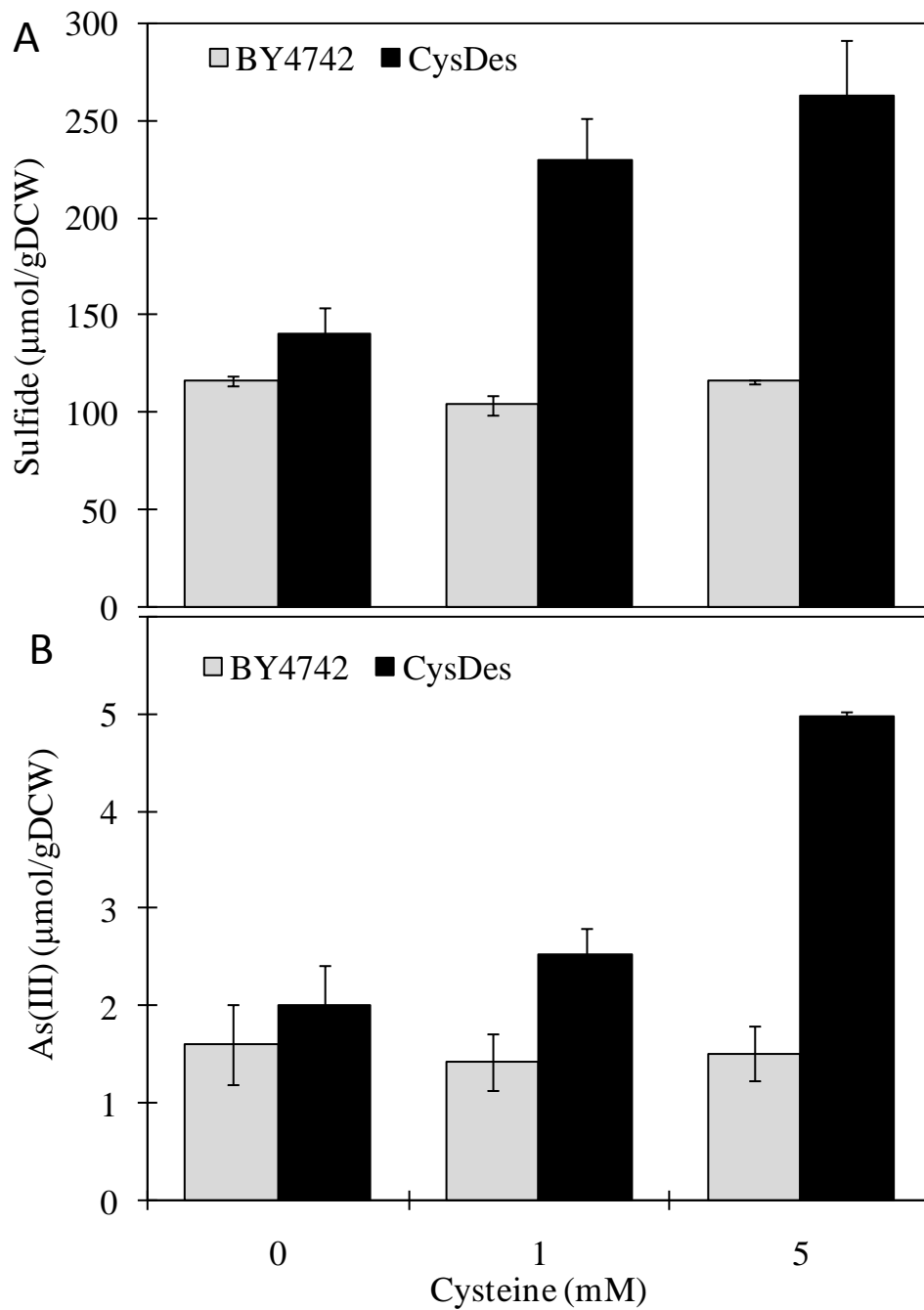


Figure 5.2. (A) Sulfide production and (B) intracellular As(III) accumulation from the engineered *S. cerevisiae* strain BY4742 expressing cysteine desulfhyrase at various cysteine concentrations.

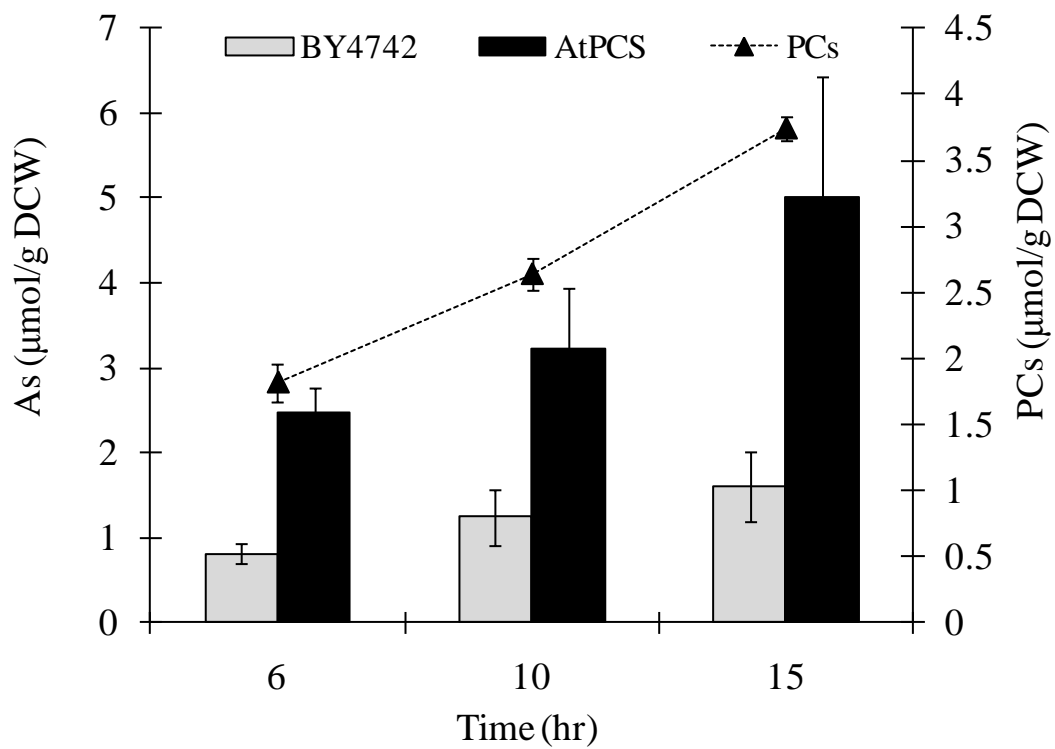


Figure 5.3. PC production and intracellular As(III) accumulation from the engineered *S. cerevisiae* strain BY4742 expressing AtPCS. DCW = dry cell weight.

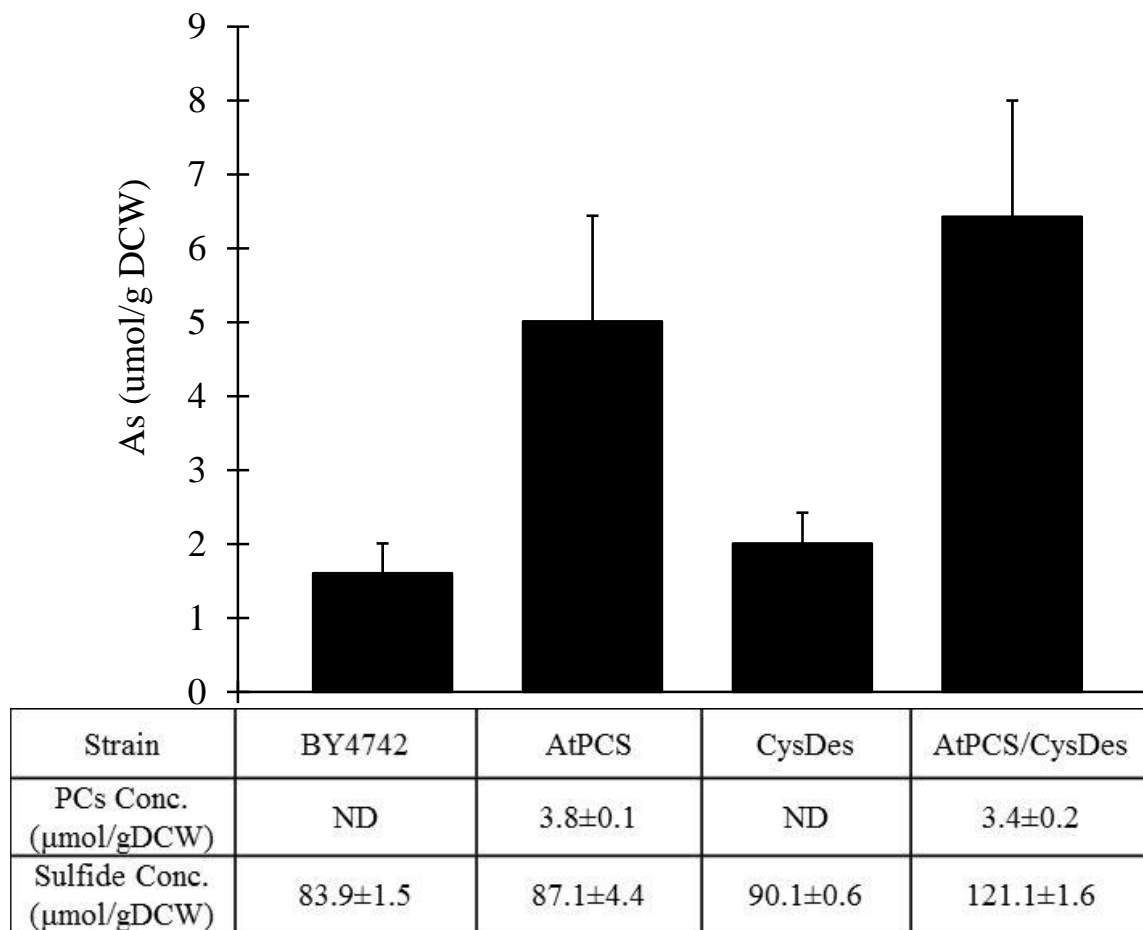


Figure 5.4. Intracellular As(III) accumulation from engineered *S. cerevisiae* strains expressing either cysteine desulfhydrase, AtPCS, or both enzymes. Data shown in the table were the average from three independent experiments. The difference of intracellular As(III) content between AtPCS and AtPCS/CysDes are statistically significant with 95% confidence. The corresponding PC and sulfide concentrations are also shown. DCW = dry cell weight.

CHAPTER 6

Conclusions

Naturally occurring microbial activities are the inspirations for all biotechnology applications. Utilizing the metabolism of microbes for the production of biofuels or the elimination of environmental pollutants has provided sustainable and economic improvements on a wide range of processes. In this dissertation, metabolic engineering has been applied to create several yeast strains with new functionalities suitable for cellulosic ethanol production and arsenic remediation.

While it is widely-accepted that fuels made from cellulosic biomass would be one of the most sustainable ways to address the issue of gasoline crisis, over the past few decades, a consensus has not been reached on the best way to engineer microbial cells for the efficient conversion of cellulose into biofuels. The main goal of these studies was to improve the overall efficiency and yield of hydrolyzed sugars from cellulosic biomass, as these factors would ultimately determine the feasibility and success of processes in biofuel commercialization. From these perspectives, anaerobic cellulolytic microorganisms that could efficiently degrade one of the most recalcitrant polymers, lignocellulose, and convert it into cell mass and products simultaneously under an energy-limited environment in nature have provided a cue.

Taking this cue from nature, we attempted to assemble several different types of cellulosome structures on the surface of the historical ethanologenic yeast *Saccharomyces cerevisiae* toward simultaneous cellulose saccharification and ethanol production. Although most of the works presented here are proof-of-concept studies, several important lessons can still be learned from them.

First, we demonstrated the functional display of a mini-scaffoldin on the yeast cell surface, consisting of three divergent cohesin domains from *Clostridium thermocellum* (t), *Clostridium cellulolyticum* (c) and *Ruminococcus flavefaciens* (f). Incubation with *Escherichia coli* lysates containing an endoglucanase (CelA) from *C. thermocellum* (At), an exoglucanase (CelE) from *C. cellulolyticum* (Ec), and an endoglucanase (CelG) from *C. cellulolyticum* fused with a dockerin domain from *R. flavefaciens* (Gf) resulted in the assembly of a functional minicellulosome on the yeast surface. The displayed minicellulosome successfully hydrolyzed cellulose by emulating the synergism of enzymatic modules in naturally occurring cellulosomes.

Second, when a β -glucosidase (BglA) from *C. thermocellum* tagged with the dockerin from *R. flavefaciens* was used in place of Gf, cells displaying the new minicellulosome exhibited significantly enhanced glucose liberation and produced ethanol directly from phosphoric acid swollen cellulose (PASC). The final ethanol concentration obtained was higher than that using the same concentration of free cellulases, confirming the synergistic contribution to simultaneous and synergistic saccharification and fermentation of cellulose to ethanol by a yeast strain displaying a functional minicellulosome containing all three required cellulolytic enzymes.

Third, we engineered a synthetic yeast consortium capable of *in vivo* surface assembly of a functional minicellulosome via intracellular complementation to accomplish simultaneous cell growth and ethanol production on cellulose. The basic design consisted of four different engineered yeast strains capable of either displaying the

miniscaffoldin or secretion of one of the three required dockerin-tagged enzymes (endoglucanase, exoglucanase, or β -glucosidase). This allowed the burden of protein expression to be distributed, effectively expediting the self-assembly of the minicellulosome. The resulting consortium grew on cellulose and produced ethanol more efficiently than a similar consortium secreting only cellulases, demonstrating the importance of the mini-cellulosome to cellulose hydrolysis and ethanol production.

Finally, a complex tetravalent cellulosome was developed for enhanced cellulose hydrolysis and ethanol production using an adaptive assembly strategy. The engineered yeasts possessing a complete tetravalent cellulosome on the surface exhibited a 4-fold increase in ethanol production than those displaying a defective divalent cellulosome, indicating the significance of enzyme proximity to the cellulosomal synergy. Furthermore, this is the first report that manifested the benefit of increasing local over bulk enzyme density in cellulosome systems for cellulose hydrolysis.

To further extend the metabolic engineering strategy toward environmental sustainability, the last part of this dissertation focused on creating a low-cost and efficient biosorbent for arsenic cleanup. The engineered *S. cerevisiae* strains expressing cysteine desulfhydrase and/or AtPCS were created for enhanced accumulation of arsenic. Cells expressing both AtPCS and cysteine desulfhydrase showed a higher level of arsenic accumulation than a simple cumulative effect of expressing both enzymes, confirming the importance of coordinated action of hydrogen sulfide and PCs in the overall bioaccumulation of arsenic.

The success of metabolically engineered cellulosic biofuel production and arsenic bioremediation indicates that sophisticated metabolic techniques will continue to be implemented to advance the field. Although tremendous amount of work remains to be done, the work presented here suggests a promising future for the application of molecular techniques in environmental cleanup and sustainable energy production.